UNIVERSITAT POLITÈCNICA DE VALÈNCIA

FUNDAMENTAL AND APPLIED RESEARCH IN ABA SIGNALING:

Regulation by ABA of the chromatin remodeling ATPase BRAHMA and biotechnological use of the PP2CA promoter

Tesis doctoral realizada por

Marta Peirats-Llobet

Y dirigida por

Prof. Pedro L. Rodriguez Egea

València, Febrero 2017

ABSTRACT

Optimal response to drought is critical for plant survival and will affect biodiversity and crop performance during climate change. Mitotically heritable epigenetic and dynamic chromatin state changes have been implicated in the plant response to the drought stress hormone abscisic acid (ABA). The Arabidopsis SWI/SNF chromatin-remodeling ATPase BRAHMA (BRM) modulates response to ABA by preventing premature activation of stress response pathways during germination. Here, we show that the core ABA signalosome formed by ABA receptors, PP2Cs and SnRK2s physically interact with BRM to regulate BRM activity and post-translationally modify BRM by phosphorylation/dephosphorylation. Genetic evidence suggests that BRM acts downstream of SnRK2.2/2.3 kinases and biochemical studies identified evolutionary conserved SnRK2 phosphorylation sites in the C-terminal region of BRM. Our data suggest that SnRK2-dependent phosphorylation of BRM leads to its inhibition, and PP2CA-mediated dephosphorylation of BRM restores the ability of BRM to repress ABA response.

ABA plays a key role to regulate germination and post-germination growth and the AP2-type ABI4 and bZIP-type ABI5 transcription factors (TFs) are required for ABA-mediated inhibition of post-germination growth when the embryo encounters water stress. The growth arrest induced by ABI4 and ABI5 involves ABA signaling and in the case of ABI5, it has been demonstrated that ABA inhibits the activity of BRM to induce ABI5 transcription. Loss of BRM activity leads to destabilization of a nucleosome involved in repression of ABI5 transcription. Therefore reduction of BRM activity in the *brm-3* allele leads to enhanced expression of ABI5 in 2-d-old seedlings and enhanced sensitivity to ABA. Novel genetic evidence obtained in this work indicates that ABI4 is one of

the redundant TFs regulated by BRM that mediate ABA response during germination and early seedling growth. Thus, the association of BRM with the *ABI4* locus together with the observed derepression of *ABI4* expression in *brm-3* suggests that BRM directly regulates *ABI4* expression.

Finally, this work provides a direct link between the ABA signalosome and the chromatin-remodeling ATPase BRM, which enables ABA-dependent modulation of BRM activity as a possible mechanism to enhance plant drought tolerance. Additionally, we identified and characterized the promoter of PP2CA as a stress-inducible promoter and we have used it to drive the expression of ABA receptors from *Arabidopsis* and *Solanum lycopersicum*. This technology appears to be promising for the expression of ABA receptors in an inducible manner and to generate drought tolerant plants.

RESUMEN

La respuesta óptima a la sequía es crítica para la supervivencia de las plantas y afectará a la biodiversidad y al rendimiento de los cultivos durante el cambio climático. Las modificaciones epigenéticas y los cambios dinámicos del estado de la cromatina han sido implicados en la respuesta de la planta al ácido abscísico (ABA), la conocida como la hormona del estrés hídrico. La ATPasa remodeladora de cromatina de tipo SWI/SNF de *Arabidopsis*, BRAHMA (BRM), modula la respuesta al ABA mediante la prevención de la activación prematura de las vías de respuesta al estrés durante la germinación. Aquí, mostramos que el núcleo del señalosoma de ABA formado por los receptores de ABA, las PP2Cs y las SnRK2s interaccionan físicamente con BRM para regular su actividad y modificarla post-traduccionalmente por mecanismos de fosforilación/desfosforilación. La evidencia genética sugiere que BRM actúa aguas abajo de las quinasas SnRK2.2/2.3 y los estudios bioquímicos identificaron la presencia en la región C-terminal de BRM de sitios de fosforilación de las SnRK2 que estaban conservados evolutivamente. Nuestros datos sugieren que la fosforilación de BRM que depende de las SnRK2 conduce a su inhibición, y que la desfosforilación de BRM mediada por PP2CA restaura la capacidad de BRM para reprimir la respuesta a ABA.

El ABA juega un papel clave en la regulación de la germinación y el crecimiento post germinativo y los factores de transcripción de tipo AP2 como ABI4 y de tipo bZIP como ABI5, son necesarios para la inhibición del crecimiento post germinativo mediado por ABA cuando los embriones encuentran estrés hídrico. La detención del crecimiento inducida por ABI4 y ABI5 implica la señalización de ABA y en el caso de ABI5, se ha demostrado que el ABA inhibe la actividad de BRM para

inducir la transcripción de ABI5. La pérdida de actividad de BRM conduce a la desestabilización de un nucleosoma implicado en la represión de la transcripción de ABI5. Por lo tanto, la reducción de la actividad de BRM en el alelo *brm-3* conduce a una mayor expresión de ABI5 en plántulas de 2 días y una mayor sensibilidad a ABA. La nueva evidencia genética obtenida en este trabajo indica que ABI4 es uno de los factores de transcripción redundantes regulados por BRM que median la respuesta a ABA durante los estadios de germinación y crecimiento temprano de las plántulas. La asociación de BRM con el locus *ABI4*, junto con la desrepresión de la expresión de *ABI4* observada en el mutante *brm-3* sugiere que BRM regula directamente la expresión de *ABI4*.

Por último, este trabajo proporciona una relación directa entre el señalosoma de ABA y la ATPasa remodeladora de cromatina BRM, que permite la modulación de la actividad de BRM de modo dependiente de ABA como un posible mecanismo para mejorar la tolerancia a sequía de las plantas. Además, hemos identificado y caracterizado el promotor de PP2CA como un promotor inducible por estrés y lo hemos utilizado para dirigir la expresión de los receptores de ABA de *Arabidopsis* y *Solanum lycopersicum*. Esta tecnología parece ser prometedora para la expresión de receptores de ABA de modo inducible y para generar plantas tolerantes a la sequía.

RESUM

La resposta òptima a la sequera és crítica per a la supervivència de les plantes i afectarà la biodiversitat i al rendiment dels cultius durant el canvi climàtic. Les modificacions epigenètiques i els canvis dinàmics de l'estat de la cromatina han estat implicats en la resposta de la planta a l'àcid abscísic (ABA), la coneguda com hormona de l'estrès hídric. L'ATPasa remodeladora de cromatina de tipus SWI/SNF d'*Arabidopsis*, BRAHMA (BRM), modula la resposta a l'ABA mitjançant la prevenció de l'activació prematura de les vies de resposta a l'estrès durant la germinació. Ací, mostrem que el nucli del senyalosoma d'ABA format pels receptors d'ABA, les PP2Cs i les SnRK2s interaccionen físicament amb BRM per regular la seva activitat i modificar-la post-traduccionalment per mecanismes de fosforilació/desfosforilació. L'evidència genètica suggereix que BRM actua aigües avall de les quinases SnRK2.2/2.3 i els estudis bioquímics van identificar la presència, a la regió C-terminal de BRM, de llocs de fosforilació de les SnRK2 que estaven conservats evolutivament. Les nostres dades suggereixen que la fosforilació de BRM que depèn de les SnRK2, condueix a la inhibició de BRM, i que la desfosforilació de BRM mediada per PP2CA restaura la capacitat de BRM per reprimir la resposta a ABA.

El ABA juga un paper clau en la regulació de la germinació i el creixement post germinatiu i els factors de transcripció de tipus AP2 com ABI4 i de tipus bZIP com ABI5, són necessaris per a la inhibició del creixement post germinatiu mediat per ABA quan els embrions pateixen estrès hídric. La detenció del creixement induïda per ABI4 i ABI5 implica la senyalització d'ABA i en el cas d'ABI5, s'ha demostrat que l'ABA inhibeix l'activitat de BRM per induir la transcripció d'ABI5. La pèrdua d'activitat de BRM condueix a la desestabilització d'un nucleosoma

implicat en la repressió de la transcripció d'ABI5. Per tant, la reducció de l'activitat de BRM a l'al·lel *brm-3* condueix a una major expressió d'ABI5 en plàntules de 2 dies i una major sensibilitat a l'ABA. La nova evidència genètica obtinguda en aquest treball indica que ABI4 és un dels factors de transcripció redundants regulats per BRM que medien la resposta a l'ABA durant els estadis de germinació i creixement primerenc de les plàntules. L'associació de BRM amb el locus *ABI4*, juntament amb la desrepressió de l'expressió de *ABI4* observada al mutant *brm-3* suggereix que BRM regula directament l'expressió d'ABI4.

Finalment, aquest treball proporciona una relació directa entre el senyalosoma d'ABA i l'ATPasa remodeladora de cromatina BRM, que permet la modulació de l'activitat de BRM de manera dependent d'ABA com un possible mecanisme per millorar la tolerància a sequera de les plantes. A més, hem identificat i caracteritzat el promotor de PP2CA com un promotor induïble per estrès i l'hem utilitzat per dirigir l'expressió dels receptors d'ABA d'*Arabidopsis* i *Solanum lycopersicum*. Aquesta tecnologia sembla ser prometedora per a l'expressió de receptors d'ABA de manera induïble i per generar plantes tolerants a la sequera.

INDEX

INTRODUCTION

Plants and environment

Sessile nature of plants makes them very sensitive to environmental changes. Due to their nature, plants have to deal daily with several stress conditions as drought, light, salinity, wounding, pathogen attack and more. Therefore, plants have to be plastically enough to integrate these conditions and respond to them accordingly. This plasticity is managed in plants by hormones (Weake & Workman, 2010).

Plant hormones are a collection of small signaling molecules that coordinate stress responses and developmental pathways through complex signaling pathways to increase plant fitness (Santner & Estelle, 2009). There are five classical hormones in plants: auxins, gibberellins (GAs), cytokinins (CKs), ethylene (ET) and abscisic acid (ABA). They can work together or display independent roles in plant growth and development. Auxins, GAs and CKs are mainly implicated in growth in different ways (Verma et al., 2016). Auxins are involved in cell growth and cell expansion (Liscum & Reed, 2002). GAs acts in a similar way to auxins in growth and development but they are a completely different hormones (Swain & Singh, 2005). CKs are responsible of cell division and their balance with auxins is very important in regulating apical meristems, the patterning of the root, the development of the gynoecium and female gametophyte, and organogenesis and phyllotaxy in the shoot (Schaller et al., 2015). ET is a peculiar hormone; it is the only gas hormone known to date and participates in processes like plant growth, fruit ripening and flowering (Van de Poel et al., 2015). And last, ABA that is known as the drought stress hormone however is implicated in a lot of different developmental processes (Finkelstein & Rock, 2002, Finkelstein et al., 2002). Other plant hormones and growth regulators are brassinosteroids (BRs) that stimulates cell elongation and division

(Gudesblat & Russinova, 2011), salicylic acid (SA), nitric oxide (NO) and jasmonates (JA) that are involved in defense responses to pathogens (Klessig et al., 2000, Spoel & Dong, 2008, Cao et al., 2011, Gimenez-Ibanez & Solano, 2013), polyamines (PAs) that regulates growth, division and cell death (Tiburcio et al., 2014) and strigolactones (SLs), which act in developmental processes like branching (Zwanenburg et al., 2016).

Environmental stresses induce large amount of changes at transcriptional level. In response to ABA, more than 10% of the transcriptome is modified indicating that, high plasticity of the genome is needed to allow genes to be activated or repressed by this hormone (Wang et al., 2011, Bechtold et al., 2016). Chromatin-remodeling activity in plants plays an essential role to sustain these massive changes in gene expression providing the necessary flexibility for developmental plasticity and stress adaptation (Jarillo et al., 2009, Ahmad et al., 2010, Weake & Workman, 2010).

Abscisic acid

ABA synthesis and catabolism

The ABA molecule is synthesized in response to water deprivation and catabolized very quickly to avoid a sustained stress response. ABA is a sesquiterpenoid derived from the modification and cleavage of zeaxanthin, a C_{40} carotenoid in the chloroplast. The first step of the biosynthetic pathway involves 9-cis-epoxycarotenoid dioxygenase (NCED) (Schwartz et al., 2003). This enzyme cleaves the C_{40} substrate into a C_{25} metabolite and another C_{15} compound, xanthoxin. Xanthoxin is converted to ABA in two reactions. First, xanthoxin is translocated to the cytoplasm of the cell and converted to abscisic aldehyde by aba deficient 2 (ABA2), a short-chain dehydrogenase encoded by a single *ABA2* gene (Gonzalez-Guzman et al., 2002, Cheng et al., 2002). Finally, abscisic aldehyde is oxidized to ABA by an abscisic aldehyde oxidase (AAO) (Seo et al., 2000, Gonzalez-Guzman et al., 2004).

To inactivate ABA, its catabolism also involves a series of reactions that will breakdown the molecule in response to environmental conditions. There are two major pathways for ABA catabolism. One of them involves hydroxylation of ABA molecule to 8-OH-ABA by a family of cytochrome P450 monooxygenase called CYP707A. 8-OH-ABA is spontaneously isomerized to phaseic acid (PA), a metabolite less active than ABA (Saito et al., 2004). ABA can also be inactivated by conjugation to another molecule as glucosyl ester. ABA suffers esterification to ABA-glucosyl ester (ABA-GE), which is an inactive conjugated storage or transportable form of ABA (Lim et al., 2005). ABA-GE can be stored in the vacuoles and apoplast but also translocated to endoplasmic reticulum when drought is perceived. This has been described as a fast mechanism, which allows plants to quickly adjust the ABA levels in response to

environmental conditions (Dietz et al., 2000, Lee et al., 2006, Xu et al., 2012). The balance between biosynthesis and catabolism processes will determine the bioactive ABA levels and is responsible for the plant adaptation to stress.

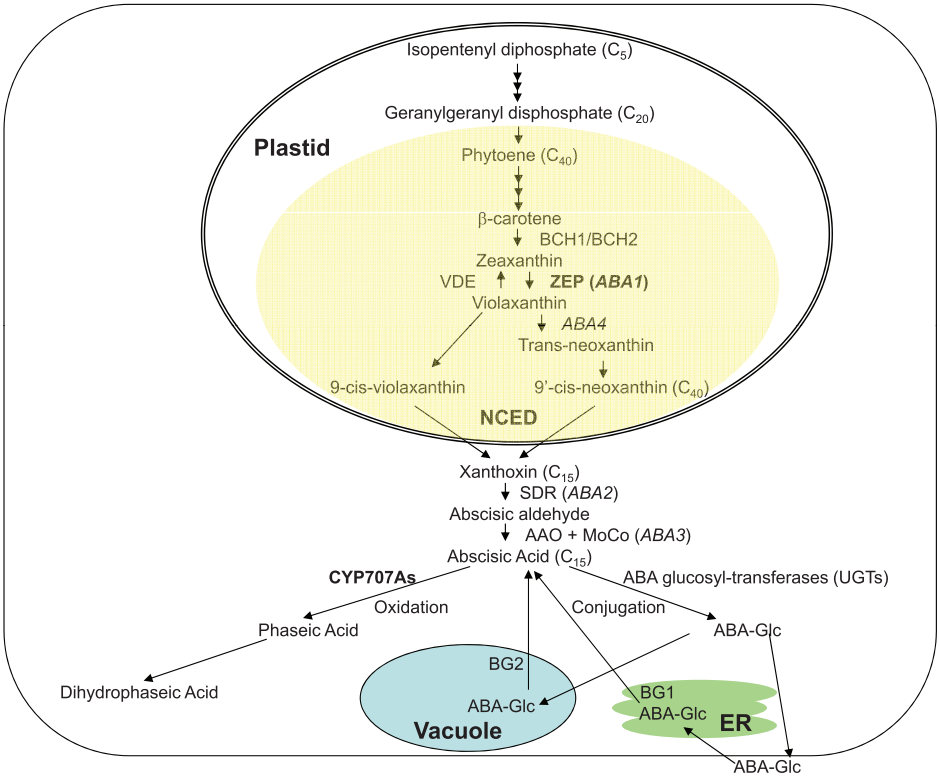

Figure 1. ABA metabolism overview. ABA biosynthetic pathway occurs in the chloroplasts and cytoplasm. The carotenoid intermediates are highlighted in yellow. ABA catabolism depends on its oxidation. Inactive ABA, ABA-GE can be stored in the vacuole and can be reused through endoplasmic reticulum. Reprinted from (Finkelstein, 2013).

ABA transport

Roots are the first part of the plant to experience drought conditions because they contact directly with the drying soil. The reduced soil water availability causes an increase in the synthesis of ABA that will promote root growth in the search of water. Furthermore, the expression pattern of ABA biosynthetic genes indicates that the synthesis of ABA takes place in the seeds, in the vasculature and in guard cells (Bauer et al., 2013). ABA synthesized in the vascular tissues is transported to shoots and roots through xylem and phloem. Under drought stress conditions, ABA is also accumulated in leaves. The accumulation in the leaves is several-fold higher than that in the roots. This is in part due to ABA is being translocated from the root but also because exists *de novo* ABA synthesis in the leaves (Bauer et al., 2013).

Due to the nature as a weak acid of ABA, it is in a pH-dependent equilibrium between a charged (ABA^-) and an uncharged (ABAH) form. Although the uncharged form is thought to move by passive diffusion across cell membranes, the anionic form presumably requires a transporter (Wilkinson & Davies, 2002, Schachtman & Goodger, 2008). There are two different groups of transporters reported so far, the transporters belonging to the ATP-binding cassette (ABC) transporter family and those from the family of low-affinity nitrate transporters. AtABCG25 and AtABCG40 (*A. thaliana* ABC subfamily G25 and 40 respectively) are members of the large and diverse ABC family of transporter proteins. AtABCG25, which is primarily expressed in vascular tissue, appears to serve as an ABA efflux transporter. Overexpression of AtABCG25 reduces water loss from detached leaves (Kuromori et al., 2010). AtABCG40 is expressed in guard cells and is also an influx transporter of ABA. Loss-of-function *abcg40* mutants have guard cells with reduced sensitivity to ABA and are more susceptible to drought

stress (Kanno et al., 2012, Kuromori & Shinozaki, 2010). The ABA-importing transporter1 (AIT1), also known as NRT1.2 or At-NPF4.6 (Tsay et al., 2007, Kanno et al., 2012, Leran et al., 2014), mediates influx as well, demonstrating the variety of transporter types that are able to mediate ABA transport. Recently, the ABC subfamily C (ABCC) transporters ABCC1 and ABCC2 have been shown to transport ABA-GE into the mesophyll vacuole (Burla et al., 2013).

ABA roles in plants

ABA is the major hormone involved in controlling plants' ability to survive in the changing environment. To be able to respond to all the challenges happening everyday in nature, ABA signaling regulates stress responses as well as plant growth and development (Cutler et al., 2010, Finkelstein, 2013). ABA plays major roles in abiotic and biotic stress responses. It is implicated in guard cell regulation triggering stomatal closure to maintain water balance (Sirichandra et al., 2009, Merilo et al., 2015, Munemasa et al., 2015), antagonizes gibberellins (GAs) effects to fine tune growth in adverse situations (Golldack et al., 2013), controls gene expression to help with plant adaptation to stress (Bechtold et al., 2016) and also has a role in the promotion of plant resistance to pathogens restricting its entrance via stomata (McLachlan et al., 2014). Despite of the well known functions in abiotic and biotic stress, ABA is also important for the regulation of several physiological and developmental events as embryo maturation, promotion of seed desiccation tolerance and dormancy, germination and seedling establishment, primary and lateral root growth and transition from vegetative to reproductive stage (Finkelstein et al., 2002, Cutler et al., 2010, Finkelstein, 2013, Harris, 2015).

Germination and dormancy

Seeds are structures designed to protect the genetic material that will establish the next generation of plants. To assure that protection plants have developed several strategies such as regulation of seed development, desiccation tolerance or regulation of germination. Despite the fact that ABA has a role in several developmental processes, its effect on seed maturation and germination are the most studied processes. Seed maturation process begins with a transition between embryo cell division arrest and embryo cellular expansion and differentiation. This transition is marked by the storage reserves accumulation in the embryo (Raz et al., 2001) which is coordinated by ABA signaling and transcriptional regulators. In this transition phase there are two peaks of ABA accumulation. The first peak occurs in the early seed maturation phase where the ABA is produced by maternal tissues and in combination with FUS3 and LEC1/2 transcription factors, prevent the premature germination (Raz et al., 2001).

Seed dormancy is an adaptive trait that delays germination until the environmental conditions are favorable to assure survival. The second ABA peak occurs in the late maturation phase and is derived from the embryo tissues (Kanno et al., 2010). These high ABA levels prevent precocious germination under non-favorable conditions. After seed dispersal, the after-ripening process prepares the dry seed to germinate after imbibition (Carrera et al., 2008). Seed imbibition activates ABA metabolism and dramatically reduces ABA levels to allow germination (Okamoto et al., 2006). At this level, crosstalk among the different hormones is necessary to integrate environmental signals. The major components implicated in dormancy are light, cold and plant hormones (Holdsworth et al., 2008). Several studies along the years concluded that the plant hormones GAs and ABA play central and antagonistic roles in

germination. While ABA is a positive regulator of dormancy, GAs release dormancy and promote germination counteracting the effects of ABA. GAs promotes proteasome-mediated degradation of the DELLA protein RGL2, that acts as a germination repressor (Golldack et al., 2013). On the other hand, ABA blocks germination by inducing the expression of seed specific transcription factors, such as members of B3-domain (ABI3), AP2 domain (ABI4) and bZIP domain (ABI5) families (Finkelstein, 2013). ABI5 causes early seedling growth arrest due to the promotion late embryogenesis abundant (LEA) genes (Lopez-Molina & Chua, 2000, Finkelstein & Lynch, 2000, Shu et al., 2016c). At the end, the balance between GAs and ABA is the responsible for the regulation of seed dormancy and germination.

Stomatal dynamics

Guard cells are specialized cells surrounding stomatal pores in the epidermis of plant leaves. Stomatal pores are essential for the CO_2 uptake required for photosynthetic carbon fixation. Movement of guard cells is therefore necessary for the regulation of gas exchange in stomata. Importantly, plants lose 95% of their water by transpiration through these structures. Guard cells are able to integrate several stimuli (hormones, light, water status, CO_2, temperature) through different signaling cascades to modulate stomatal aperture/closure. ABA is a master regulator in this process, it promotes stomatal closure and, at the same time, inhibits their aperture (Schroeder et al., 2001). ABA perception in guard cells is mediated by PYR/PYL/RCAR receptors through a kinase cascade. This pathway controls ion channels in the plasma membrane that will create an ion gradient controlling water intake by guard cells and stomata pore opening or closure (Schroeder et al., 2001, Daszkowska-Golec & Szarejko, 2013, Merilo et al., 2015). Recently, new data from

Bauer et al. (2013) indicates that guard cells possess the entire ABA biosynthetic pathway indicating that ABA is autonomously synthesized in guard cells.

Root development

It is known that ABA is essential for the regulation of root development and architecture, likely by interaction with hormones like auxins (Swarup et al., 2005, Peret et al., 2009), gibberellins (Ubeda-Tomas et al., 2009) or brassinosteroids (Hacham et al., 2011). New insights on ABA function in roots have been recently reported. ABA signaling in the root is required for the maintenance of primary root elongation and the repression of lateral root formation when water availability is reduced (Sharp et al., 2004, Deak & Malamy, 2005).

Additionally, ABA plays a major role in the regulation of hydrotropism that consists in the differential growth of the root towards a water gradient (Takahashi et al., 2002). Antoni et al. (2013) described the importance of sensing drought conditions in the root tip in order to trigger growth towards a water source. In addition, lateral roots also respond to hydrotropism although the involvement of ABA signaling in this process is still not clear (Bao et al., 2014). Moreover, gravitropic response, known as growing along the gravity vector, is also very important in roots. It is known that both processes, hydro- and gravitropic responses, are linked through the degradation of amyloplasts in seedling roots when those are hydrotropically- and water-stressed stimulated. The degradation of the amyloplasts in the columella cells lets to reduced gravitropic responsiveness and allows the roots to exhibit hydrotropism (Takahashi et al., 2003, Sharp et al., 2004, Antoni et al., 2013).

Control of flowering time

In *Arabidopsis*, flowering time is finely regulated by environmental and internal cues. It is well known in the literature that GAs promotes flowering, but recent studies pointed out the relevance of ABA signaling in suppression of the floral transition (Wang et al., 2013b). The ABA-insensitive mutants, ABA deficient 1 (*aba1*), ABA insensitive1 (*abi1-1*) and ABA insensitive 3 (*abi3-4*) mutants exhibit early flowering phenotype while hyponastic leaves (*hyl1*) mutant, an ABA hypersensitive mutant, shows delayed flowering. These phenotypes are consistent with a negative role of ABA in floral transition (Lu & Fedoroff, 2000).

Recently, it has been reported that ABA inhibits the floral transition by activating transcription of Flowering locus C (FLC) gene through ABA insensitive 4 (ABI4) binding to FLC promoter. FLC is a MADS box-containing transcription factor that acts as an integrator of developmental and environmental cues in flowering transition (Shu et al., 2016b).

Biotic stress

The signaling pathways of ABA, SA, JA and ET are known to activate different transcription factors related with defense responses, which require certain level of crosstalk (Klessig et al., 2000, Spoel & Dong, 2008, Bari & Jones, 2009, Cao et al., 2011). In general, ABA plays a multifaceted and pivotal role in disease susceptibility, resistance to pathogen infection and interaction with other biotic stress hormones. ABA is reported to play an ambivalent role in pathogen defense; it can act as a positive or negative regulator depending on the plant species, on the pathogen and on their mode of infection (Cao et al., 2011). In the early defense responses, ABA promotes stomatal closure to block the entrance of most of the pathogens and enhances the production of

reactive oxygen species (ROS) intermediates and callose deposition in the apoplast to interfere with pathogen entry (Melotto et al., 2006). However, ABA is also important for late defense responses through the modulation of crosstalk among other hormones. Thereby, ABA suppresses SA- and JA/ET-dependent responses and modulates synergistic crosstalk with JA signaling (Cao et al., 2011).

ABA-mediated gene regulation

Like most signaling transduction pathways, ABA response leads to changes in gene expression. These changes are controlled at different steps including transcription, transcript processing and transcript stability and they generally regulate genes that contribute to stress tolerance. Along evolution, plants have adopted different strategies to overcome water limitation. At cellular level, plants respond to drought with changes in gene expression and protein and metabolite abundances, which are part of the defense mechanisms (Bechtold et al., 2016).

Extensive transcriptome profiling studies have been produced in the past years. Comparison of transcriptomes of *Arabidopsis* and rice exposed to various stresses including ABA, have shown changes affecting 5-10% of the genome and more than half of them are common to drought, salinity and ABA treatments. The ABA-regulated genes in *Arabidopsis* seedlings included more than 10% of the genes (Nemhauser et al., 2006). Comparison between seeds and seedling transcriptome analysis showed that two-thirds of the ABA-induced genes in imbibed seeds are the same than in ABA-treated seedlings. Another large-scale study identified over 1000 ABA-regulated genes in guard cells, roughly 300 of which are uniquely ABA-regulated in guard cells (Wang et al., 2011).

Core signaling pathway

ABA response has been largely studied during many years but it was not until 2009 when a chemical-genetic approach and protein-protein interaction studies allowed the discovery of proteins with ABA receptor characteristics (Park et al., 2009, Ma et al., 2009, Santiago et al., 2009a, Nishimura et al., 2010). Since then, this family of ABA receptors has proved real and represents today the only reliable proteins with ABA perception function. The discovery of the ABA receptors allowed the establishment of the ABA core signaling pathway. Briefly, the ABA signaling mechanism is based on the activity of a four-component module constituted by the PYR/PYL/RCAR family of ABA receptors (Pyrabactin resistance 1 (PYR1) /PYR1-like (PYL) /regulatory components of ABA receptors (RCAR)), protein phosphatases type 2C (PP2Cs), sucrose-non fermenting 1 (SNF1)-related protein kinase 2 (SnRK2s) and the ABA responsive transcription factors (TFs). The core pathway was first reported *in vitro* using PYR1, ABI1, OST1, and ABF2 components by Fujii et al. (2009). In this work the authors used protoplasts to introduce this four components systematically resulting in ABA-responsive expression of a RD29B-LUC reporter. They also proved how mutations of the different components prevent the activation of the signaling pathway ($PYR1^{P88S}$, $ABI1^{G180D}$ and $SnRK2.6^{K50N}$). Although the core elements are sufficient to recapitulate the ABA signaling pathway, other elements, i.e. ion channels, are also part of the cellular response to ABA. The current model for ABA action in plant cells through these components is summarized in Figure 2.

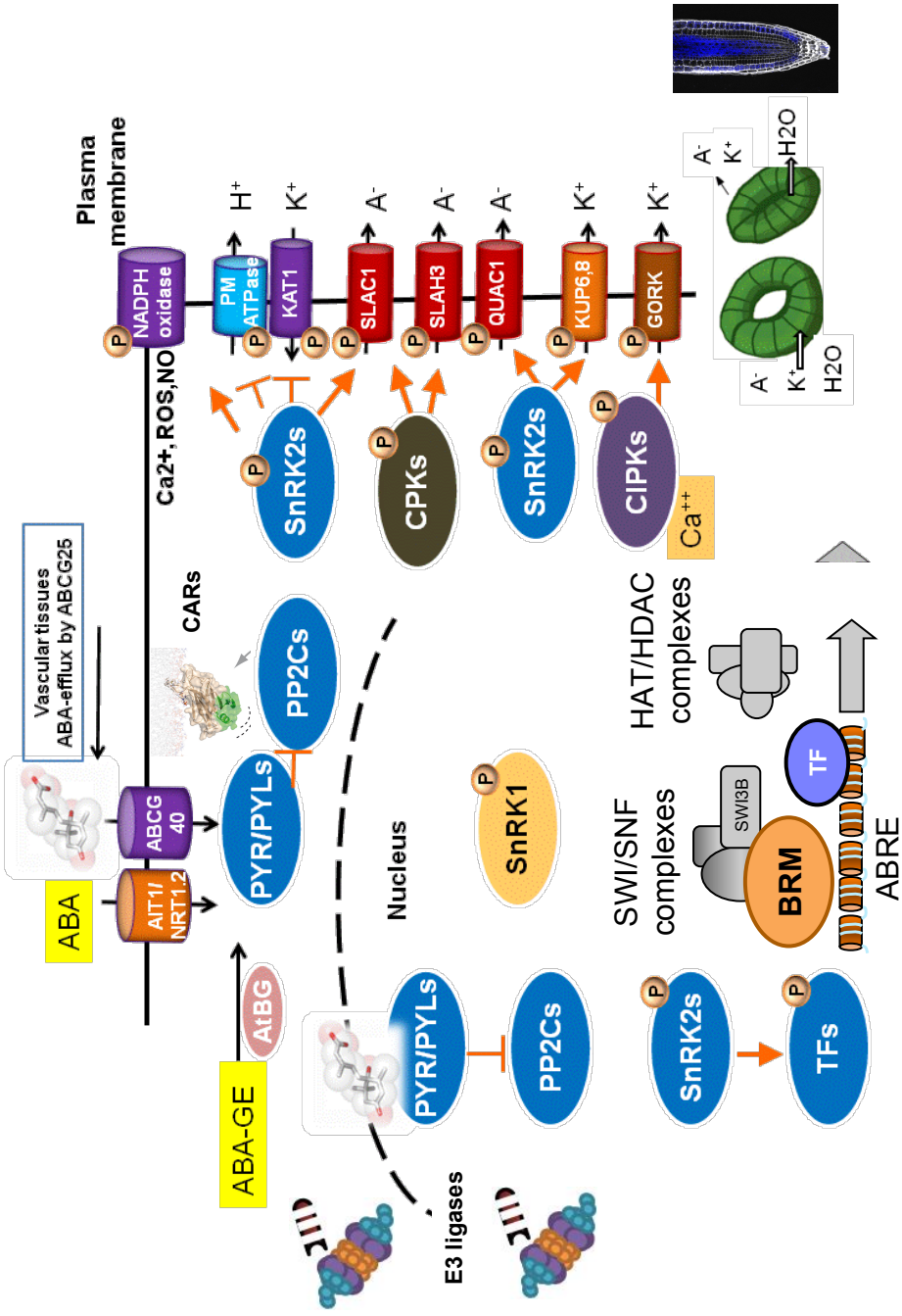

Figure 2. Overview of the ABA signaling pathway. The illustration includes the most remarkable proteins involved in the pathway and their relationship known to date. Adapted from Antoni et al. (2011).

The ABA signaling pathway is not only important at the nucleus but it also plays an essential role at the plasma membrane. When drought stress occurs, ABA level rises and plants activate the primary ABA response at the membrane level. ABA is transported through the vascular tissues and imported by AtABCGs and nitrate membrane transporters, which are responsible for the up take from the vasculature (Kuromori et al., 2010, Leran et al., 2014). When the ABA molecule is bound to the receptor, this complex recruits the PP2Cs, generating a ternary complex ABA-PYR/PYL/RCAR-PP2C, blocking the PP2C phosphatase activity. Thus the SnRK2s are released and *cis*- and *trans*-activated to phosphorylate their targets (Ma et al., 2009, Park et al., 2009, Umezawa et al., 2009, Vlad et al., 2009, Gonzalez-Guzman et al., 2012). These targets are usually integral-membrane proteins like ion channels and H^+ ATPases or enzymes associated such as NADPH oxidases. As a result, the ion and water fluxes are regulated for a fast ABA response and secondary messengers of stress like ROS, NO, Ca^{2+} are produced (Kwak et al., 2003, Mori et al., 2006, Planes et al., 2015).

Focusing now in the nuclear part of the ABA signaling pathway, ABA is also perceived by the nuclear PYR/PYL/RCAR ABA receptors. This perception mediates the recruiting of the PP2Cs in the ternary complex allowing SnRKs to phosphorylate their targets in the nucleus. The most known function of the SnRKs in the nucleus is to phosphorylate transcription factors. SnRKs-mediated phosphorylation is capable of activate/inhibit their targets as the bZIP transcription factors ABF1, ABF2/AREB1, ABI5, and the ABI3 (AP2 type TF) (Yoshida et al., 2015), but this is not the only function of the kinases.

ABA receptors

The discovery of the ABA receptors has been a long race. The first ABA binding protein discovered was Flowering time control protein A (FCA) (Razem et al., 2006). Although the protein showed some ABA-binding activity *in vitro*, this work was later retracted after the impossibility to reproduce the previous binding results (Razem et al., 2008, Risk et al., 2008). The second postulated ABA binding protein was the Chloroplastic magnesium protoporphyrin-IX chelatase H subunit (CHLH), which is a component of the Mg-chelatase, a multisubunit plastid complex related to chlorophylls biosynthesis (Shen et al., 2006). This was proposed to be the link among nuclear and chloroplast gene expression in Arabidopsis, but its function in ABA binding and signaling has not been reproduced by others suggesting that CHLH protein has not ABA-binding activity. Later, the G-protein coupled receptor-type G-proteins (GTG) 1 and 2, were proposed to bind ABA *in vitro* (Liu et al., 2007). However, contradictory results were found in the analysis of mutant phenotypes and this protein is believed as not being an ABA receptor.

One of the top breakthroughs of 2009 in plant biology was the identification of the PYR/PYL/RCAR family of ABA receptors. These receptors were identified separately by four independent research groups, Ma et al. (2009), Nishimura et al. (2010), Park et al. (2009) and Santiago et al. (2009a) its mode of action connected with well known components of ABA signaling, pointing to this family of proteins as the true ABA receptors. The discovery of the PYR/PYL/RCAR receptors by Park et al. (2009) was mediated by the use of the small molecule, pyrabactin. This compound was isolated through a phenotype-based chemical screening seeking for molecules able to inhibit germination. Mutants impaired in the ABA response, like *abi1-1*, were insensitive to pyrabactin, suggesting its role on ABA signaling. The subsequent genetic

screening lead to the identification of PYR1, as the protein responsible for pyrabactin-induced germination inhibition. Further work characterizing PYR1 showed how this protein is able not only to bind pyrabactin but also ABA, describing the family of PYR/PYL/RCAR proteins as the ABA receptors.

PYR/PYL/RCAR proteins are members of the lipid/sterol-binding STAR-related lipid transfer (START) proteins that contain a hydrophobic pocket able to accommodate diverse ligands. In *A. thaliana,* PYR/PYL/RCAR receptor family is constituted by 14 members. They can be grouped in three subfamilies based on their sequences homology as shown in the figure 3.

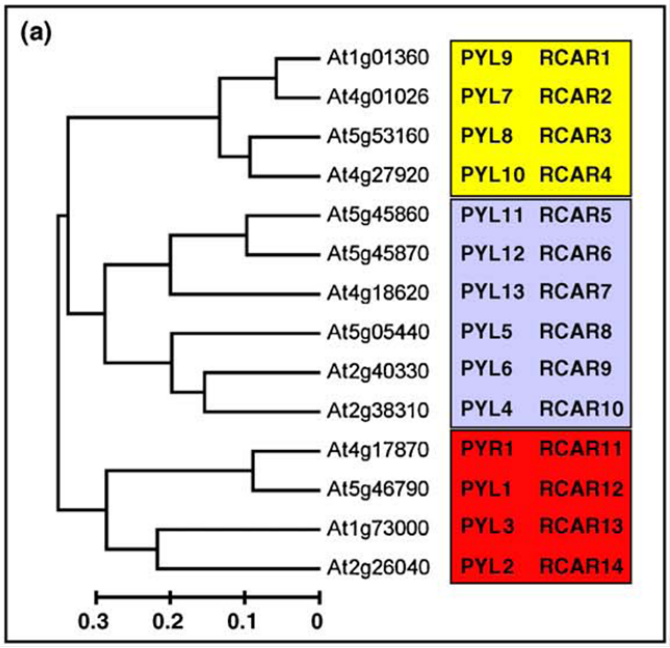

Figure 3. Phylogenetic tree for ABA receptors family in *A. thaliana*. PYR/PYL/RCAR proteins are organized in three families based on their sequences homology.

Based on their biochemical properties, PYR/PYL/RCAR receptors can be also classified in two groups based on their oligomeric state. Several experimental data indicate that PYR1, PYL1 and PYL2 receptors exist as dimers in solution; however, the receptor-PP2C complex has a 1:1 stoichiometry. This implies that receptor dimers have to dissociate before interacting with the PP2C (Nishimura et al., 2009, Santiago et al., 2009a, Yin et al., 2009). Other receptors are monomeric proteins (Dupeux et al., 2011b, Hao et al., 2011). Detailed analysis of their ABA-dissociation constant (Kd) for ABA shows that the dimeric receptors have higher Kd for ABA (> 50 μM) than the monomeric ones (1 μM). However, in the presence of clade A PP2Cs, both groups of receptors form ternary complexes with high affinity for ABA (Kd, 30 to 60 nM) (Ma et al., 2009, Santiago et al., 2009a, Santiago et al., 2009b).

The family of PYR/PYL/RCAR ABA receptors is the largest family of plant hormone receptors described to date. This implies a high level of functional redundancy among them. It also opens up some interesting questions: are they able to respond to different signals? Or, do they respond in a tissue- or developmental-specific manner? Several works have been able to address these questions. First, Antoni et al. (2013) described a unique role of PYL8 in the regulation of root growth. This work was the first describing a phenotype associated to a single mutant in the ABA receptors. Second, they showed functional redundancy in other ABA-responses and accordingly, several members of the family have to be inactivated in order to get an ABA-insensitive phenotype (Park et al., 2009, Gonzalez-Guzman et al., 2012). The redundancy among ABA receptors was analyzed in studies reported by Gonzalez-Guzman et al. (2012) where they found a quantitative regulation of stomatal aperture and transcriptional response to ABA by PYR/PYL/RCAR proteins. They analyzed the expression pattern for six of the PYR/PYL/RCAR receptors

(*PYR1, PYL1, PYL2, PYL4, PYL5* and *PYL8*) and generated a great number of multiple mutants including a sextuple knock out mutant that is "blind" to ABA. Taken together these results indicate that there is a large level of functional redundancy among ABA receptors being PYL8 the only one that has a specific role to date.

Whole-genome microarray data show low expression levels for PYL3 and PYL10-13 whereas PYL1-9 present significant expression levels (Kilian et al., 2007, Winter et al., 2007). Promoter-GUS fusion analysis including the promoters of *PYR1*, *PYL1*, *PYL2*, *PYL4*, *PYL5* and *PYL8* reveal overlapping expression in some tissues such as seeds, guard cells and roots, although some differences could also be observed (Gonzalez-Guzman et al., 2012).

In addition to biochemical, genetic and genomic data, researchers have provided very valuable information about the crystal structure of some PYR/PYL/RCAR proteins. The elucidation of the structure of the receptors showed the importance of different amino acids, both for ligand binding and for the formation of the ternary complex with the PP2Cs. ABA binds to a hydrophobic cavity in the ABA PYR/PYL/RCAR receptors (Melcher et al., 2009, Miyazono et al., 2009, Nishimura et al., 2009, Yin et al., 2009). This binding induces a conformational change in two loops of the protein, named as gate and latch. When closed, the surface of the loops creates a favorable platform necessary for the interaction with PP2Cs (Melcher et al., 2009, Dupeux et al., 2011a). Additionally, after the ternary complex PYR/PYL/RCAR–ABA–PP2C is generated some residues of the receptor establish contacts with important residues of the PP2C active site, leading to the inhibition of the phophatase (Figure 4) (Miyazono et al., 2009, Dupeux et al., 2011b, Yin et al., 2009, Melcher et al., 2009). The elucidation of the PYR/PYL/RCAR receptors in complex

with ABA and PP2Cs also has illuminated the way to develop more receptors with increased activity by directed mutagenesis into important residues of the ABA binding pocket and the receptor–PP2C interactions surface. X-ray structures have also allowed the structure-guided design of small molecules with antagonistic and agonistic activities (Okamoto et al., 2013). Thus, the atomic resolution of the ABA receptor protein structures has been an important step to understand ABA signaling which might have implications in agriculture.

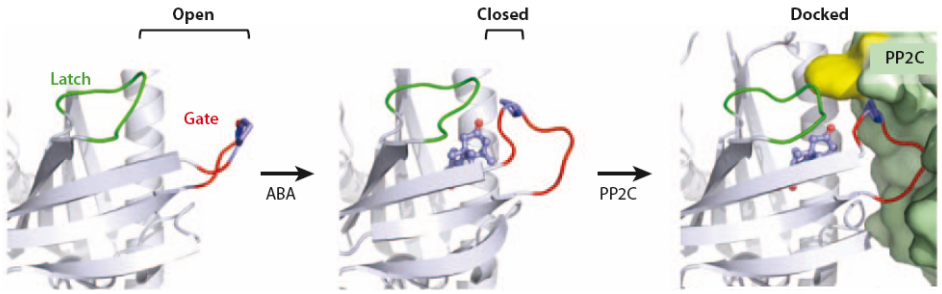

Figure 4. Structural representation for the ternary complex generated by the interaction of Receptor–ABA–Phosphatase (PYR1–ABA–HAB1). Reprinted from Cutler et al. (2010).

PYR/PYL/RCAR ABA receptors in *Solanum lycopersicum*

Arabidopsis thaliana PYR/PYL/RCAR receptors have been largely studied and their implications on drought tolerance are known. Consequently, the basal knowledge of *Arabidopsis* has to be transferred into crops in order to improve their agricultural traits. Since the discovery of *Arabidopsis* PYR/PYL/RCAR receptors, several orthologous genes had been discovered in important crops as tomato, rice, strawberry and soybean (Sun et al., 2011, Chai et al., 2011, Kim et al., 2012, Bai et al.,

2013). Deeper characterization of tomato PYR/PYL/RCAR receptors was done by Gonzalez-Guzman et al. (2014). Tomato PYR/PYL/RCARs are highly expressed in roots and present differential sensitivity to quinabactin, a synthetic agonist of ABA receptors (Okamoto et al., 2013). Quinabactin mimics the effects of ABA in the ligand-dependent activation of a subset of PYR/PYL/RCAR receptors. Based on Gonzalez-Guzman et al. (2014) studies, there are 15 putative tomato PYR/PYL/RCAR receptors. They could be grouped in 3 subfamilies correlated with *Arabidopsis* orthologous (Figure 5). Subfamily I includes two tomato receptors that are closely related to AtPYL1/PYR1 representing putative dimeric receptors. Subfamily II includes six tomato receptors related with AtPYL4/PYL5/PYL6 and in the subfamily III, four tomato receptors were related with AtPYL7/PYL8/PYL9/PYL10. Tomato receptors are very similar to their *Arabidopsis* counterparts in their amino acid sequence. Importantly, overexpression of tomato ABA receptors in *Arabidopsis* plants increases the sensitivity to ABA and enhances plant drought tolerance.

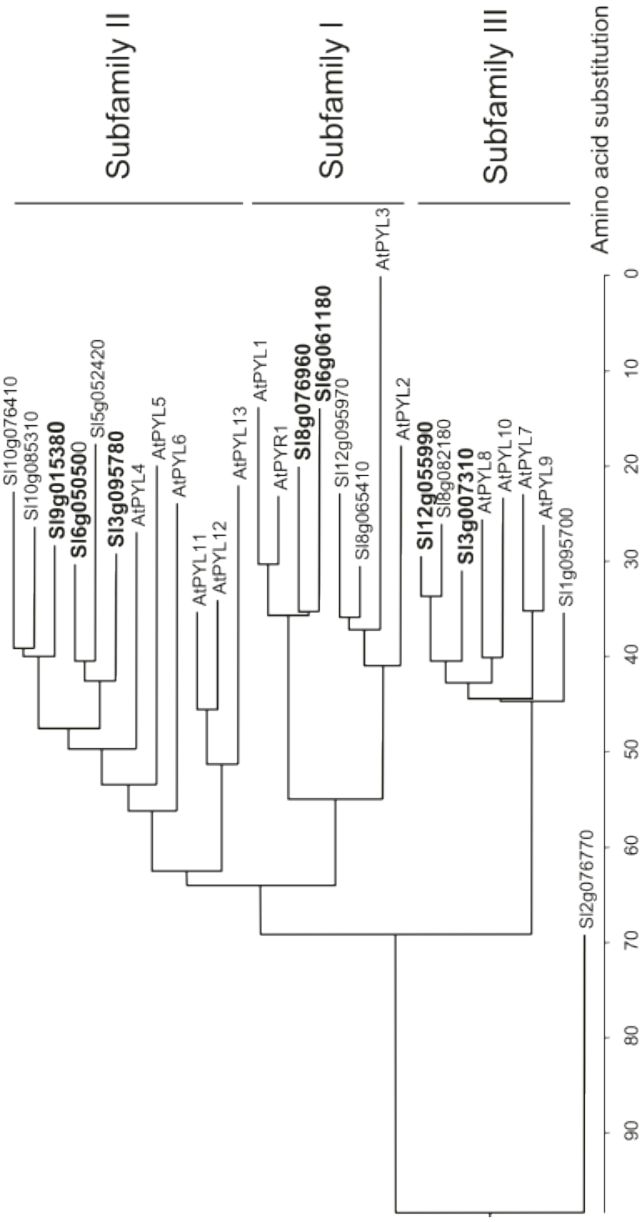

Figure 5. Cladogram of tomato PYR/PYL/RCAR ABA receptors. Cladogram of the multiple sequence alignment of tomato and *A. thaliana* PYR/PYL/RCAR receptors. Three major subfamilies can be distinguished from the similarity analysis. Reprinted from Gonzalez-Guzman et al. (2014).

Next step of the ABA signaling pathway rely on the protein phosphatases.

Protein Phosphatases type 2C, PP2Cs

Protein phosphatases are enzymes that remove a phosphate group from a phosphorylated amino acid. Plant protein phosphatases are divided in three groups depending on their substrate specificity: Serine/Threonine (Ser/Thr), Tyrosine (Tyr) and dual-specificity classes. Depending on their features, plant Ser/Thr phosphatases can be organized in PP1, PP2A and PP2C groups (Luan, 2003). The expansion of the family of PP2C proteins found in the *Arabidopsis* genome, which has 76 putative proteins, many of them without known function, organized in ten clades from A to J (Schweighofer et al., 2004), contrasts with the no more than 15 PP2Cs are found in the human genome (Cheng et al., 2000) and only 6 found in the yeast genome (Stark, 1996) which highlights the importance of the PP2C class of protein phosphatases in plants.

A genetic screening focused on the isolation of ABA insensitive mutants involved in ABA signaling (Koornneef et al., 1984) identified the first PP2C, it was the *abi1-1* mutant. Ten years later, ABA-insensitive 1 (ABI1) was identified by map-based cloning (Meyer et al., 1994, Leung et al., 1994). ABI1 belongs to the clade A subfamily of PP2Cs. This clade is divided in two separate branches based on amino acid sequence alignments (Schweighofer et al., 2004) (Figure 6). ABI1, ABI2, hypersensitive to ABA 1 (HAB1) and HAB2 are grouped in the same branch, whereas the second branch is formed by ABA-hypersensitive germination 1 (AHG1), AHG3/PP2CA and highly ABA inducible 1 (HAI1), HAI2 and HAI3.

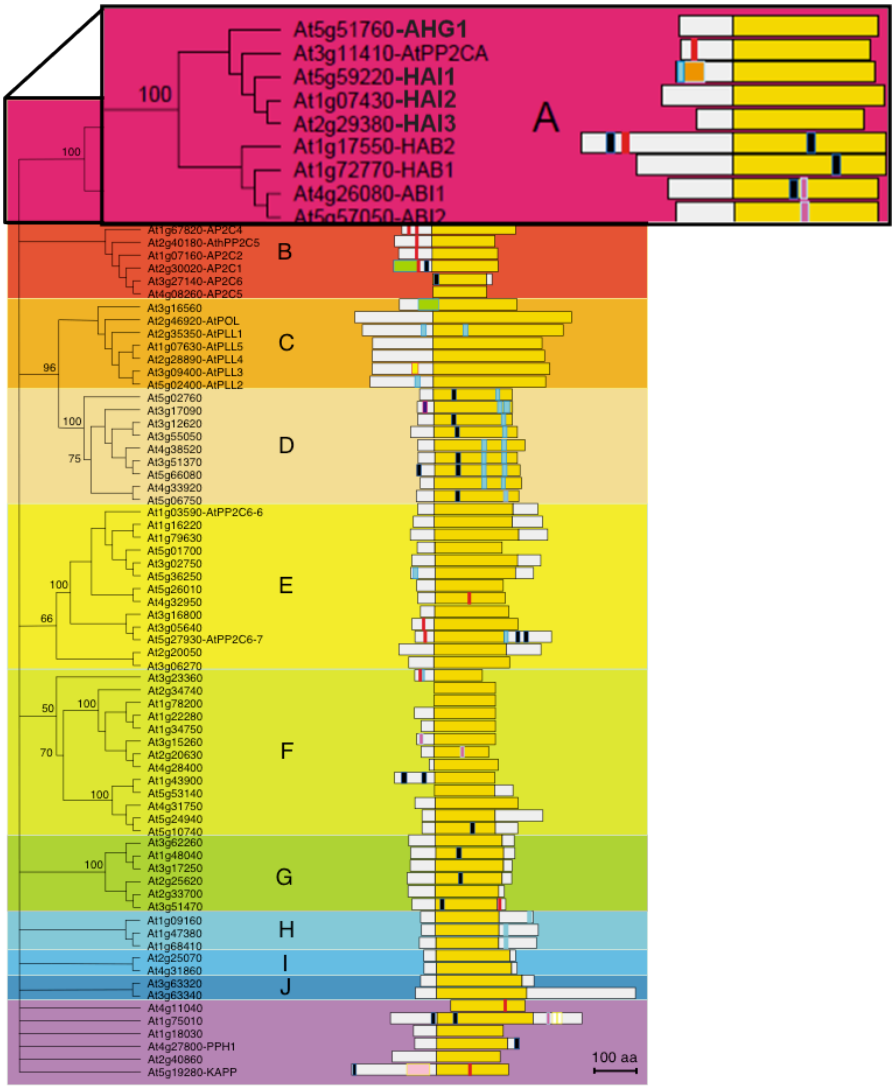

Figure 6. Topographic cladogram and domain structure based on amino acid sequence alignment of *A. thaliana* type-2C protein phosphatases (PP2Cs). The highlighted pink box is emphasizing clade A subfamily of phosphatases. Adapted from Schweighofer et al. (2004).

A second ABA-insensitive mutant, *abi2-1*, was also identified by Koornneef et al. (1984) and the locus was cloned by Leung et al. (1997) and Rodriguez et al. (1998). Both mutants, *abi1-1* and *abi2-1,* encode for

abi1^{G180D} and abi2^{G168D} proteins that display equivalent mutations in their catalytic domains (conserved Gly, G residue to Asp, A), which causes a diminished phosphatase activity in the absence of ABA as compared to wild-type (Santiago et al., 2012). These hypermorphic mutations reduce ABA responses and lead to strong insensitivity to ABA in seed germination, root growth, stomatal regulation and gene expression responses (Meyer et al., 1994, Leung et al., 1994, Leung et al., 1997, Rodriguez et al., 1998, Gosti et al., 1999). The characterization of some of the single loss-of-function mutants, *hab1-1*, *abi1-2*, *abi2-2,* showed they were weak ABA-hypersensitive, but the combination of double or triple PP2C loss-of-function showed an elevated ABA-hypersensitivity. This reflects the partial overlapping functions between them and confirmed the negative role of clade A protein phosphatases in ABA signaling (Gosti et al., 1999, Kuhn et al., 2006, Yoshida et al., 2006, Nishimura et al., 2007, Rubio et al., 2009).

Another important structural feature of PP2Cs is the presence of a critic tryptophan residue (Trp, W) (W300A in ABI1 and W385A in HAB1) in the active site that is essential for the ABA-dependent inactivation of the phosphatase by PYR/PYLs. However, these mutants are able to interact with their downstream targets such as SnRKs (Dupeux et al., 2011a). These data provided key structural support to understand the formation of the ternary complex between PYR/PYL-ABA-PP2C (Figure 7), which is required for fully inhibition of the PP2C activity (Miyazono et al., 2009, Dupeux et al., 2011a, Santiago et al., 2012).

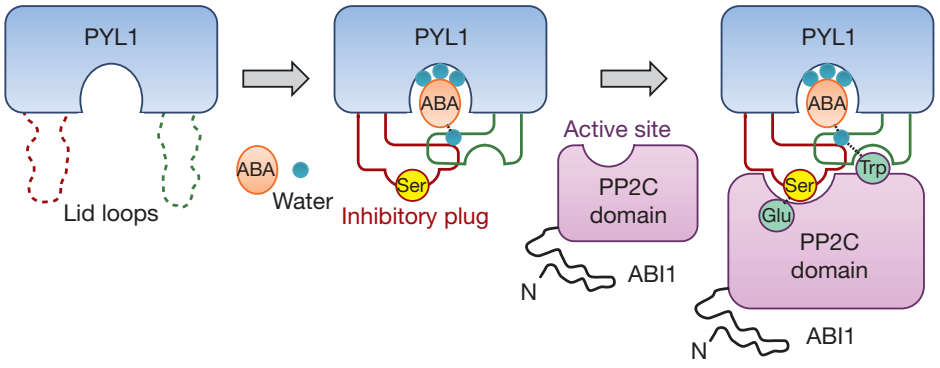

Figure 7. Model of ABA-induced phosphatase regulation by the receptors. The example in the figure represents PYL1 inhibition of ABI1 upon ABA sensing. The picture shows some of the important residues implicated in the main interactions for the ternary complex formation. Gate loop (red) and latch loop (green). Reprinted from Miyazono et al. (2009).

In addition to the redundant functions presented by clade A PP2Cs family, it is important to mention that at the same time, they have specific roles controlling the ABA signaling pathway. Subcellular localization studies indicate that PP2Cs are present at the nucleus and cytosol, which is in agreement with their reported interaction with SnRK2s (Fujita et al., 2009). In addition to dephosphorylation of SnRK2s (Umezawa et al., 2009, Vlad et al., 2009), additional targets of clade A PP2Cs have been described, such as SnRK1, SnRK3s/calcineurin B-like (CBL)-interacting protein kinases (CIPKs), calcium-dependent protein kinases (CDPKs/CPKs), ion transporters such as the K^+ channel AKT1 and AKT2 or the slow anion channel 1 (SLAC1) and SLAC1 homolog 3 (SLAH3), and transcriptional regulators, such as bZIP transcription factors and chromatin-remodeling complexes (SWI2/SNF2) (Cherel et al., 2002, Guo et al., 2002, Lee et al., 2007, Saez et al., 2008, Geiger et al., 2009, Lee

et al., 2009, Antoni et al., 2012, Brandt et al., 2012, Lynch et al., 2012, Pizzio et al., 2013, Rodrigues et al., 2013).

Although a major portion of PP2Cs is localized in the cytosol, the presence of PP2Cs is also detected in microsomal membranes, where two PP2C-interacting proteins are localized (i.e. AKT2 and SLAC1) (Cherel et al., 2002). Interestingly, a minor portion of PP2Cs co-localize with the nuclear insoluble fraction (chromatin associated), in agreement with the reported interaction of HAB1 with SWI3B, a putative component of chromatin-remodeling complexes (Saez et al., 2008).

PP2CA/AHG3

PP2CA was originally cloned by Kuromori and Yamamoto (1994). Transient-assay experiments using protoplasts and studies with antisense genes implicated PP2CA in ABA signaling as a negative regulator (Sheen, 1998, Tahtiharju & Palva, 2001). PP2CA was found to be expressed ubiquitously in plant organs with the highest transcript levels taking place in leaf tissue. However extended expression analyses showed that *PP2CA* is up-regulated by several stresses, including ABA, cold, drought, and salt treatment (Tahtiharju & Palva, 2001, Cherel et al., 2002). Later on the *pp2ca/ahg3* mutant was isolated in a screening for mutants with enhanced sensitivity to ABA (Nishimura et al., 2004). In this study, seven putative *Arabidopsis* mutants were isolated and named as ABA-hypersensitive germination (*ahg*). After map-based cloning, *ahg3* was confirmed to have a mutation in AT3G11410 gene corresponding to PP2CA (Yoshida et al., 2006). Analysis of those knock out mutants on the ABA response during germination indicates an ABA-hypersensitive phenotype. Interestingly, *ahg3/pp2ca* had the strongest effect indicating a major role of AHG3/PP2CA during seed germination and early growth.

pp2ca-1 also shows moderate ABA-hypersensitivity in root tissue that indicates a partial redundancy with other PP2Cs. Conversely, overexpression of *PP2CA* showed an ABA-insensitive phenotype in seed germination and the regulation of stomatal closure (Kuhn et al., 2006, Yoshida et al., 2006). All these data together indicate that PP2CA has a strong negative role in the regulation of ABA signal transduction during seed germination, but it is also involved in other processes (Kuhn et al., 2006, Yoshida et al., 2006).

ABA controls K^+ and other ion channels. PP2CA was found to interact and inhibit AKT2 (Cherel et al., 2002) and SLAC1, which is very important ion channel for stomatal closure regulation. PP2CA inhibits SLAC1 channel activity in two ways, due to direct interaction with SLAC and by dephosphorylation of the kinase OST1 leading to kinase-dependent phosphorylation inhibition (Lee et al., 2009). Another study trying to elucidate implications of PP2CA in ABA signaling pathway came from Pizzio et al. (2013). This work generated an allele library composed of 10,000 mutant clones of *Arabidopsis* PYL4 receptor where mutations that promoted ABA-independent interaction with PP2CA/AHG3 were selected. $PYL4^{A194T}$ mutant selected because was able to form stable complexes with PP2CA in the absence of ABA, in contrast to wt PYL4. This interaction did not lead to significant inhibition of PP2CA in the absence of ABA; however, it improved ABA-dependent inhibition of PP2CA.

PP2CA and ABI1 were also found to be related to energetic stress (Rodrigues et al., 2013). PP2CA negatively regulates SnRK1 that is a heterotrimeric complex composed of an α-catalytic subunit (SnRK1.1/1.2/1.3 in *Arabidopsis*) and two regulatory subunits, β and γ. In this study, ABI1 and PP2CA inhibited SnRK1 by dephosphorylation.

Accordingly, double and quadruple *pp2c* knockout mutants are sugar hypersensitive because of their failure in the repression of SnRK1, similarly to SnRK1 overexpression. They also demonstrate that ABA presence inactivates PP2CA and results in an activation of SnRK1, which promotes SnRK1 signaling during energetic stress. Hence, the PP2Cs generate a hub that allows a coordinated activation of ABA and energy signaling, strengthening the stress response through the cooperation of two key and complementary pathways.

PP2C dephosphorylation of key components of ABA signaling has been largely studied but the regulation of the stability of PP2Cs has been described only lately. Recent works by Kong et al. (2015) and Wu et al. (2016) describe the putative pathways for PP2Cs degradation. Kong et al. (2015) discovered a degradation pathway that includes U-box E3 ligases (PUB12/13) that ubiquitylate ABI1 only when ABI1 is interacting with the ABA receptor. This suggests that under stress conditions, ABI1 would be ubiquitylated and degraded to enhance ABA response. Wu et al. (2016) discovered another family of E3 ubiquitin ligases, RGLGs, implicated in PP2Cs degradation. Particularly, RGLG1/5 mediate ABA-dependent ubiquitylation of PP2CA, which promotes degradation in the proteasome.

SNF1-related protein kinases2, SnRK2s

Although phosphatases are very important proteins in the ABA signaling, they are negative regulators. This suggests that there must be kinases that act in opposition to them as positive regulators in the signaling. The *Arabidopsis* genome codifies for 38 SnRKs related with the SNF1 (Sucrose non-fermenting-1) kinases of yeast. They can be organized in three groups, SnRK1, SnRK2 and SnRK3 depending on their sequence similarity and domain structure (Hrabak et al., 2003). The SnRK1 and SnRK2 subfamilies are calcium-independent kinases whereas SnRK3s are calcium dependent and interact with a calcium sensor, calcineurin B-like (CBL), thus these proteins are also known as CBL-interacting protein kinases (CIPKs).

The group of SnRK2 in *Arabidopsis* is formed by 10 members named from SnRK2.1 to SnRK2.10 (Hrabak et al., 2003) (Figure 8). They are classified into three subclasses: subclass 1, activated by osmotic stress but not ABA, subclass 2, activated by osmotic stress and weakly by ABA and the subclass 3 that are activated by both ABA and osmotic stress. In this group, subclass 3, is represented by SnRK2.2/SnRK2D, SnRK2.3/SnRK2I and SnRK2.6/SnRK2E/OST1, which are activated by ABA (Boudsocq et al., 2004). OST1/SnRK2.6 was first identified in a genetic screening using thermal imagining to detect mutants with defective stomatal closure on drought stressed plants (Merlot et al., 2002). This mutant showed reduced ABA responsiveness in guard cells suggesting that OST1 has a positive role in ABA signaling in stomata (Yoshida et al., 2002, Mustilli et al., 2002). However, although ABA does not induce OST1/SnRK6 gene expression, it stimulates the kinase activity (Yoshida et al., 2002, Mustilli et al., 2002). Genetic evidence showed that SnRK2.6 is expressed to high levels in guard cells but to low levels in other tissues, which explains why *ost1/ snrk2.6* single mutant

was impaired only in ABA-mediated stomatal closure and not other ABA responses. SnRK2.2 and SnRK2.3 were also identified later on as positive regulators of the ABA signaling pathway (Fujii et al., 2007). Although the *snrk2.2* and *snrk2.3* single mutants showed no differences in ABA sensitivity compared to the wild type, their combination in the *snrk2.2snrk2.3* double mutant let to a high ABA-insensitive phenotype in germination, dormancy and seedling growth assays (Fujii et al., 2007). This indicates a tissue-specific specialization of this group of kinases being SnRK2.6 very important regulating stomata closure and SnRK2.2 and SnRK2.3 having also roles in other organs. Interestingly, the *snrk2.2/2.3/2.6* triple mutant shows extreme ABA-insensitivity, which suggests that these three ABA-activated SnRKs play a major role in ABA signaling. Thus, this triple mutant showed dramatic insensitivity to ABA in stomatal closure, germination, shoot and root growth, ABA regulation of gene expression and water loss (Fujii & Zhu, 2009). This phenotype established that SnRK2s are the core positive regulators of ABA signaling (Yoshida et al., 2002, Fujii & Zhu, 2009, Fujita et al., 2009, Nakashima et al., 2009). The isolation and characterization of a decuple mutant affected in all 10 SnRK2s indicated that other SnRK2s have a more specific role controlling adaptation to osmotic stress (Fujii et al., 2011).

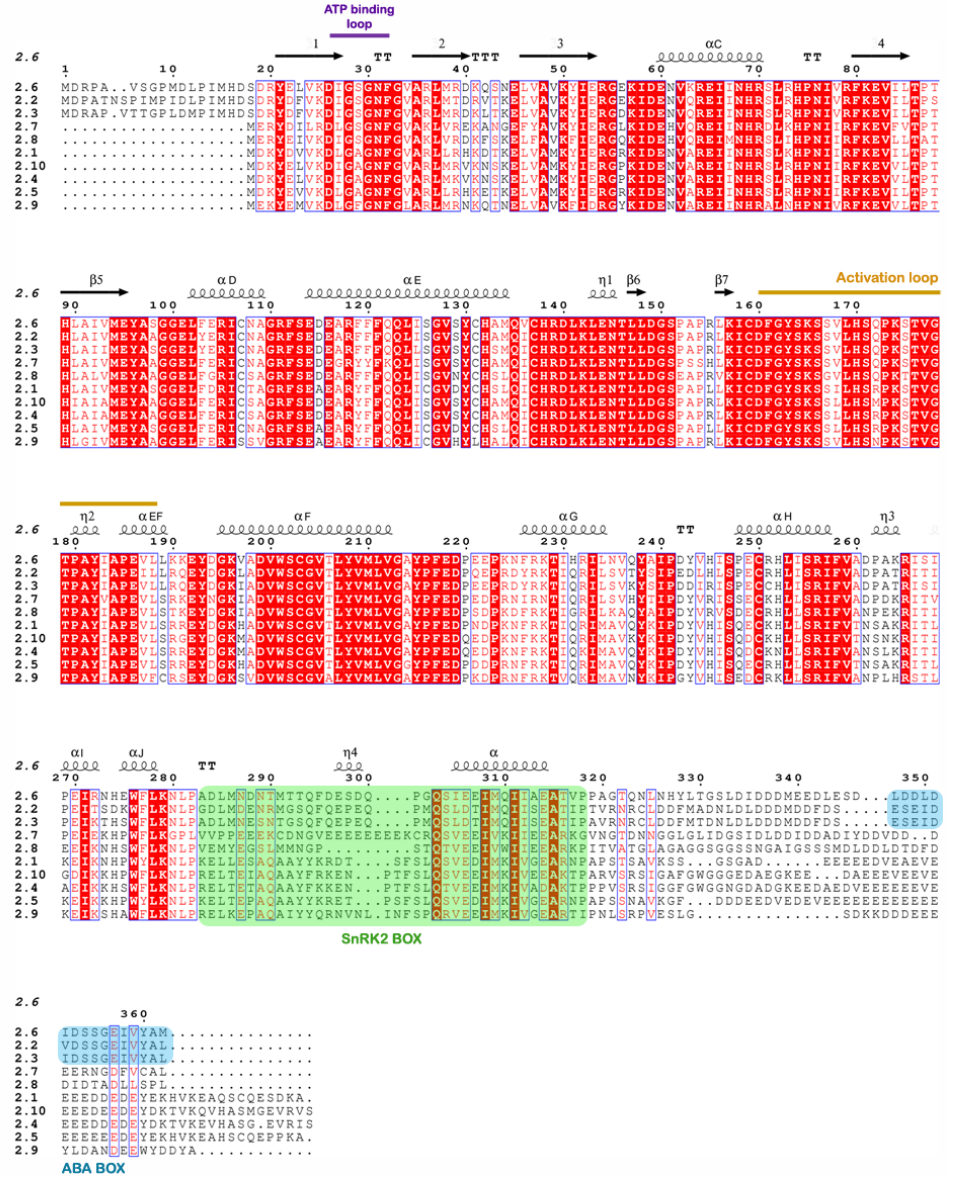

Figure 8. Sequence alignment of the ten SnRK2s of *Arabidopsis* based on SnRK2.6/OST1 structure. All ten kinases present a conserved C-terminal domain called SnRK-box (green) responsible of the activation of all SnRK2 kinases under osmotic stress. In addition to this domain, the three kinases ABA activated posses a specific region at the C-terminus called ABA-box (blue),

whereby the kinases interact with the PP2Cs and responsible of the ABA-dependent activation of these ABA kinases.

Structurally, SnRK2 family contains a highly conserved kinase domain in N-terminal and a variable regulatory domain in C-terminal. This regulatory domain is divided in two subdomains, subdomain I is conserved in all the SnRK2s and subdomain II, conserved only in the ABA-regulated SnRK2 kinases. This subdomain II is responsible for their differential activation by ABA and for the interaction with clade A PP2Cs (Yoshida et al., 2006, Yoshida et al., 2010). Biochemically, SnRK2s are activated through the phosphorylation of Ser/Thr residues of their conserved activation loop. In the absence of ABA, PP2Cs interact with the subclass 3 SnRK2 kinases leading to the dephosphorylation of the activation loop (Yoshida et al., 2006, Ma et al., 2009, Park et al., 2009, Vlad et al., 2009, Umezawa et al., 2009, Soon et al., 2012). In the presence of ABA, PYR/PYL/RCAR receptors bind to PP2Cs and inhibit them. This allows SnRK2.6 to autophosphorylate certain Ser of their activation loop and to de-repress the ABA signaling pathway through direct phosphorylation of downstream targets (Fujii et al., 2009, Umezawa et al., 2009, Vlad et al., 2009, Vlad et al., 2010). SnRK2.2 and 2.3 seem to be trans-phosphorylated by SnRK2.6 or by yet unidentified kinases. Clade A PP2Cs also regulates other SnRKs, for instance, Rodrigues et al. (2013) showed that stress generated by energy deprivation activates the SNF1-related protein kinase 1 (SnRK1), which was found to be dephosphorylated and inactivated by ABI1 and PP2CA. This work shows that PP2Cs can act as a hub to coordinate the activation of ABA and energy signaling pathways.

After SnRK2 *cis*- and *trans*-activation, they phosphorylate their downstream targets in order to fully activate the ABA response. Several proteins have been identified as substrates of the SnRK2s. Those include basic-region leucine zipper (bZIP) transcription factors, ion channels as the slow anion channel 1 (SLAC1), the R-type ion channel/QUAC1 and aquaporins (Geiger et al., 2009, Meyer et al., 2010, Imes et al., 2013, Grondin et al., 2015) that are critical factors involved in ABA regulation of stomatal movement. NADPH oxidases are also phosphorylated by SnRK2.6 to activate reactive oxygen species (ROS) production in guard cells (Sirichandra et al., 2009). Also, SnRKs can phosphorylate their targets to inactivate them as is the case of the plasma membrane ATPase and the potassium channel, KAT1 (Planes et al., 2015, Sato et al., 2009). All these targets are responsible of keeping the cellular homeostasis controlled in order to close the stomata and avoid water loss.

Recent quantitative *in vivo* phosphoproteomic studies revealed numerous targets of SnRKs, which have important roles in RNA processing, epigenetic modifications, chloroplast processes and control of flowering time (Wang et al., 2013a, Umezawa et al., 2013). In these phosphoproteomic studies, the analysis of the triple *snrk2.2/2.3/2.6* mutant revealed that several chromatin regulators including SWI/SNF BRM ATPase were putative substrates of the SnRK2 kinases. However, direct biochemical evidence was lacking in these studies.

Transcription factors in ABA signaling

In biology, a transcription factor is a protein that can bind to specific sequences of DNA to regulate gene expression. ABA-regulated gene expression is directly controlled by transcription factors that bind to specific regions in the DNA. Promoter analysis of ABA-inducible genes identified the ABA-responsive element (ABRE; PyACGTGG/TC) as a conserved *cis*-element. Yeast one-hybrid screening using ABREs as a bait identify a group of bZIP transcription factors designated as ABRE-binding proteins (AREBs) or ABRE-binding factors (ABFs) (Uno et al., 2000, Choi et al., 2000). Among the nine members of AREB/ABFs family in *Arabidopsis* (Yoshida et al., 2010), AREB1/ABF2, AREB2/ ABF4 and ABF3 are highly induced by ABA and osmotic stress treatments in vegetative tissues (Choi et al., 2000, Uno et al., 2000, Fujita et al., 2005, Yoshida et al., 2010). Large-scale transcriptome analysis of the *areb1 areb2 abf3 abf1* quadruple mutant revealed that a majority of downstream genes of SnRK2.2/2.3/2.6 are directly and indirectly regulated by the four AREB/ABFs (Yoshida et al., 2015).

The bZIP TFs have been functionally characterized and are grouped in two subfamilies depending on their expression in the plant (Figure 9). ABI5/Dc3 promoter-binding factor (AtDPBF) subfamily genes are mainly expressed in seeds and during germination and seed maturation, whereas AREB/ABF subfamily genes are mainly expressed in vegetative tissues under abiotic stress conditions (Fujita et al., 2013).

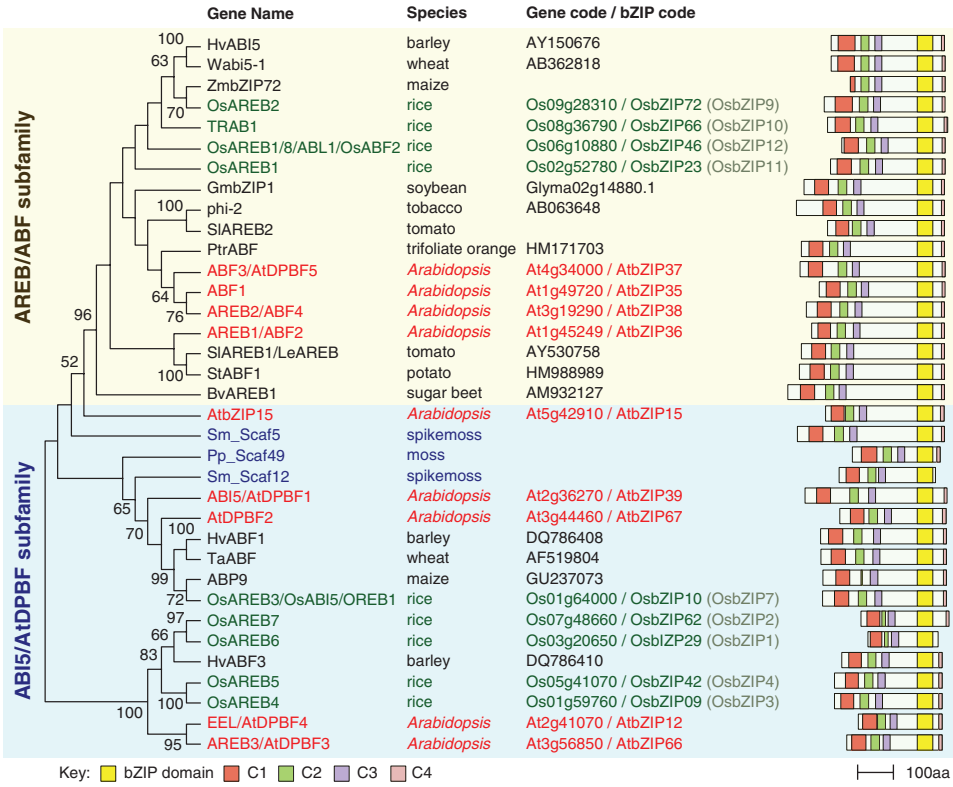

Figure 9. Phylogenetic tree and domain structure of bZIP TFs of AREB/ABF and ABI5/AtDPBF subfamilies. bZIP TFs in *Arabidopsis,* rice, bryophytes and other species of vascular plants are shown in red, green, blue and black letters, respectively (Fujita et al., 2013).

ABRE elements have been shown to play a central role in regulation of ABA-mediated gene expression in stress response (Fujita et al., 2011, Fujita et al., 2013). Besides the ABREs, there are other regulatory regions recognized by different ABA-related transcription factors. Some genes contain GC-rich sequences as the drought response elements (DRE) recognized by the Apetala2 (AP2) family of transcription factors including ABI4 (Finkelstein et al., 1998, Liu et al., 1998). Other ABA-

responsive genes display W-box sequence in their promoter regions for the binding of WRKY transcription factors as WRKY63 and WRKY40 (Ren et al., 2010, Shang et al., 2010) and other regions as the RY/Sph elements recognized by different transcription factors that are bonded by B3 domain proteins as ABI3 (Ezcurra et al., 2000) or MYC2 and MYB2 that are bHLH- and MYB-related transcription factor, respectively (Abe et al., 2003) that are also implicated in ABA signaling.

Transcriptional activity of AREB/ABF TFs requires its ABA-dependent activation by phosphorylation of multiple conserved RXXS/T sites, which is mediated by ABA-activated SnRK2s (Fujii et al., 2007, Yoshida et al., 2010, Fujita et al., 2013). On the other hand, it was also found that AREB/ABFs are direct targets of the clade A PP2Cs (Lynch et al., 2012). This highlights the importance of the phosphorylation regulatory mechanism in the activation/deactivation of the ABA transduction pathway when plants are challenged by water deficit. The first bZIP TF identified and characterized was ABA-insensitive 5 (ABI5) (Finkelstein, 1994, Finkelstein & Lynch, 2000). ABI5 binds to ABREs in the promoters of ABA-responsive genes and activates gene expression (Finkelstein & Lynch, 2000, Lopez-Molina & Chua, 2000). The analysis of *abi5* loss-of-function mutant revealed its key role as a positive regulator of ABA signaling during seed development, maturation, germination and early seedling growth (Lopez-Molina et al., 2002, Lopez-Molina & Chua, 2000, Finkelstein et al., 2002, Lopez-Molina et al., 2001). Post-germination developmental checkpoint is controlled by ABA and it is known that ABI5 expression is induced in this process (Lopez-Molina et al., 2001). In addition, the expression level of *ABI5* is severely reduced in the *snrk2.2snrk2.3snrk2.6* triple mutant at different stages suggesting that these kinases also regulate ABI5 (Nakashima *et al.,* 2009). Other AREB/ABFs with partly redundant functions, such as AREB1/ABF2,

AREB2/ABF4, ABF3 and ABF1 were characterized as positive regulators of ABA signaling in vegetative tissues (Fujita et al., 2005, Yoshida et al., 2010, Yoshida et al., 2015).

In addition to *abi5*, other ABA-insensitive mutants, *abi3* and *abi4*, were identified in genetic screenings performed in seeds (Koornneef et al., 1984, Finkelstein, 1994, Finkelstein et al., 1998). Cloning of the corresponding loci revealed the TFs ABI3 and ABI4, which belong to the B3 and AP2 transcription factor families, respectively, play important roles in seed germination and early seedling establishment (Parcy et al., 1994, Finkelstein et al., 1998). ABI4 expression was think to be restricted to seed development and early germination stages (Finkelstein et al., 1998). At these stages, ABI4 was shown to be involved in glucose signaling, sugar signaling and response pathways, ABA signaling and lipid mobilization in the embryo and germinated seeds as well as in chloroplast functioning and retrograde signaling. *abi4* loss-of-function mutants are insensitive to ABA (Soderman et al., 2000) but also display reduced sugar sensitivity (Huijser et al., 2000), sucrose insensitivity (Laby et al., 2000) and glucose insensitivity (Arenas-Huertero et al., 2000). ABI4, is a very versatile TF that fulfills other important roles in the regulation of plant development, such as glucose responses (Arenas-Huertero et al., 2000), nitrate-modulated root branching (Signora et al., 2001) and chloroplast-to-nucleus retrograde signaling pathways (Kaliff et al., 2007, Koussevitzky et al., 2007) and also, mitochondria-to-nucleus retrograde signaling pathways (Giraud et al., 2009). Recent studies have shown that ABI4 integrates redox, sucrose, ABA and JA signaling (Kerchev et al., 2011). Furthermore, the ABI4 protein binds to *cis*-acting elements mediating both sugar- and ABA-inducible gene expression (Bossi et al., 2009, Reeves et al., 2011).

The expression levels of ABI3, ABI4, and ABI5 during the plant life cycle show they are tightly co-expressed. All three genes are expressed through seed development, reaching their highest transcript levels at seed maturity, but decreasing during germination unless they are exposed to stresses that inhibit maturation such as ABA or dehydrating conditions (Wind et al., 2013, Finkelstein et al., 2011). A recent study shows that ABA induces transcription of *ABI4* and ABI4 protein stabilization (Shu et al., 2016a).

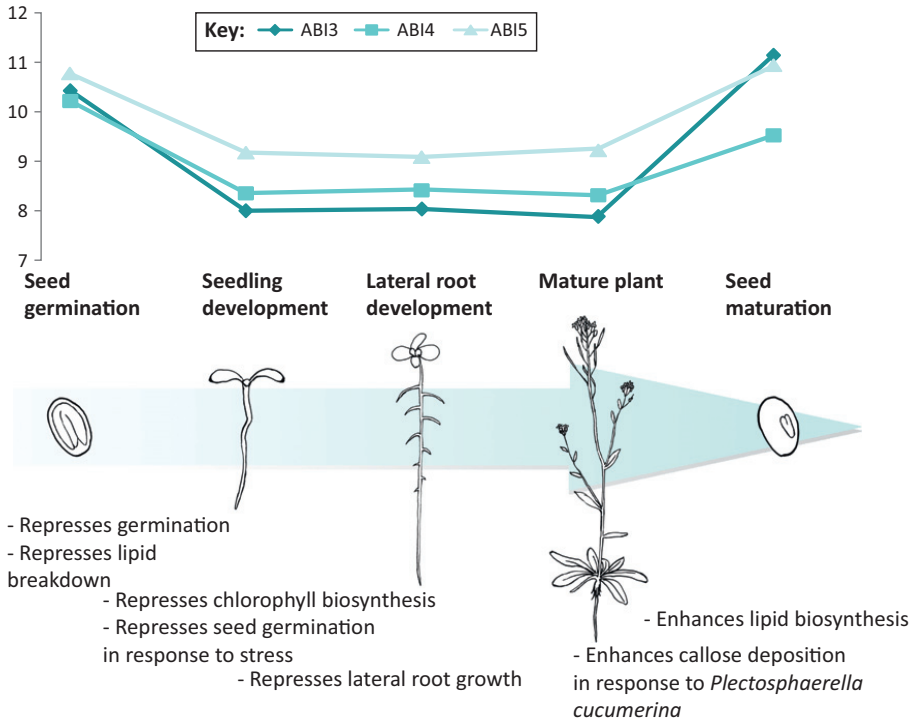

Figure 10. Expression levels of ABI3, ABI4, and ABI5 during the plant life cycle (Wind et al., 2013). Expression of these ABA-insensitive mutants shows a peak in germination and the levels are kept low until seed maturation when they accumulate again.

Chromatin remodeling and ABA signaling

Eukaryotic cells have developed a highly organized structure called chromatin to compact the genomic DNA. This packaging allows the cell to have large amount of DNA in a small space in the nuclei. The nucleosome is the basic structural unit of chromatin in eukaryotic cells. A nucleosome consists in a DNA sequence of approximately 147 bp wrapped around a core structure formed by eight histone proteins called histone octamer. The octamer is composed by two H2A-H2B dimers and one H3-H4 tetramer. Each nucleosome is connected to the next by a linker DNA of approximately 20-90 bp depending on the species and tissues (Szerlong & Hansen, 2011). Thus, nucleosomes function is to compact and restrict the access to DNA in the nucleus.

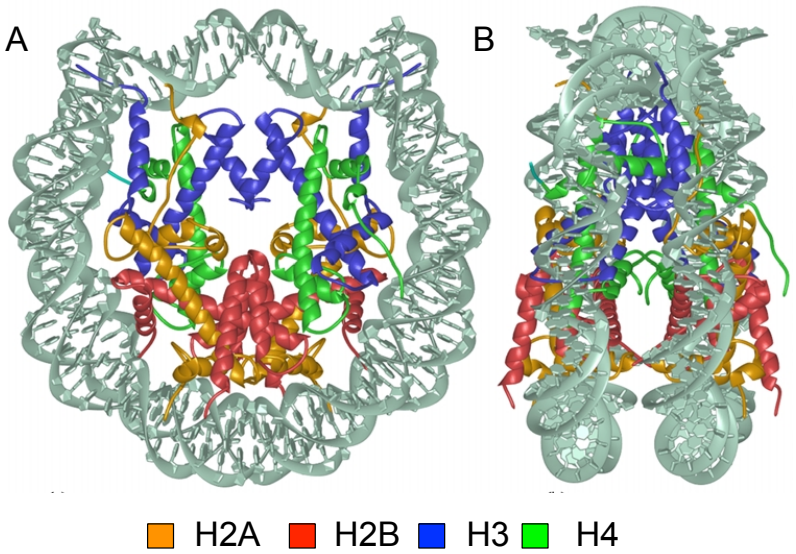

Figure 11. Overview of the nucleosome core particle structure, viewed in two different orientations. α-helices of the histone proteins are shown as spirals. (A) The nucleosome core particle viewed down the superhelical axis. (B) The same structure is rotated by 90º around the y-axis to emphasize the disc-like shape of the particle. Luger, K. 2001

The representation of a nucleosome shown in figure 11 is obtained from high-resolution crystal structure and demonstrates how DNA can achieve a 5-fold compaction by wrapping it around the histone octamer core. This highly condensed structure, the chromatin, is normally associated to inactive chromosomal regions (Jarillo et al., 2009, Chodavarapu et al., 2010). The binding of transcription factors to the DNA requires accessible or also the called “open” chromatin state. Recent studies have shown that ABA is also implicated in the modification of the access to the DNA via chromatin remodeling.

Signaling transduction mediated by clade A of PP2C phosphatases and SnRK2 kinases plays an important role in the coordination of the environmental signals and the alteration of gene expression in water stress responses. Saez et al. (2008) reported a direct interaction between a core element of the ABA signaling pathway, the HAB1 phosphatase, and a component of the SWI/SNF chromatin remodeling complexes, SWI3B. They found that this protein interaction blocked the induction of a subset of ABA regulated genes. HAB1 could induce a direct dephosphorylation of SWI/SNF complexes containing SWI3B in an ABA-dependent manner. Sokol et al. (2007) identified that ABA was also responsible for the induction of rapid changes in gene expression through histone modification. They discovered that some abiotic stresses as high salinity, cold and ABA can induce global H3S10 phosphorylation and H4K4 acetylation, which are modifications associated with the open state of chromatin. These studies established the first steps to link ABA response to mitotically heritable and dynamic chromatin state changes. Recently, it has been reported that chromatin remodeling (Han et al., 2012), histone deacetylation (Ryu et al., 2014, Luo et al., 2012), and histone demethylation (Zhao et al., 2015b) can regulate ABA response.

SWI/SNF Chromatin Remodeling Complexes (CRC)

Chromatin is subjected to dynamic modifications and chromatin-mediated control of gene expression involves two different mechanisms (Smith & Peterson, 2005, Kwon & Wagner, 2007, Weake & Workman, 2010). One mechanism depends on enzymes that covalently modify histones (for example by acetylation, methylation, phosphorylation and ubiquitylation) or the DNA (by methylation) and the other, is based on non-covalent changes of nucleosome occupancy or positioning through chromatin-remodeling complexes (CRCs).

In chromatin terminology, there are two terms that need clarification; one is **nucleosome positioning** which is referred to indicate where the nucleosomes are located with respect to the genomic DNA sequence. This positioning is critical for gene expression and most DNA-related processes. The genome-wide pattern of nucleosome positioning is determined by the combination of DNA sequence, ATP-dependent nucleosome remodeling enzymes and transcription factors that include activators, components of the pre-initiation complex and elongating RNA polymerase II. Thus, **nucleosome occupancy** reflects the fraction of cells from the population in which a given region of DNA is occupied by a histone octamer. While most genomic DNA is occupied by nucleosomes, many functional regions (promoters, enhancers, terminators) are depleted of nucleosomes (i.e. have low occupancy) and some regions are largely nucleosome-free (Struhl & Segal, 2013).

Chromatin remodeling consists of a change of the interactions between DNA and histones. The canonical role of the non-covalent type of chromatin remodelers to use the energy derived from ATP hydrolysis to alter the density or the position of nucleosomes on the DNA or the composition of the histone octamer (Cairns, 2009, Hargreaves &

Crabtree, 2011, Narlikar et al., 2013). Therefore, certain ATPases play a key role in chromatin remodeling (CR). In particular, the *Arabidopsis* genome codifies for 41 ATPases, which are grouped in 19 subfamilies. Some of them are known to be key regulators in several developmental stages or to have essential functions in nuclear DNA organization, however function of many of them remains still unclear (Knizewski et al., 2008). Plants chromatin remodeling complexes (CRCs) can be also classified in five major subfamilies according to their conserved ATPase subunit: ISWI, SNF2, CHD, Swr1 and INO80 (Figure 12). Each subfamily has unique domains besides the catalytic ATPase domain, which allows them to act in specific chromatin environments (Manning & Peterson, 2013). For example, ISWI and Mi-2/Chd1 families have unique function in nucleosome spacing in chromatin assembly after replication (Corona & Tamkun, 2004). The unique property of SWI/SNF family is that they are capable to disassemble nucleosomes to induce stable alterations in the nucleosomal DNA (Whitehouse et al., 1999). Finally, INO80 and SWR1 subfamilies play a role in histone variant exchange. The presence of H2A versus H2A.Z variant in the octamer of histones affects stability of the nucleosome (Mizuguchi et al., 2004, Papamichos-Chronakis et al., 2011).

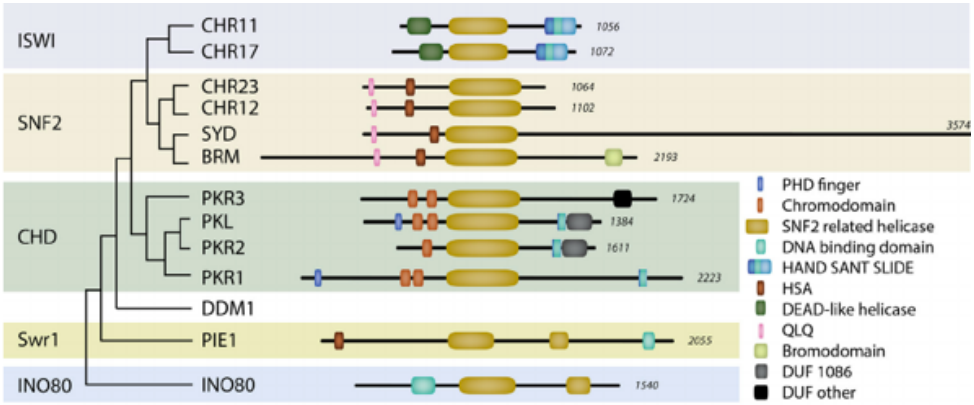

Figure 12. Characteristic protein domains defining the major SWI2/SNF2 family members in *Arabidopsis thaliana*. Reprinted from Gentry and Hennig (2014).

The most studied family in the ATP-dependent CRC is the SWI2/SNF2 (Switch/Sucrose non-fermenting) subgroup. *SWI2* and *SNF2* genes were originally discovered in *Saccharomyces cerevisiae* by screening for mutants affected in mating-type switch (Switch) and ability to growth on carbon sources other than glucose (Sucrose non-fermenting) (Abrams et al., 1986). In *Arabidopsis thaliana*, SWI/SNF complexes are involved in modulating various developmental and regulatory processes, including both vegetative and generative development, flowering time and hormonal signaling (Sarnowski et al., 2005, Bezhani et al., 2007, Saez et al., 2008, Han et al., 2012, Wu et al., 2012, Archacki et al., 2013, Efroni et al., 2013, Sarnowska et al., 2013, Vercruyssen et al., 2014, Zhao et al., 2015a, Peirats-Llobet et al., 2016).

The SWI/SNF complexes are highly conserved, although their composition is different. This feature reflects the gain of complexity of the complexes during evolution. Plant SWI/SNF complexes can be

potentially assembled from combinations of identified core subunits and an unknown number of putative accessory subunits (Figure 13). Developmental processes are responsible for the generation of different patterns of gene expression and this expression requires, at the same time, different composition of the SWI/SNF complex to regulate them tightly in a spatial or temporal manner.

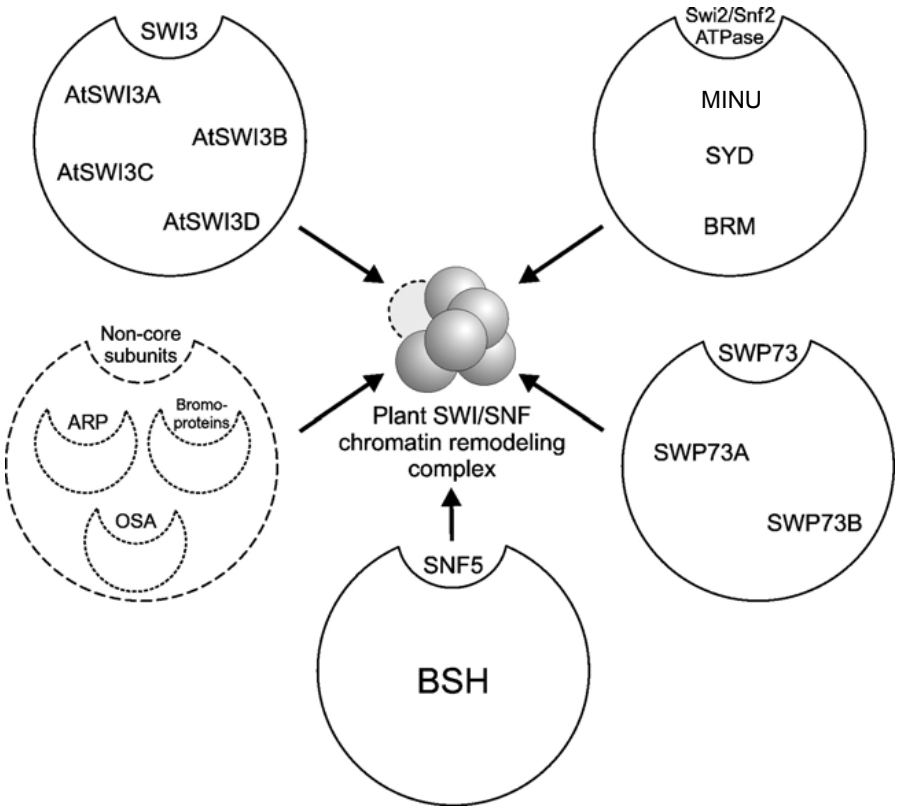

Figure 13. Plant SWI/SNF chromatin remodeling complexes with annotated subunits (solid line) and unknown candidate auxiliary subunits (broken line). The most important component of the CRCs are the ATPases, other conserved groups of accessory subunits are the SWI3 group, SNF5 and SWP73 group. Adapted from Jerzmanowski (2007).

SWI/SNF chromatin remodelers have been proposed as “general transcription activators” because of their function in sliding nucleosomes but they do not have the possibility to assemble them (Clapier & Cairns, 2012) and display the opposite function to Policomb Group (PcG) proteins that are identified as chromatin repressors (Tamkun et al., 1992, Wu et al., 2012). However, recent studies have shown that these remodeling complexes can also repress gene expression directly (Zhao et al., 2015a, Zhu et al., 2013, Han et al., 2012).

All land plants encode three types of SWI/SNF subfamily ATPases: BRM, SPLAYED (SYD) and MINUSCULE (MINU) (Sang et al., 2012). Although they belong to the same family they show structural differences. BRM is the most similar to its metazoan counterparts, while SYD shows a larger and acidic C-terminal domain of 200 kDa. This C-terminal domain is considered as autoinhibitory and is related to the control of the SYD protein accumulation (Su et al., 2006). Besides, MINU proteins are the shortest family members showing N- and C-terminal truncated domains. The *Arabidopsis* genome encodes for four members of this subfamily, one BRM, one SYD and two MINU.

The work of this thesis will be focused on the BRM ATPase and next paragraph will highlight some of its main features.

BRM, the core ATPase of SWI/SNF CRC

Structure of BRM protein

BRM is the most studied member of the SWI/SNF subgroup. It has the canonical domains found in this family of proteins (Farrona et al., 2004, Han et al., 2015). BRM protein includes a N-terminal region with a glutamine-rich domain and a helicase SANT-associated domain (HSA).

This HSA domain frequently serves as docking site for recruiting transcription factors such as LFY and TCP4 (Farrona et al., 2004, Szerlong et al., 2008, Wu et al., 2012, Efroni et al., 2013). The HSA domain is followed by the catalytic helicase-like ATPase domain and the Snf2 ATP-coupling (SnAC) domain, which is very important for catalytic activity of BRM. The ATPase domain is the catalytic subunit that displays helicase activity. It is the responsible of providing the energy for nucleosome dynamics. The ATPase hydrolyzes the ATP molecule to obtain the energy to modify the contacts between the DNA and the histones in order to reposition or disassemble nucleosomes. The SnAC domain is known to be required for mobilizing nucleosomes and its presence is required *in vivo* for transcription regulation but not for the complex organization, the substrate recognition or the recruitment function (Sen et al., 2013, Sen et al., 2011). BRM has a C-terminal domain that contains an AT-hook and a bromodomain (Farrona et al., 2007, Sen et al., 2011, Han et al., 2015). The AT-hook and the bromodomain are important domains for the BRM association with chromatin. The AT-hook motif consists in a GRP tripeptide surrounded by basic amino acid residues. AT-hook binds to A+T-rich sequences in the minor groove of the DNA (Reeves & Beckerbauer, 2001). The bromodomain was first reported in the *Drosophila* protein BRAHMA (Zeng & Zhou, 2002) and consists in a conserved module of approximately 110 residues responsible for the binding of acetylated histones. Both domains are evolutionarily conserved protein modules found in many chromatin-associated proteins and in nearly all known nuclear histone acetyltransferases (HATs) (Zeng & Zhou, 2002). The figure 14 is a scheme of the BRM domain organization.

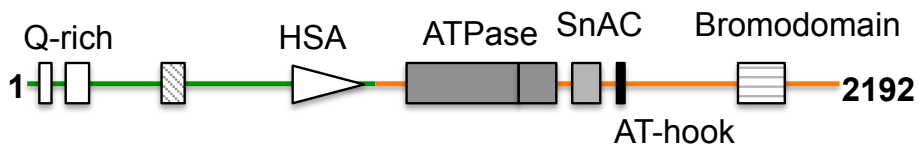

Figure 14. Domain architecture of the *A. thaliana* BRM protein. Schematic representation of the putative domains identified in BRM protein. N-terminal domain (green) includes domains related with protein interactions and C-terminal domain (orange) includes the catalytic subunit, the ATPases and several domains related to DNA-histones interactions.

BRM mutants

BRM is a 6582 nucleotides gene that encodes for a protein of 2193 residues, whose Mw is around 250 kDa. The studies to date identified three BRM T-DNA alleles (*brm-1, brm-2* and *brm-3*) that were characterized by Hurtado et al. (2006) and Farrona et al. (2007). *brm-1* and *brm-2* represent null mutations, in contrast, the *brm*-3 expresses a truncated BRM protein that lacks a C-terminal segment of 454 amino acids encompassing the bromodomain motif. Additionally, three EMS alleles (*brm-101–brm-103*) were identified by Kwon et al. (2006) when they were studying *Arabidopsis* cotyledon boundary genes. These alleles correspond to nonsense mutations that presumably permit the synthesis of truncated protein products lacking various domains important for the biological function of BRM. Two more alleles (*brm-4*, *brm-5*) were described later by Tang et al. (2008) in the study of seed maturation genes. The *brm-5* point mutation results in the exchange of Gly to Arg in the catalytic domain of BRM protein. Archacki et al. (2009) identified *brm-6* insertional mutant that has a phenotype indistinguishable from that of *brm-1* null mutant. Recently Xu et al. (2016) described a new allele, *brm-*

7, which was a substitution of a G by an A at the 5663-bp position of *BRM* coding sequence. This mutant exhibited an accelerated vegetative phase change phenotype and have more serrated leaves. The *brm-3* and *brm-5* mutants displayed less severe developmental alterations showing intermediate elongation and growth defects compared with wild-type and *brm* null mutant plants (Hurtado et al., 2006, Tang et al., 2008).

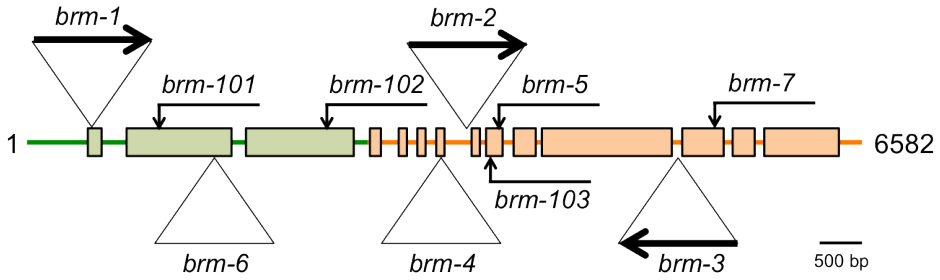

Figure 15. Characteristics of *brm* mutants and point mutations. Triangles indicate T-DNA insertional mutants where the arrows indicate the direction of the insertion. Point mutations are indicated with arrows. Modified from Archacki et al. (2009).

Along this thesis we performed most of our experiments with *brm-3* and *brm-1* mutants. *brm-1* is a null mutant that has a T-DNA insertion in the first translated exon, 20 pb downstream the first translated nucleotide. *brm-1* display a dwarf phenotype with characteristic short and branched roots, dark green coloration, curled leaves, homeotic changes in flowers, underdeveloped stamens, male sterility and delayed flowering under non-inductive short-day conditions (Hurtado et al., 2006). *brm-3* is an hypomorphic mutant, this allele carries a T-DNA insertion just upstream of the bromodomain. The insertional mutation causes formation of a truncated BRM polypeptide lacking the last 454 residues. Both mutants

impair BRM function, but *brm-1* has an extreme phenotype. *brm* mutants are slow growing and dwarfed, have defects in cotyledon separation, defects in leaves and exhibit reduced apical dominance. *brm* null mutants also have unique root growth phenotypes, defects in the flowering time and are male sterile (Farrona et al., 2004, Su et al., 2006, Kwon et al., 2006, Hurtado et al., 2006, Xu et al., 2016, Sarnowski et al., 2005).

BRM as a growth and development regulator

Pluripotency and differentiation

In plants and mammals, SWI/SNF subfamily of chromatin remodelers are required to promote both stem cells fate and differentiation (Farrona et al., 2004, Tang et al., 2008, Farrona et al., 2011, Wu et al., 2012, Sang et al., 2012, Efroni et al., 2013, Vercruyssen et al., 2014, Zhao et al., 2015a). BRM has been proposed as a regulator of the root cell stem niche through alteration of auxin distribution. *brm* mutant plants showed defects in the root stem cells that can be rescued by the overexpression of the PLETHORA genes, which maintain the root cell fate (Yang et al., 2015). On the other hand, BRM and SYD promote differentiation of floral organs. *brm* mutants show transcription repression of all the classes of flower homeotic genes (Hurtado et al., 2006). BRM and SYD regulate floral homeotic genes through direct interaction with floral transcription factors as LFY and SEP3 (Wu et al., 2012). This indicates that SWI/SNF remodelers have a promoting function in floral organ identity. Moreover, BRM interacts with TCP4, ANGUSTIFOLIA3 (AN3) and BREVIPEDICELLUS (BP/KNAT1) to regulate leaf development and inflorescence architecture (Efroni et al., 2013, Vercruyssen et al., 2014, Zhao et al., 2015a). TCP4 is a member of the CIN-TPC transcription factor family, which promotes leaf maturation, AN3 is a transcriptional activator of cell proliferation in leaf development and BP/KNAT1 is a

KNOX transcription factor controlling the inflorescence shape by directly repressing other KNOX genes.

Developmental phase transitions

BRM is involved in the two major developmental transitions occurring in plants. One is the transition from embryo to seedling whereby the plant acquires the autotrophic capacity (Bezhani et al., 2007). Upon germination in the darkness, seedlings grow up to reach the light, in a process called skotomorphogenesis. When seedlings reach the light, growth stops, cotyledons expand and photosynthesis begins. *brm* mutants gene expression analysis show that several seed maturation and embryonic genes are derepressed during the vegetative development and BRM bind to several of this loci (Tang et al., 2008). Recent work has focus on this specific role of BRM in juvenile-to-adult transition. Xu et al. (2016) identified a direct interaction of BRM to miRNA165 promoter that represses its function. miRNA156 is a master regulator in this transition in plants. SWINGER (SWN), which is a key component of PCR2 (PcG repressive complex 2) acts antagonically to BRM at the nucleosome level to assure a fine-tuning of the vegetative phase change in *Arabidopsis*.

The second major transition occurs when plants change from vegetative to reproductive growth. This is the phase where plants allocate resources for flower production (Farrona et al., 2011). *brm* mutants show early flowering phenotype in SD and LD conditions, which correlates with a derepression of the flowering integrator FLOWERING LOCUS T (FT) and the photoperiod-pathway gene CONSTANS (CO) (Farrona et al., 2004). Kwon et al. (2006) found that SWI/SNF CRC enhance the expression of a set of CUP-SHAPED COTYLEDON (CUC) genes, which are in charge

of the control of cotyledon separation in *Arabidopsis.* Thus, BRM repressive function is very important in the control of floral transition when the conditions are not favorable for the plant.

Stress response and growth

Plants are constantly exposed to environmental changes from which they cannot scape. This sessile state requires a delicate balance of the molecular responses to maintain the integrity of the cellular structures. This balance is achieved by fine transcriptional reprogramming of the plant responses through, for instance, changes on the accessibility to the DNA mediated by chromatin remodeling (Shinozaki & Yamaguchi-Shinozaki, 2007, Han & Wagner, 2014). *brm* mutants are hypersensitive to ABA and the expression of a key transcriptional regulator of ABA response, ABI5, is elevated in the absence of the stress hormone (Han et al., 2012). BRM is constitutively bound to the ABI5 promoter and inhibit its transcription until the stress triggers the ABA response (Han et al., 2012). *brm* mutants also have reduced levels of GAs, and GA exogenous application can partial or fully rescue the reduced growth and late flowering in short days (Archacki et al., 2013).

Beyond transcription

Chromatin remodeling ATPases can act in many different pathways, but how is that selectivity achieved remains unclear. One proposed mechanism of selectivity is via recruitment of the complexes to the target loci by transcription factors or lncRNAs (spatiotemporally or environmentally controlled). Zhu et al. (2013) discovered a mechanism to explain how a long non coding RNA (lncRNA) is capable to guide SWI/SNF CRC to silence specific loci. SWI3B, a subunit of the SWI/SNF

CRC interact with IDN2, a lncRNA binding protein to direct the complex to specific loci to establish their nucleosome positioning.

Chromatin is also important in other processes like DNA repair, recombination and replication, processes that control genome integrity. SWI/SNF and CHD3 have also been implicated in DNA repair (Bennett et al., 2013).

OBJECTIVES

General objectives of this thesis are the study of ABA regulation of the SWI2/SNF2 chromatin remodeling complex BRAHMA and the generation of a stress-inducible promoter for biotechnological use.

Specific objectives are:

1. Characterization of the SWI2/SNF2 chromatin remodeling ATPase BRAHMA in ABA signaling and its interaction with core ABA signaling components.

2. Study of the BRM role in the regulation of *ABI4* gene expression during post-germination growth.

3. Characterization of the PP2CA promoter and its application for stress-inducible expression of ABA receptors.

RESULTS

Chapter One: A direct link between the core ABA signaling pathway and the chromatin remodeling ATPase BRAHMA

CHARACTERIZATION OF *brm-3* MUTANT

Previous results of our laboratory showed a relationship between chromatin remodeling through the protein SWI3B, a component of SWI/SNF chromatin remodeling complex and the ABA signaling phosphatase HAB1. Saez et al. (2008) reported a direct interaction between these two processes suggesting that ABA signaling could regulate chromatin status. Later on, Han et al. (2012) reported that *brm-3*, a mutant impaired in the core of the SWI/SNF chromatin remodeling complexes, the ATPase BRAHMA, showed hypersensitivity to ABA in seed germination and seedling establishment assays (Figure 16). This implies that BRM acts as a negative regulator of the ABA signaling pathway.

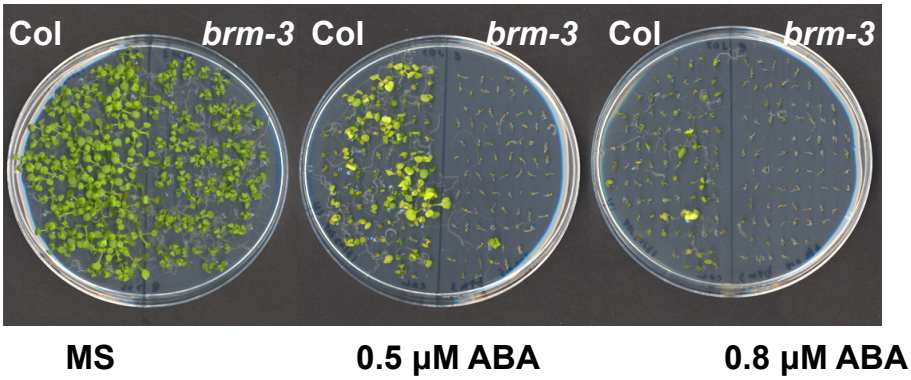

Figure 16. *brm-3* mutant is hypersensitive to ABA. Seedlings were grown in MS plates supplemented or not with the indicated ABA concentrations. Photographs were taken 11 (MS) and 18 (ABA) days after stratification. Reprinted from Han et al. (2012).

INTERACTIONS BETWEEN BRM AND CORE ABA SIGNALING PATHWAY ELEMENTS

Genetic Interaction between SnRK2.2/2.3 and BRM

To test for a functional link between the core ABA signaling pathway and BRM, we crossed the ABA-hypersensitive *brm-3* mutant to the ABA-insensitive *snrk2.2/2.3* mutant to generate the *snrk2.2/2.3/brm-3* triple mutant. ABA-mediated inhibition of seedling establishment was compared among the different genetic backgrounds (Figure 17A). We found that the ABA-insensitive phenotype of the *snrk2.2/2.3* double mutant was attenuated when *brm-3* was introduced in this genetic background. Likewise, the reduced sensitivity of *snrk2.2/2.3* to ABA-mediated inhibition of root growth was attenuated in the *snrk2.2/2.3/brm-3* triple mutant (Figure 17B).

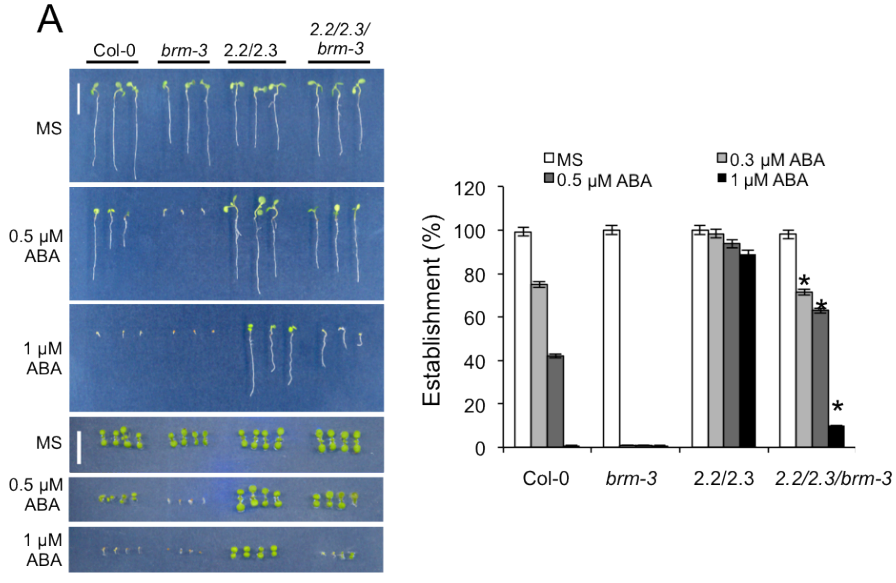

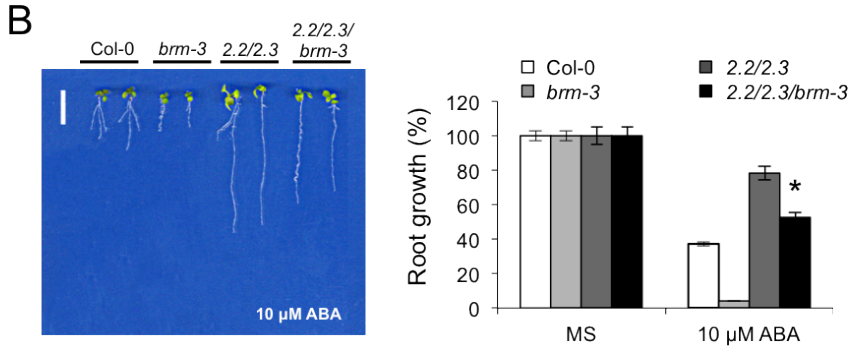

Figure 17. ABA insensitivity is dependent on BRM activity in different genetic backgrounds. (A) Left: Photographs of Col-0 wild-type (white), *brm-3* mutant (light grey), *snrk2.2/2.3* (dark grey) and *snrk2.2/2.3/brm-3* triple mutant (black) grown for 7 days on MS medium either lacking or supplemented with the indicated ABA concentrations. Seeds were germinated in plates lacking or supplemented with ABA, and after 7 days seedlings were rearranged on agar plates to illustrate seedling growth. Scale bar corresponds to 1 cm. Right: Quantification of ABA-mediated inhibition of seedling establishment for the indicated genetic backgrounds. Approximately 100 seeds of each genotype were sown on each plate and scored for the presence of both green cotyledons and the first pair of true leaves 7 days later. Values are averages ± SE of three independent experiments. * indicates $P < 0.05$ (Student's *t-test*) compared with *snrk2.2/2.3* in the same assay conditions. (B) The root ABA-insensitive phenotype of *snrk2.2/2.3* is attenuated in *snrk2.2/2.3/brm-3*. Quantification of ABA-mediated root growth inhibition in the indicated genetic backgrounds. Scale bar corresponds to 1 cm. Data are averages ± SE from three independent experiments (n = 30). * indicates $P < 0.05$ (Student's *t-test*) compared with *snrk2.2/2.3* in the same assay conditions.

These results suggest that the ABA insensitivity of *snrk2.2/2.3* mutant is in part dependent on BRM repressing the ABA response. To further test this idea, we took advantage of a double mutant previously generated that combines the *brm-101* null mutant and a 35S:HAB1 overexpressing (OE) line (Saez et al., 2004, Han et al., 2012). HAB1 OE leads to enhanced dephosphorylation of SnRK2s at serine (Ser, S) residues of the kinase-activating loop, which prevents SnRK2 activation and ABA signaling (Umezawa et al., 2009, Vlad et al., 2009, Antoni et al., 2013), and thus phenocopies higher-order *snrk2* mutants. HAB1 OE causes ABA insensitivity in the root. The ABA-insensitive phenotype of HAB1 OE lines was attenuated in *brm-101* HAB1 OE plants (Figure 18), which likewise suggests that the HAB1 gain-of-function effect on ABA signaling is partially dependent on BRM activity.

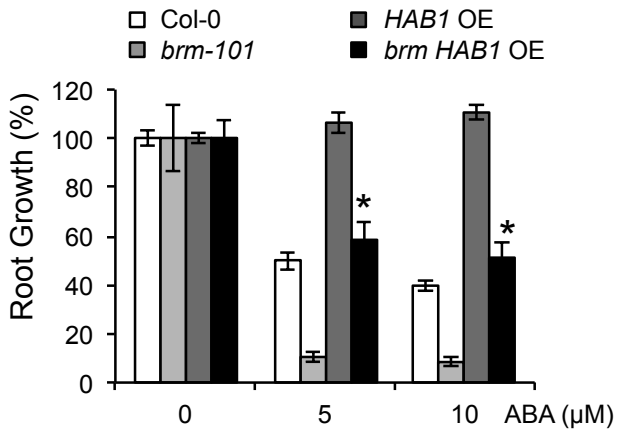

Figure 18. The root ABA-insensitive phenotype of HAB1 OE line is attenuated in *brm-101* HAB1 OE. Data are averages ± SE from three independent experiments (n = 30, except *brm-101* with n = 14). * indicates $P < 0.05$ (Student's *t-test*) compared with HAB1 OE line in the same assay conditions.

Finally we tested the effect of stratification time on the germination rate of *brm-3* mutant and other ABA-insensitive mutants as *snrk2.2/2.3* and *snrk2.2/2.3/brm-3*. Snrk2s mutants are insensitive to ABA and did not display dormancy phenotype. In contrast, as shown in the figure 19, without stratification, the *brm-3* mutant germinates poorly whereas *snrk2.2/2.3* and *snrk2.2/2.3/brm-3* mutants germinate well. Stratification of the seeds for 24 h in darkness at 4ºC improved the germination rate in Col-0 and *brm-3.* Moreover, all mutants dramatically improved their germination rate reaching close to 100% after 72 h of stratification.

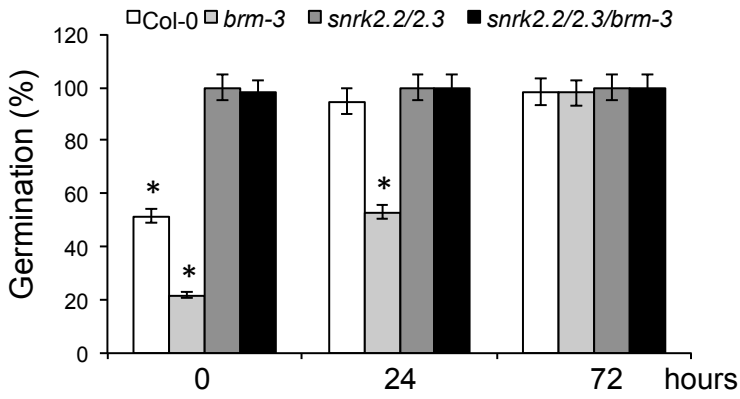

Figure 19. Dormant phenotype of *brm-3* seeds. Quantification of Col-0 wild-type (white), *brm-3* mutant (light grey), *snrk2.2/2.3* (dark grey) and *snrk2.2/2.3/brm-3* triple mutant (black) seeds without stratification, 24 and 72 h of stratification in darkness at 4ºC. Averages of three independent experiments are shown in SD. Approximately 50 seeds/genotype were used in each experiment. * indicates $P < 0.05$ (Student's *t-test*) compared with *snrk2.2/2.3* in the same assay conditions.

Physical interaction of BRM with SnRK2s and clade A PP2Cs

BRM is an SWI/SNF subgroup ATPase and has the canonical domains found in this family of proteins (Han et al., 2015) (Figure 20). BRM has an N-terminal region with a glutamine-rich domain and a helicase SANT-associated domain (HSA), which frequently serves as docking site for recruiting transcription factors such as leafy (LFY) and TCP family transcription factor 4 (TCP4) (Farrona et al., 2004, Szerlong et al., 2008, Wu et al., 2012, Efroni et al., 2013). This is followed by the catalytic helicase-like ATPase domain, the Snf2 ATP-coupling (SnAC) domain, and a C-terminal domain which contains an AT-hook and a bromodomain; these domains are important for catalytic activity of BRM and for BRM association with chromatin, respectively (Farrona et al., 2007, Sen et al., 2011, Han et al., 2015).

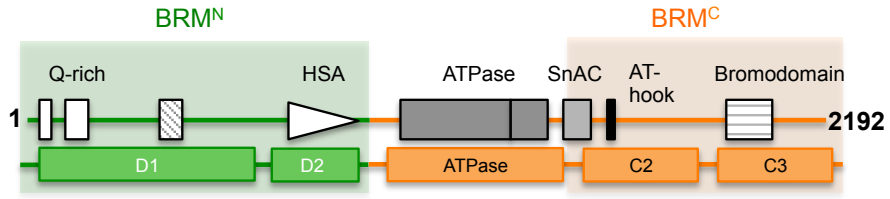

Figure 20. Domain architecture of the *A. thaliana* BRM protein. Colored boxes correspond to special nomenclature followed along this work. Adapted from Farrona et al. (2004).

The genetic interaction between BRM and SnRK2s, together with data obtained in phosphoproteomic studies (Umezawa et al., 2013, Wang et al., 2013a), combined with the known role of BRM in

preventing ABA response in the absence of stress (Han et al., 2012), prompted us to test whether BRM is a direct target of the core ABA signaling pathway. Because BRM is a large protein (2193 amino acid residues (aa)), it is difficult to express transiently; to overcome that inconvenience, we first generate and express in tobacco leaves different BRM proteins fragments, BRM N (1–950 aa), BRM C2 (1541-1890 aa), BRM C3 (1891-2193 aa) and BRM C2C3 (691-2193 aa), fused to green fluorescent protein (GFP). All the fusion proteins were localized to the nucleus of plant cells (Figure 21), as expected for a chromatin related protein. Location in nuclear speckles was observed for BRM C2-GFP and BRM C3-GFP, whereas BRM N-GFP showed a nuclear pattern as nuclear GFP, which was also expressed in the cytoplasm.

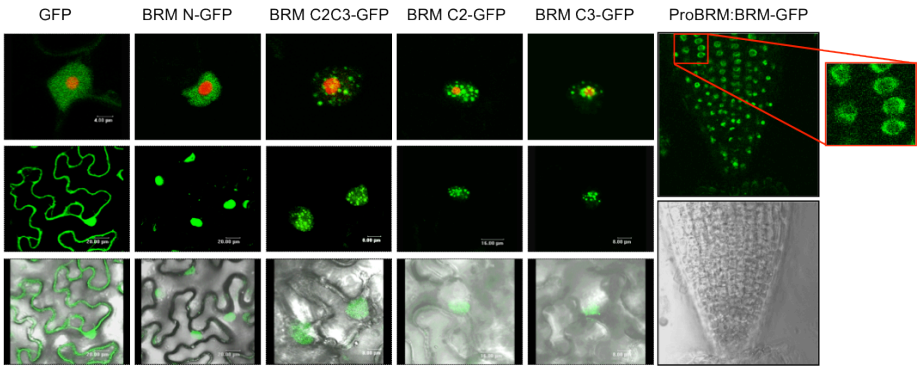

Figure 21. BRM fragments are localized in the nucleus of *Agrobacterium*-infiltrated tobacco leaves. Confocal microscopy of transiently transformed *N. benthamiana* epidermal cells co-expressing green fluorescent protein (GFP) or GFP-BRM fusions and the nucleolar marker, fibrillarin, tagged with red fluorescent protein (RFP). Bars correspond to 20 µm. Right panel shows CSLM images of roots from transgenic lines expressing full-length BRM-GFP under the control of their own promoter.

Next, we generate translational fusions of the N-terminal 1–950 (BRMN) and C-terminal 1541–2193 (BRMC) residues to N-terminal part of the yellow fluorescence protein (YFP^N). We used BiFC technique in *A. thaliana* leaf protoplasts (Figure 22) and tobacco leaf epidermal cells (Figure 23) to test whether BRM physically interacts with key components of the ABA signaling pathway, namely SnRK2s and clade A PP2Cs. We found that both BRMN and BRMC were able to interact with either the OST1/SnRK2.6 kinase or the HAB1 PP2C phosphatase in the nucleus of *A. thaliana* protoplasts (Figure 22). A negative control was provided by an unrelated nuclear localized protein (NC) that lacks interaction with both HAB1 and OST1/SnRK2.6 (Figure 22) (Wu et al., 2012).

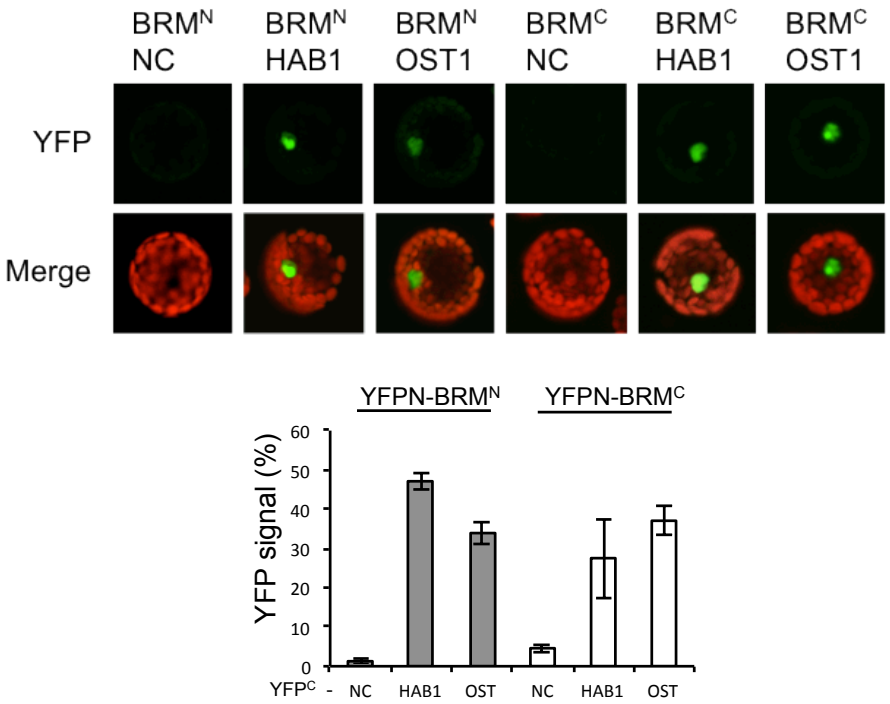

Figure 22. BiFC interaction of HAB1 and OST1/SnRK2.6 with BRMN and BRMC in the nucleus of *A. thaliana* leaf protoplasts. Top: The

YFP fluorescence was merged with red fluorescence generated by chloroplasts. Bottom: Quantification of the percentage of YFP-positive cells observed. Values are averages ± SE from three independent experiments. The number of protoplasts scored per interaction test was >600. NC, negative control.

We confirmed and extended this interaction by BiFC assays in tobacco epidermal cells, and showed that SnRK2.2, SnRK2.3 and SnRK2.6 kinases were able to interact with BRMN and BRMC (Figure 23A). SnRK2.6 Δ280, which lacks the C-terminal ABA box (Vlad et al., 2009), was no not able to interact with BRMN or BRMC. The interaction of BRMN with SnRK2s was confirmed by using yeast two-hybrid (Y2H) interaction assays. The BRMC fragment, which contains chromatin interacting domains, could not be assayed in Y2H assays because of autoactivation (Figure 23C, left panel). Likewise, two clade A PP2Cs, PP2CA and HAB1, were able to interact with BRMN and BRMC on the basis of BiFC (Figure 23B). In contrast, the closely related HAI1 PP2C did not interact with BRM in BiFC assays. The interaction of BRMN with HAB1 and PP2CA was confirmed using Y2H assays (Figure 23C, right panel). In addition we found that AHG1, another clade A PP2C expressed mainly in seeds, interacted with BRMN in Y2H tests. In more stringent Y2H assay conditions (medium lacking Ade and His) we could not detect an interaction between HAB1 or ABI2 and BRMN; however, in medium lacking His and supplemented with 3AT, we confirmed the interaction of HAB1 with BRMN (Figure 23C, bottom right panel).

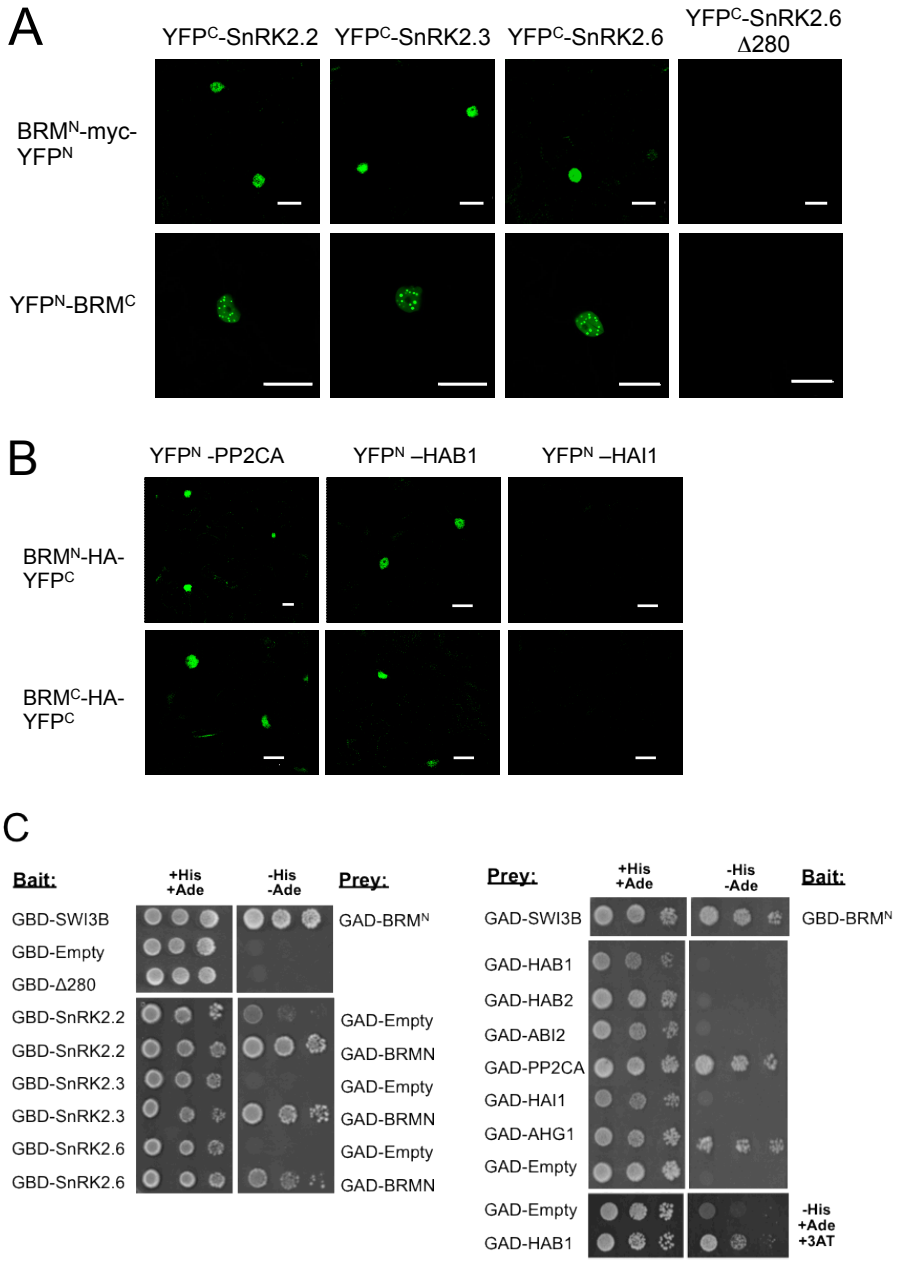

Figure 23. BiFC and Y2H analyses show interaction between BRM and SnRK2s/PP2Cs. (A) BiFC interaction of SnRK2.2, SnRK2.3, and SnRK2.6 with BRMN and BRMC in the nucleus of tobacco leaf cells. Tobacco leaves were infiltrated with a mixture of *A. tumefaciens*

suspensions harboring the indicated constructs and the silencing suppressor p19. (B) BiFC interaction of PP2CA and HAB1 with BRMN and BRMC. Scale bars on A and B corresponds to 20 µm. (C) Left: The BRMN interaction in (A) was confirmed in Y2H assays. Dilutions (10^{-1}, 10^{-2}, and 10^{-3}) of saturated cultures were spotted onto the plates, and photographs were taken after 5 days. Interaction was determined by growth assay on medium lacking His and Ade. Right: Interaction in (B) was confirmed in Y2H assays conducted as BRM-SnRKs assay except for the growth in the case of HAB1 that was also tested on medium lacking His and supplemented with 0.1 mM 3AT.

To test whether full-length BRM protein is able to interact with SnRK2 kinases and PP2C phosphatases in plant cells we performed co-immunoprecipitation (coIP) experiments using the full-length BRM protein expressed in *brm-1* background as ProBRM:BRM-HA. First, we demonstrated that a fraction of HA tagged-SnRK2.2/2.3 and of HA-PP2CA proteins, as well as of BRM-HA itself, could be detected in soluble nuclear extracts by biochemical fractionation (Figure 24).

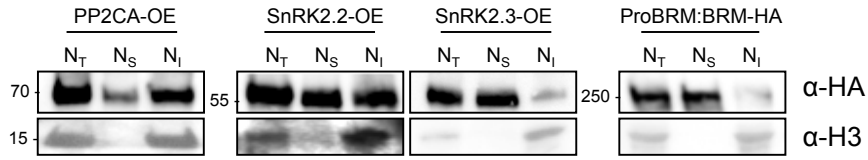

Figure 24. Biochemical fractionation and immunoblot analysis of protein extracts prepared from *A. thaliana* transgenic plants expressing 35:3HA-PP2CA, 35:3HA-SnRK2.2, 35:3HA-SnRK2.3, and ProBRM:BRM–HA. Nuclear total (Nt), nuclear soluble (Ns) and nuclear insoluble (Ni) protein extracts were analyzed by immunoblotting using α-HA and α-H3 antibodies.

Next, we transformed ProBRM:BRM-GFP plants with 35S:3HA-SnRK2.2 or 35S:3HA-PP2CA and generated stable transgenic lines. After anti-HA antibody immunoprecipitation in nuclear extracts from ProBRM:BRM-GFP 35S:3HA-SnRK2.2 plants, we tested for coIP of BRM-GFP using anti-GFP monoclonal antibody (Figure 25). BRM was co-immunoprecipitated with SnRK2.2 in the absence or presence of ABA (50 μM for 1 h). Hence, ABA-mediated activation of SnRK2.2 is not a prerequisite for its interaction with BRM. This result is in agreement with Y2H assays, which show that non-ABA-activated SnRK2s are able to interact with BRMN (Figure 23C, left panel).

To test the interactions between BRM and PP2CA in plant cells, we first immunoprecipitated BRM-GFP with anti-GFP antibody and tested for coIP of 3HA-PP2CA using anti-HA. We detected PP2CA coIP in the absence but not the presence of ABA (50 μM for 1 h). In the presence of ABA, PP2CA forms a highly stable PP2C–ABA–receptor complex in both the nucleus (predominantly) and cytosol of plant cells (Pizzio et al., 2013). Thus ABA treatment impairs the interaction of PP2CA with BRM (Figure 25), which may be the result of PP2CA being hijacked by ternary phosphatase–ABA–receptor complexes.

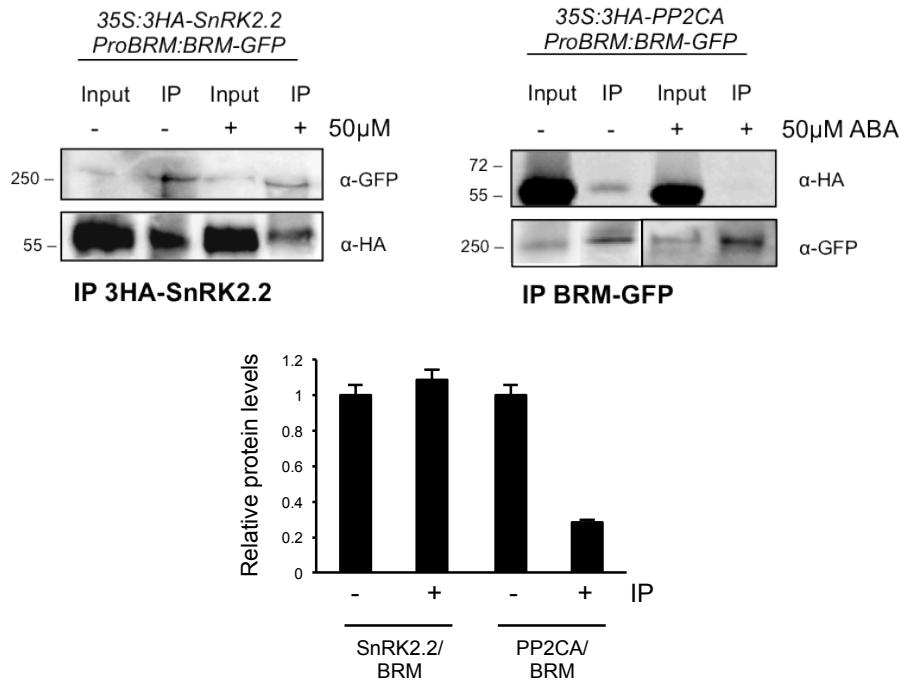

Figure 25. coIP of BRM and SnRK2.2 or PP2CA. Double transgenic lines containing ProBRM:BRM-GFP and HA-tagged SnRK2.2 or PP2CA were used for coIP experiments. Top: Nuclear soluble protein extracts prepared from mock- or ABA-treated plants (50 µM for 1 h) were immunoprecipitated using either α-HA (left) or α-GFP (right). CoIP was revealed using α-GFP or α-HA, respectively. Bottom: Histograms show the quantification of the protein signal obtained with analyzer LAS3000 and Image Guache V4.0 software.

CORE ABA SIGNALING COMPONENTS MEDIATE PHOSPHORYLATION/DEPHOSPHORYLATION OF BRM

In vitro phosphorylation/dephosphorylation of the carboxy-terminal region of BRM by OST1/PP2CA

Several large-scale experiments have identified phosphorylation sites in BRM by mass spectrometry (The Arabidopsis Protein Phosphorylation Site Database [PhosPhAt 4.0; http:// phosphat.uni-hohenheim.de/ phosphat.html]) (Durek et al., 2010, Umezawa et al., 2013, Wang et al., 2013a). In particular, more than 10 phosphopeptides in the C-terminal domain of BRM were identified following ABA treatment in the wt that were absent in *snrk2.2/2.3/2.6* triple mutant or were induced by osmotic stress (Umezawa et al., 2013, Wang et al., 2013a, Xue et al., 2013); Supplemental Excel and Figure 31). These studies suggest that BRM phosphorylation is dependent on SnRK2s; however, direct *in vitro* evidence was not provided.

Phosphoproteomic studies identified S1760 and S1762 as putative phosphorylation targets of SnRK2.2/2.3/2.6 that lay in the well-known LxRxxS consensus site for OST1 phosphorylation (Sirichandra et al., 2010, Umezawa et al., 2013, Wang et al., 2013a). We reasoned that residues critical for BRM function in this region should be evolutionarily conserved. For instance, S1760 and S1762 were found to be conserved in the analyzed plant genomes (Figure 26).

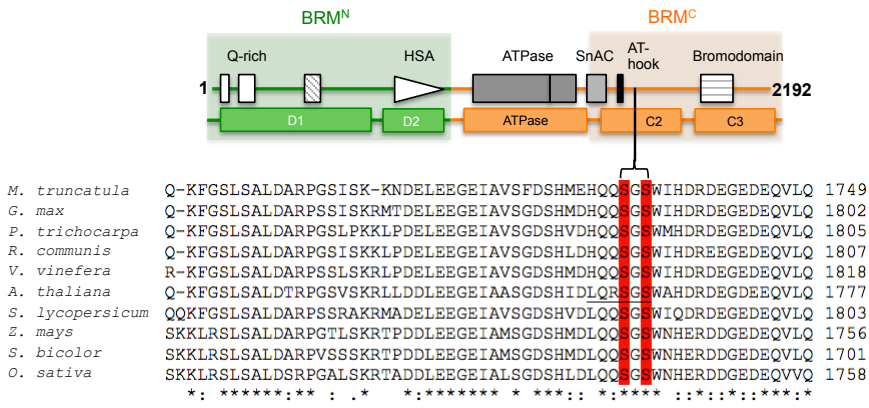

Figure 26. Residues S1760 and S1762 of *A. thaliana* BRM are evolutionary conserved in different plant species. C-terminal amino acid sequence of BRM in different plant species such as *Medicago truncatula, Glycine max, Populus trichocarpa, Ricinus communis, Vitis vinifera, Solanum lycopersicum, Zea mays, Sorghum bicolor, Oryza sativa.*

The C-terminal region of BRM contains domains that are critical for nucleosome interaction and normal function of BRM (Farrona et al., 2007). For instance, the potential phosphorylation sites (S1760 and S1762) are located between the AT hook, which is a non-specific DNA-binding domain rich in lysines (Lys, K) and arginines (Arg, R) required for tethering of BRM to chromatin (Bourachot et al., 1999) and the bromodomain, which is known to interact with acetylated Lys of histones H3 and H4 (Dhalluin et al., 1999, Farrona et al., 2007) (Figure 20). Further support for the importance of this domain comes from the *brm-3* allele, which carries a T-DNA insertion just upstream of the bromodomain. This insertional mutation causes formation of a truncated BRM polypeptide lacking the last 454 residues and impairs BRM function (Farrona et al.,

2007). Finally, additional potential SnRK2 phosphorylation sites are located after the bromodomain (Supplemental Excel and Figure 26).

To test whether BRM is a direct target of SnRK2s, we generated recombinant fragments of this chromatin remodeling ATPase for *in vitro* phosphorylation assays. We purified two histidine-tagged C-terminal domain fragments (BRM C2 [residues 1541–1890] and BRM C3 [residues 1891–2193]) and one N-terminal fragment as an MBP fusion protein (MBP-BRM D2 [residues 684–950], which contains the HSA domain) (Figure 27).

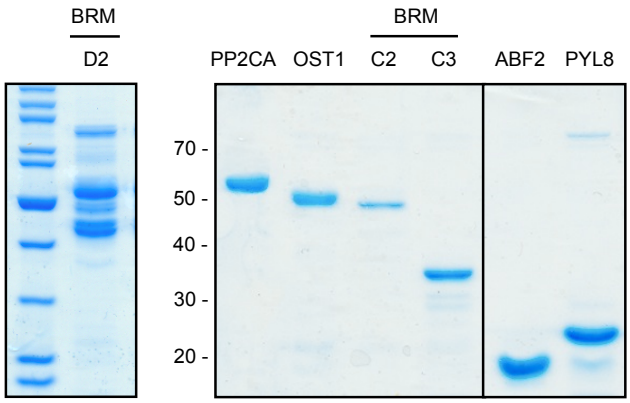

Figure 27. Coomassie gel staining of the proteins used in the phosphorylation assay. MBP-BRM D2 was purified using amylose affinity chromatography (left panel), whereas His-tagged PP2CA, OST1, BRM C2, BRM C3, ABF2ΔC and PYL8 were purified using Ni-NTA affinity chromatography. ABF2 is a direct target of OST1 used as a positive control of phosphorylation.

Next, we tested these fragments as *in vitro* substrates in a phosphorylation assays with the OST1/SnRK2.6 kinase (Figure 28). Recombinant OST1 is 10-fold more active than SnRK2.2 and SnRK2.3 in phosphorylation assays as determined by [γ-32P] ATP labeling (Ng et al., 2011). Fragment BRM C2, which migrates just below OST1, and fragment BRM C3 were phosphorylated *in vitro* by OST1 and, as previously reported (Dupeux et al., 2011a, Ng et al., 2011), OST1 was autophosphorylated and is able to phosphorylate directly a target protein such as the transcription factor ABF2 (Figure 28). In contrast to BRM C2 and BRM C3, the BRM D2 fragment was not phosphorylated by OST1 (Figure 28, right panel). Addition of the PP2CA phosphatase 45 min after the phosphorylation reaction took place led to dephosphorylation of both the OST1 and the BRM fragments (Figure 28, left panel). However, addition of the PP2CA phosphatase together with PYL8 and ABA did not result in BRM or OST1 dephosphorylation (Figure 28, left panel). This was expected, since PYL8 inhibits PP2CA activity in an ABA-dependent manner (Antoni et al., 2012). These results suggest that ABA-mediated activation of SnRK2s initiated by PYR/PYL ABA receptors leads to phosphorylation of BRM, whereas the clade A PP2CA is able to dephosphorylate BRM when ABA levels are low.

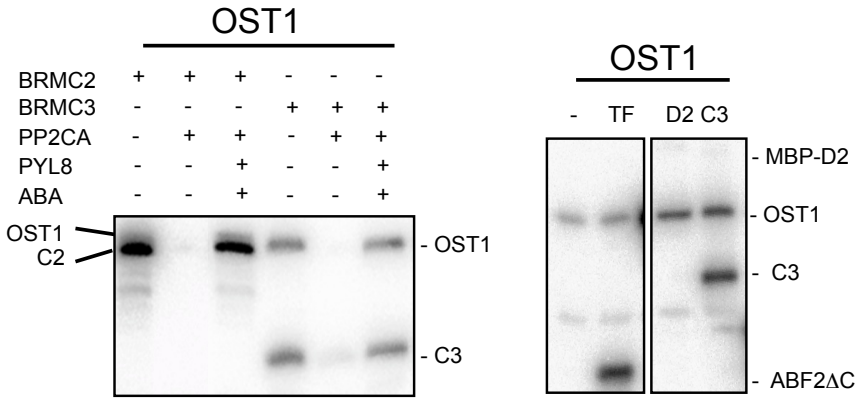

Figure 28. *In vitro* phosphorylation of BRM C2 and BRM C3 fragments by OST1/SnRK2.6. Subsequent addition of PP2CA dephosphorylates BRM C2 and BRM C3, whereas co-incubation of PP2CA with PYL8 in the presence of ABA (10 µM) prevents the dephosphorylation of BRM C2 and BRM C3. The BRM D2 fragment is not phosphorylated by OST1, in contrast to a positive control, ABF2ΔC (Pizzio et al., 2013) or the BRM C3 fragment.

Identification of BRM phosphorylated sites by OST1

Next, we performed *in vitro* cold phosphorylation of BRM C2 and BRM C3 by OST1 to identify by proteomic analysis the precise residues phosphorylated. After incubation of BRM C2 and BRM C3 with OST1, phosphopeptides were enriched by immobilized metal affinity chromatography (IMAC) and Oligo R3 reversed-phase chromatography (Navajas et al., 2011). Phosphopeptide analysis was performed using CID/ETD fragmentation of the most abundant ions and liquid chromatography–tandem mass spectrometry (LC–MS/MS) (Navajas et al., 2011). For protein identification, CID and ETD spectra obtained by LC–MS/MS system were searched

against the SwissProt database using a licensed version (v.2.3.02) of Mascot (Matrix Science, London, UK) as the search engine. Using this strategy, we identified one phosphopeptide in BRM C2, SGpS1762WAHDR, and three phosphopeptides in BRM C3: NALSFSGSAPTLVS(T)2029P(T)2031PR, TGGS(S)2120(S)2121 PVSPPPAMIGR, and SPVpS2139GGVPR, whose CID/ETD spectra are shown in Figure 30. The fragmentation pattern of some of the phosphorylated peptides in the CID/ETD spectra did not allow the unambiguous assignment of the phosphate group to specific S/T residues (shown in parentheses in Figure 30). In these cases, the peptide sequence and the number of phosphorylation sites in the peptide could be derived from the mass spectrum, but not the precise location within the sequence. However, for the SGpS1762WAHDR and SPVpS2139GGVPR phosphorylated peptides, the precise location of the phosphorylation site was derived from the mass spectrum.

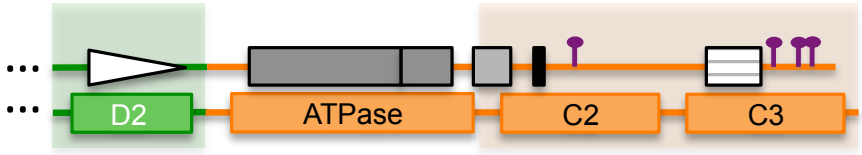

Figure 29. Schematic representation of partial BRM protein. The locations of the four phosphorylation sites in the C-terminal part of BRM identified in this work are indicated with violet symbols.

The four BRM phosphopeptides identified here (Figure 29) matched those deposited in PhosPhAt database based on *in vivo* phosphoproteomics (Durek et al., 2010). In particular, the genetic-phosphoproteomic studies performed by Wang et al. (2013a) and

Umezawa et al. (2013) yielded BRM phosphopeptides that matched those identified in our *in vitro* analysis (Supplemental Excel). However, those studies did not discern whether the identified BRM phosphopeptides were a direct target of SnRK2s or downstream targets of MAPKs/GSKs that might be dependent on SnRK2 function (Umezawa et al., 2013). Motif analysis of ABA-responsive phosphopeptides has identified four groups of motifs (Umezawa et al., 2013). Motif analysis of the phosphorylated BRM peptides identified in our assays revealed that SGpS1762WAHDR matched motif 1: (K/R) xx(pS/pT), whereas SPVpS2139GGVPR matched motif 4: (S) xx(pS). The LQRSGS1762WAHDR peptide, moreover, matches a well-known LxRxxS consensus site for OST1 phosphorylation (Sirichandra et al., 2010), and phosphorylation of both Ser1760 and Ser1762 was found in BRM phosphopeptides present in PhosPhAt 4.0 (Umezawa et al., 2013, Wang et al., 2013a). The phosphopeptides TGGS(S)^{2120}(S)^{2121}PVSPPPAMIGR, NALSFSGSAPTLVS(T)^{2029}P(T)^{2031}PR, and SPVpS^{2139}GGVPR match motif 3 (pS/T-P; pSxP; pSPxpS), and we found in PhosPhAt 4.0 evidence for *in vivo* existence of the corresponding phosphopeptides (Umezawa et al., 2013, Wang et al., 2013a). In addition to the OST1 phosphorylation sites identified in this study, other putative SnRK2 phosphorylation sites, for instance EIEDDIAGYpS^{1629}EEpS^{1632}pS^{1633}EERNIDpS^{1640}NEEE, were previously identified in the C terminus of BRM that match the [acidic pS acidic] consensus (Umezawa et al., 2013, Wang et al., 2013a).

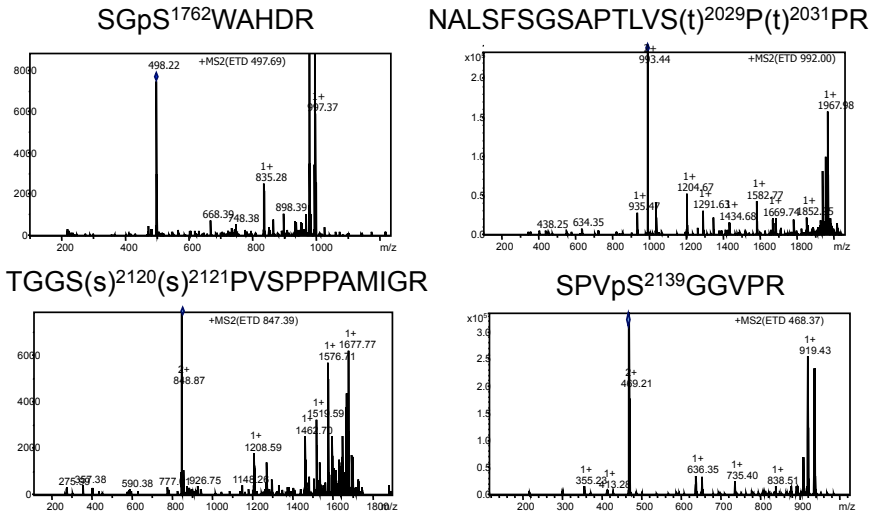

Figure 30. Identification of four phosphorylation sites in BRM C-terminal region. Spectra obtained by MS/MS of phosphorylated peptides are shown and annotated.

In summary, our *in vitro* phosphorylation assays together with *in vivo* phosphoproteomic studies indicate that the BRM C terminus is a hotspot for ABA-dependent phosphorylation (Supplemental Excel and Figure 31). We also provide direct evidence that OST1 is able to phosphorylate Ser1762 and Ser2139 residues, and either S2120/S2121 or T2029/2031 in the C-terminal part of BRM.

M[1]QSGGSGGGPARNPAMGPAGRTASTSSAASPSSSSSSVQQQQQQQQQQQQQQQQLASRQQQQQHRN
SDTNENMFAYQPGGVQGMMGGGNFASSPGSMQMPQQSRNFFESPQQQQQQQQQGSSTQEGQQNFN
PMQQAYIQFAMQAQHQKAQQQARMGMVGSSSVGKDQDARMGMLNMQDLNPSSQPQASSSKPSGDQ
FARGERQTESSSQQRNETKSHPQQQVGTGQLMPGNMIRPMQAPQAQQLVNNMGNNQLAFAQQWQA
MQAWARERNIDLSHPANASQMAHILQARMAAQQKAGEGNVASQSPSIPISSQPASSSVVPGENSP
HANSASDISGQSGSAKARHALSTGSFApSTSSPRMVNPAMNPFSGQGRENPMYPRHLVQPTNGMP
SGNPLQTSANETPVLDQNASTKKSLGPAEHLQMQQPRQLNTPTPNLVAPSDTGPLSNSSLQSGQG
TQQAQQRSGFTKQQLHVLKAQILAFRRLKKGEGSLPPELLQAISPPPLELQTQRQIpSPAIGKVQ
DRSSDKTGEDQARSLECGKESQAAApSSNGPIFSKEEDNVGDTEVALTTGHSQLFQNLGKEAT(S
)TDVATKEEQQTDVFPVKSDQGADSSTQKNPRSDSTADKGKAVASDG(S)QSKVPPQANpSPQPP
KDTASARKYYGPLFDFPFFTRKLDSYGSATANANNNLTLAYDIKDLICEEGAEFLSKKRTDSLKK
INGLLAKNLERKRIRPDLVLRLQIEEKKLRLSDLQSRVREEVDRQQQEIMSMPDRPYRKFVRLCE
RQRLEMNRQVLANQKAVREKQLKTIFQWRKKLLEAHWAIRDARTARNRGVAKYHEKMLREFSKRK
DDGRNKRMEALKNNDVERYREMLLEQQTNMPGDAAERYAVLSSFLTQTEDYLHKLGGKITATKNQ
QEVEEAANAAAVAARLQGLSEEEVRAAATCAREEVVIRNRFTEMNAPKENSSVNKYYTLAHAVNE
VVVRQPSMLQAGTLRDYQLVGLQWMLSLYNNKLNGILADEMGLGKTVQVMALIAYLMEFKGNYGP
HLIIVPNAVLVNWKSELHTWLPSVSCIYYVGTKDQRSKLFSQEVCAMKFNVLVTTYEFIMYDRSK
LSKVDWKYIIIDEAQRMKDRESVLARDLDRYRCQRRLLLTGTPLQNDLKELWSLLNLLLPDVFDN
RKAFHDWFAQPFQKEGPAHNIEDDWLETEKKVIVIHRLHQILEPFMLRRRVEDVEGSLPAKVSVV
LRCRMSAIQSAVYDWIKATGTLRVDPDDEKLRAQKNPIYQAKIYRTLNNRCMELRKACNHPLLNY
PYFNDFSKDFLVRSCGKLWILDRILIKLQRTGHRVLLFSTMTKLLDILEEYLQWRRLVYRRIDGT
TSLEDRESAIVDFNDPDTDCFIFLLSIRAAGRGLNLQTADTVVIYDPDPNPKNEEQAVARAHRIG
QTREVKVIYMEAVVEKLSSHQKEDELRSGGpS[1452]VDLEDDMAGKDRYIGSIEGLIRNNIQQYKID
MADEVINAGRFDQRTTHEERRMTLETLLHDEERYQETVHDVPSLHEVNRMIARSEEEVELFDQMD
EEFDWTEEMTNHEQVPKWLRASTREVNATVADLSKKPSKNMLSSpS[1593]NLIVQPGGPGGERKRGR
PKSKKINYKEIEDDIAGYpS[1629]EEpS[1632]pS[1633]EERNIDpS[1640]NEEEGDIRQFDDDELpT[1657]GA
LGDHQTNKGEFDGENPVCGYDYPPGSGSYKKNPPRDDAGSSGSSPE(S)HRSKEMApS[1714]PVpS[17
18]pS[1719]QKFGpS[1723]LSALDTRPGpS[1733]VSKRLLDDLEEGEIAASGDSHIDLQRpS[1760]GpS[1762]WA
HDRDEGDEEQVLQPTIKRKRSIRLRPRQTAERVDGSEMPAAQPLQVDRSYRSKLRTVVDSHSSRQ
DQSDSSSRLRSVPAKKVASTSKLHVSSPKSGRLNATQLTVEDNAEASRE(T)WDGpT[1883]pS[1884]P
IpS[1887](S)(S)NAGARMSHIIQKRCKIVISKLQRRIDKEGQQIVPMLTNLWKRIQNGYAAGGVNN
LLELREIDHRVERLEYAGVMELASDVQLMLRGAMQFYGFSHEVRSEAKKVHNLFFDLLKMSFPDT
DFREARNALSFSGSAPTLVpS[2028]pT[2029]PTPRGAGISQGKRQKLVNEPEpT[2051]EPpS[2054]pS[2055]P
QR(s)QQRENSRIRVQIPQKETKLGGTTSHTDESPILAHPGELVICKKKRKDREKSGPKTRpT[2116]
GGSpS[2120]pS[2121]PVpS[2124]PPPAMIGRGLRpS[2136]PVpS[2139]GGVPRETRLAQQQRWPNQPTHPNNS
GAAGDSVGWANPVKRLRTDSGKRRPSHL[2192]

Figure 31. BRM phosphopheptides in PhosPhAt 4.0 identified through *in vivo* phosphoproteomic studies and *in vitro* OST1 phosphorylation assays of BRM C2 and BRM C3 fragments. Green, phosphopeptides located in N terminal; blue and red, phosphopeptides located in C terminal; red highlighted-white writing, phosphorylation sites identified in this work after *in vitro* OST1 phosphorylation.

INTERPLAY AMONG ABA CORE ELEMENTS AND BRM

PYR/PYL ABA receptors impair the interaction of PP2CA with BRM

Our *in vitro* results indicated PP2CA was able to dephosphorylate the C-terminal region of BRM after its phosphorylation by OST1 only when PP2CA was not complexed with PYL8 in the presence of ABA (Figure 28). Moreover, *in planta* ABA treatment was able to prevent coIP of PP2CA with full-length BRM (Figure 25). These data prompted us to examine whether ABA and PYR/PYL ABA receptors modulate the direct interaction between BRM and PP2CA. Toward this end we employed a yeast three-hybrid (Y3H) approach (Brachmann & Boeke, 1997). As showed in the figure 32 the interaction between the GAL4 DNA-binding domain (GBD)-BRMN and the GAL4 transcriptional activation domain (GAD)-PP2CA was disrupted in an ABA-dependent manner by the presence of PYL4 or PYL5. ABA itself did not affect the interaction of BRMN and a well-known partner of BRM, namely the SWI3C subunit of the SWI/SNF chromatin-remodeling complex (Hurtado et al., 2006, Jerzmanowski, 2007) (Figure 32).

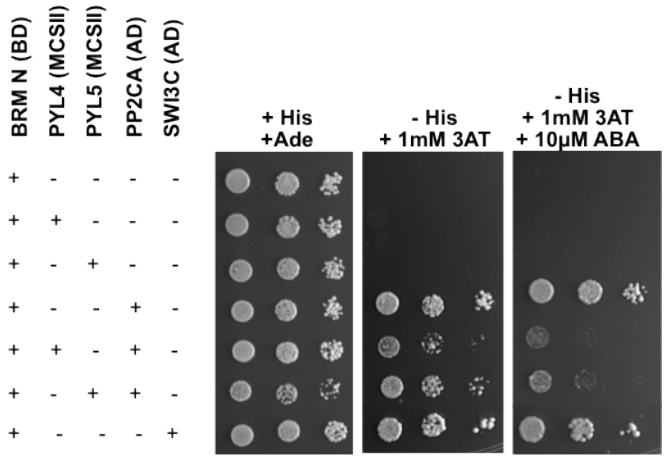

Figure 32. PYR/PYL ABA receptors block the interaction of PP2CA with BRM in an ABA-dependent manner. Dilutions (10^{-1}, 10^{-2}, and 10^{-3}) of saturated cultures were spotted onto the plates, and photographs were taken after 5 days. Interaction was determined by growth assay on medium lacking His, lacking His and supplemented with 0.1 mM 3AT and lacking His and supplemented with 0.1 mM 3AT and 10 µM ABA.

We also examined whether the interaction of SnRK2.3 with BRM was disrupted by the presence of PP2CA, which has been reported to interact with SnRK2.3 in Y2H assays (Umezawa et al., 2009). The presence of PP2CA did not disrupt the BRM–SnRK2.3 interaction (Figure 33). These results suggest that under basal low ABA levels, where PP2Cs are not forming stable ternary complexes with PYR/PYLs, the presence of free PP2C might not affect the interaction between SnRK2 and BRM, in agreement with the coIP results obtained in Figure 25. Under these conditions, however, the activation loop of SnRK2s is not phosphorylated and, hence, the kinase is not active (Fujii et al., 2009).

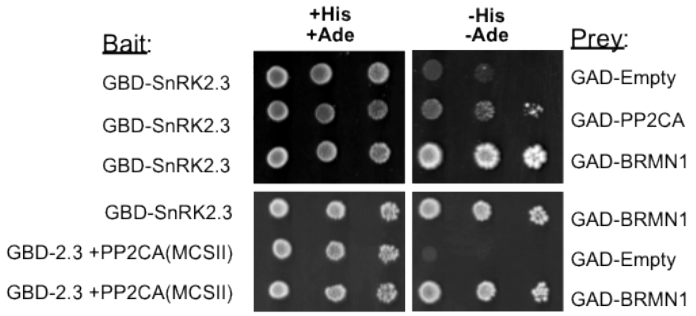

Figure 33. Presence of PP2CA does not interfere with the interaction between SnRK2.3 and BRMN in yeast. Dilutions (10^{-1}, 10^{-2}, and 10^{-3}) of saturated cultures were spotted onto the plates, and photographs were taken after 5 days. Interaction was determined by growth assay on medium lacking His and Ade.

BRM$^{S1760D\ S1762D}$ phosphomimetics display ABA hypersensitivity and increased *ABI5* expression

Because BRM represses ABA response during germination, in large part by preventing *ABI5* expression in the absence of ABA (Han et al., 2012), we hypothesized that phosphorylation of BRM by SnRK2s – key positive regulators of ABA signaling – might lead to inactivation of BRM and activation of ABA response. Direct biochemical assay of BRM chromatin-remodeling activity in the phosphorylated and non-phosphorylated form was not feasible because we could not obtain sufficient recombinant protein, either by expression in *E. coli* or insect cells using a baculovirus vector, to test *in vitro* remodeling activity. As an alternative approach to test the effect of SnRK2 phosphorylation on BRM activity and taking advantage of the phosphorylation sites identified, we designed a BRM phosphomimetic mutant where Ser residues were replaced

by aspartic acid (Asp, D). Negatively charged amino acids such as Asp or glutamic acid (Glu, E) can frequently mimic the effect of phosphorylated Ser (Konson et al., 2011). A BRM$^{\mathbf{S1760D\ S1762D}}$ phosphomimetic mutant was generated and introduced into the *brm-3* background under the control of its own promoter. Analysis of ABA-mediated inhibition of seed germination and seedling establishment assays revealed that transgenic lines expressing BRM$^{\mathbf{S1760D\ S1762D}}$ were ABA hypersensitive compared with wt (Figure 34).

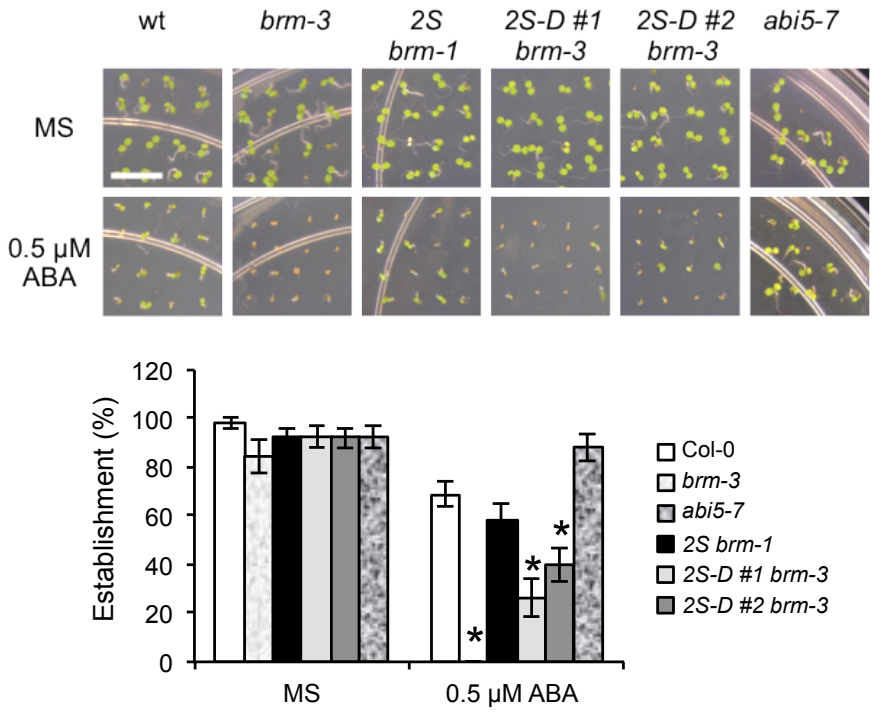

Figure 34. BRM phosphomimetic mutant (2S-D) shows ABA hypersensitivity during seedling establishment compared with wt, *brm-3* or *brm-1* mutant transformed with wt BRM (2S). Top: Photographs of the indicated genetic backgrounds grown for 4 days on

MS medium either lacking or supplemented with ABA. Scale bar corresponds to 0.5 cm. Bottom: Quantification of cotyledon greening 4 days after sowing. Values are averages of two independent biological experiments. The error bars are proportional to the standard error of the pooled percentage computed using binominal distribution. * indicates P<0.01 (Chi-squared test) compared with wt in the same assay conditions.

BRM$^{\mathbf{S1760A\ S1762A}}$ phosphomutant transgenic plants in the *brm-3* background, or BRM WT in a *brm* mutant background, by contrast, did not display ABA hypersensitivity (Figure 34 and 35).

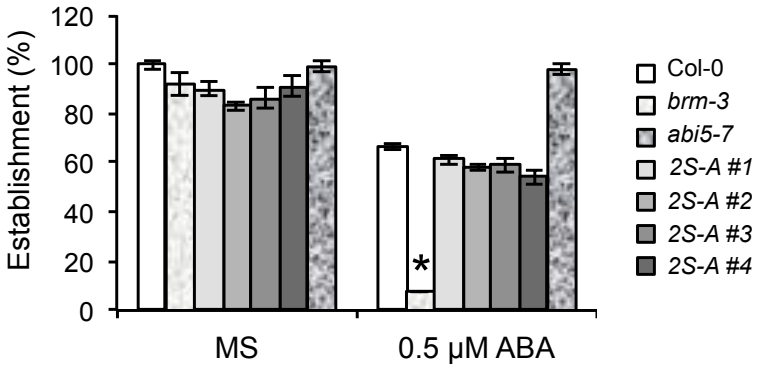

Figure 35. BRM$^{\mathbf{S1760A\ S1762A}}$ phosphomutant does not show ABA hypersensitivity during seedling establishment compared with wt. The error bars are proportional to the standard error of the pooled percentage computed using binominal distribution. * indicates P < 0.01 (Chi-squared test) compared with wt in the same assay conditions.

Moreover, the expression of a direct BRM target, *ABI5*, was elevated in BRM phosphomimetic mutant lines, relative to the wt (Figure 36). These results are consistent with the idea that phosphorylation of BRM leads to release of its inhibitory effect on ABI5 expression (Figure 37). Conversely, these results suggest that PP2C-mediated dephosphorylation of BRM serves to maintain its repressive effect on ABI5 expression.

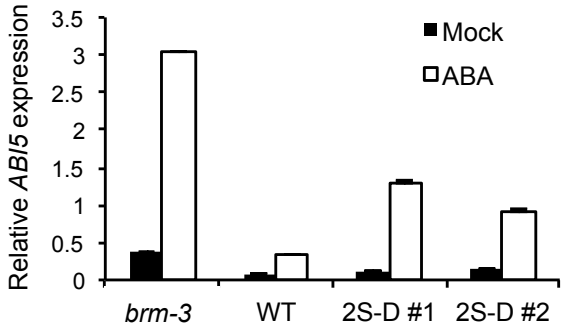

Figure 36. Expression of *ABI5* during seedling establishment in BRM phosphomimetic mutant compared to wt and *brm-3*. Two-day-old seedlings that were mock- or 50 µM ABA-treated for 1 h were used for *ABI5* expression analysis. The error bars are proportional to the standard error of the pooled percentage computed using binominal distribution.

A model integrating BRM regulation of the ABA signaling pathway is shown in figure 37, where BRM activity blocks *ABI5* expression when ABA levels are low or what is the same, when the environmental conditions do not require the activation of the stress response. In contrast, when drought stress occurs, ABA level rise and ABA signaling pathway is activated, activating at the same time the kinases that will phosphorylate BRM inducing its inhibition

and allowing ABI5 activation and the consequent activation of the ABA-regulated genes to face stress condition.

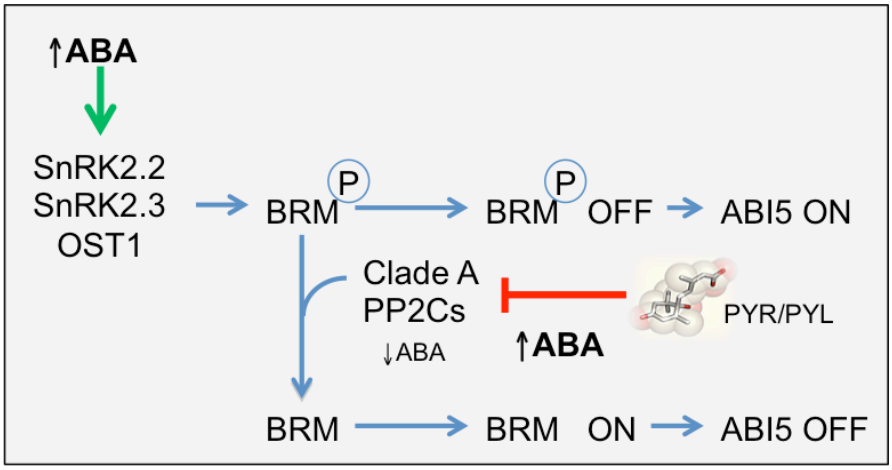

Figure 37. Model for the regulation of BRM activity through inhibitory SnRK2-dependent phosphorylation and restorative PP2C-dependent dephosphorylation. When ABA levels increase, SnRK2s are activated and clade A PP2Cs are inhibited by PYR/PYL ABA receptors. This allows SnRK2s to phosphorylate BRM, which leads to inhibition of BRM activity and *ABI5* induction. At low ABA levels, dephosphorylation of BRM by PP2CA/HAB1 restores BRM activity and repression of *ABI5* expression.

Chapter Two: The ABA signalosome interact with BRAHMA to regulate expression of ABI4 and early seedling establishment

BRM IS GENETICALLY AND PHYSICALLY RELATED WITH ABI4

Genetic Interaction between ABI4 and BRM

Loss of BRM activity leads to destabilization of a nucleosome involved in repression of ABI5 transcription and therefore ABI5 acts downstream of BRM in ABA signaling (Han et al., 2012). Reduction of BRM activity in the *brm-3* allele leads to enhanced expression of *ABI5* in 2-d-old seedlings and accordingly, *brm-3* is ABA-hypersensitive in ABA-mediated inhibition of cotyledon greening assays (Han et al., 2012). By contrast, the *brm-3 abi5-7* double mutant is not ABA hypersensitive and develops green cotyledons at 1 µM ABA, which otherwise fully inhibits cotyledon greening in *brm-3*. However, the *brm-3 abi5-7* double mutant is less sensitive to ABA-mediated inhibition of primary root growth than *brm-3*, but it is still partially inhibited by ABA, which suggests redundant activities of other ABA-dependent TFs. Since ABI4 plays a crucial role in regulating embryo responses to ABA, we investigated a possible connection between BRM and ABI4.

To this end we generated an *abi4 brm-3* double mutant by crossing the *abi4-T* (SALK_080095 line) (Shu et al., 2013) with *brm-3* mutant and analyzed the ABA response in germination and early seedling growth. Whereas *brm-3* was hypersensitive to 0.5 µM ABA, *abi4-T* was insensitive to 0.5 and 1 µM ABA. Interestingly, the *abi4 brm-3* double mutant was able to establish at 0.5-1 µM ABA as the *abi4-T* mutant (Figure 38). Thus, *abi4-T* is epistatic to *brm-3* and these data suggest BRM acts up-stream of ABI4.

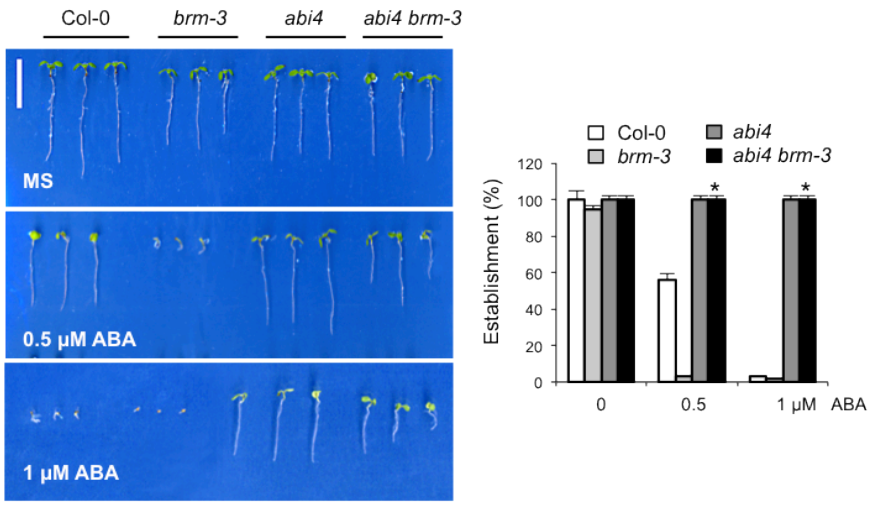

Figure 38. The ABA hypersensitive phenotype of *brm-3* is almost abolished in the *abi4 brm-3* double mutant. Right: Photographs of Col-0 wt, *brm-3*, *abi4* and *abi4 brm-3* mutants grown in MS medium lacking or supplemented with the indicated ABA concentrations. Seeds were germinated in plates lacking or supplemented with ABA, and after 8 days seedlings were rearranged on agar plates to illustrate seedling growth. Scale bar correspond to 1 cm. Left: Quantification of seedling establishment. Approximately 100 seeds of each genotype were sown in plates and scored for green cotyledons after 5 days. Values are averages ±SE of three independent experiments. * indicates $P < 0.05$ (Student's *t-test*) compared to *brm-3* mutant in the same assay conditions.

This result suggests that in addition to ABI5, ABI4 is also responsible of the *brm-3* ABA-hypersensitive phenotype and BRM might regulate ABI4 expression. Next we transfer 2-d-old seedlings germinated in MS medium to plates supplemented with 10 µM ABA and scored primary root growth after 10 days (Figure 39). The *abi4 brm-3* roots were significantly less sensitive to ABA-mediated inhibition of root growth than *brm-3*, which suggests that ABI4, as

well as ABI5, mediate ABA response in *brm-3* roots. The *abi4* single mutant was also less sensitive to ABA-mediated inhibition of root growth than wt, indicating that ABI4 is one of the redundant TFs that mediate ABA response in roots of seedlings (Finkelstein et al., 2005).

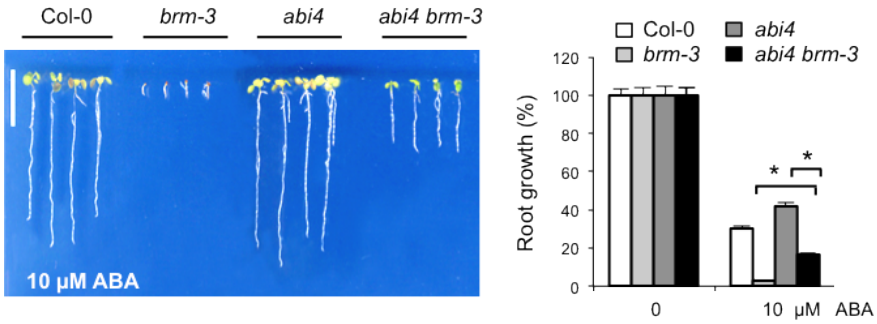

Figure 39. The ABA hypersensitive phenotype of *brm-3* is markedly reduced in the *abi4 brm-3* double mutant. Right: Photographs of the different genetic backgrounds seedlings analyzed that were germinated in MS media plates and grown for 2 days before were transferred to either new MS plates or MS supplemented with 10 µM ABA plates until the end of the experiment, 11 days after. Scale bar corresponds to 1 cm. Left: Quantification of ABA-mediated root growth inhibition in the indicated genetic backgrounds. Values are averages ±SE of three independent experiments. * indicates $P < 0.05$ (Student's *t-test*) comparing *abi4 brm-3* double mutant either with *brm-3* mutant or *abi4* mutant in the same assay conditions.

BRM regulates ABI4 through direct interaction with the *ABI4* promoter

The above data suggested that expression of *ABI4* might be regulated by BRM. However, the mechanism through which BRM regulates ABI4 was still unknown. First, we analyzed the level of *ABI4* by RT-qPCR in wt and *brm-3* mutant. We were interested in early seedling growth stage, when *ABI4* expression is up-regulated by stress, such as ABA or dehydrating responses (Finkelstein et al., 2011). We analyzed expression of *ABI4* by RT-qPCR in wt and *brm-3* and found that expression of *ABI4* was up-regulated in *brm-3*, thus suggests that BRM could act as a repressor of *ABI4* expression (Figure 40).

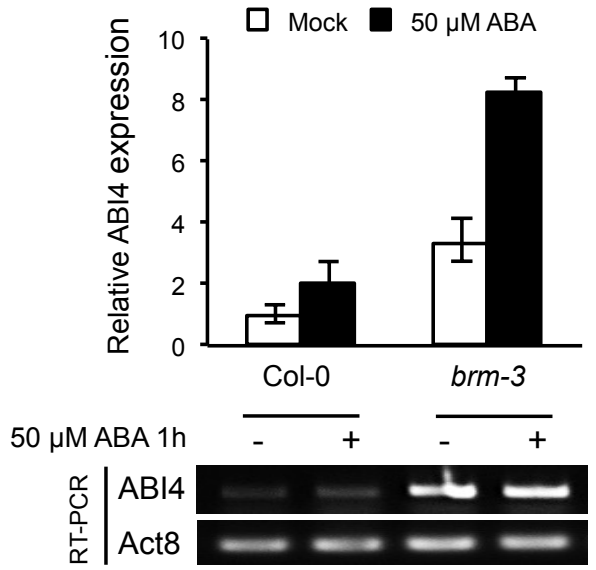

Figure 40. ABI4 expression in germinated embryos after 36 h growing in MS –sucrose medium. (Top) RT-qPCR analysis quantification and (Bottom) RT-PCR of *ABI4* expression showing the

induction of ABI4 in *brm-3* mutant in mock treatment and less induction after 1 h of 50 μM ABA treatment.

Since SWI2/SNF2 BRM complexes can repress transcription, we analyzed by chromatin immunoprecipitation (ChIP) whether BRM can bind to the ABI4 locus. To this end we used a *brm-1* ProBRM:BRM-HA line, where BRM-HA fully restores the *brm-1* null mutant (Han et al., 2012), as a substrate for ChIP. We detected binding of BRM to the *ABI4* promoter (Figure 41).

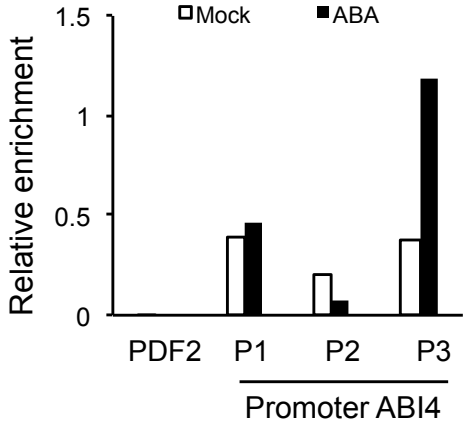

Figure 41. ChIP analysis data for ProABI4 in *ProBRM:BRM-HA* transgenic lines. qPCR after anti-HA ChIP in 36 h embryos of *brm-1* ProBRM:BRM-HA plants after mock or ABA (50 μM for 1 h). The relative enrichment represents the fold change respect to the input sample. Data were normalized over *PDF2* gene.

The association of BRM with the ABI4 locus together with the observed derepression of ABI4 expression in *brm-3* suggests that BRM directly regulates ABI4 expression. Next we performed data

mining on a genome-wide nucleosome positioning map of *Arabidopsis* obtained by massive sequencing of Micrococcal Nuclease digested nucleosomal DNA (Chodavarapu et al., 2010) that is a method for the analysis of DNA associated to nucleosomes. We found a well-positioned nucleosome in the region -501 to -364 of the *ABI4* promoter (coordinates 19798086-19797949, being 19797585 the beginning of the ATG start codon) (Figure 42). Therefore the ChIP data suggest the presence of the BRM in the *ABI4* promoter, which might be related to the presence of a well-position nucleosome in that region.

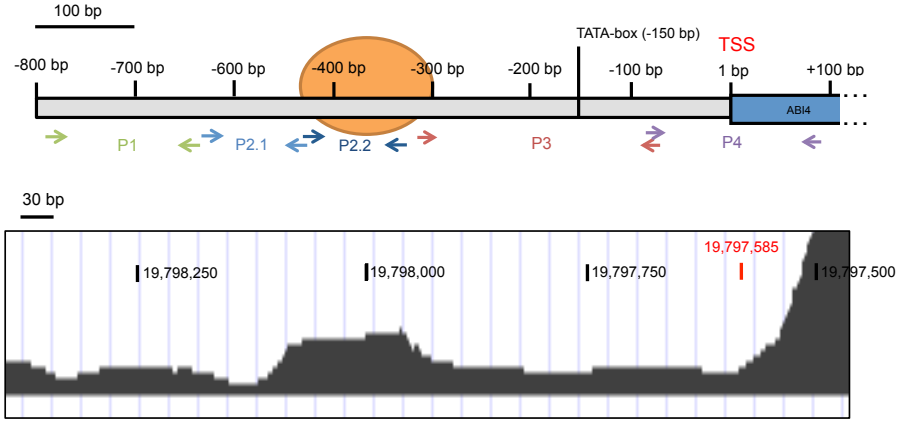

Figure 42. ABI4 promoter analysis. (A) Arrows indicate the primer pairs designed for the ChIP analysis. (B) Representative UCSC Browser screenshot of ABI4 promoter. (Chodavarapu et al., 2010)

BRM also interacts with PYR/PYL/RCAR ABA receptors

The data showed in the chapter one demonstrate that ABA-activated SnRK2s and clade A PP2Cs, which are core ABA signaling components, physically interact and modify BRM by phospho-/dephosphorylation, respectively. The interaction of PP2CA with BRM was abolished by ABA treatment (Figures 25 and 32), which indicates that ABA perception by PYR/PYL proteins disrupts the PP2CA-BRM interaction and suggests a close link between ABA receptors and BRM. Here, we have tested whether PYR/PYL proteins are able to interact with BRM. To this end we generated YFP^C-PYR1/PYL4/PYL5 protein fusions and tested their interaction with either BRMN-YFP^N (N-terminal 1-950 BRM residues) or YFP^N-BRMC (C-terminal 1541-2193 BRM residues) using BiFC assays in tobacco leaf epidermal cells and agroinfiltration. We found that all the receptors tested were able to interact with both BRMN and BRMC in the nucleus of tobacco cells (Figure 43A). As negative control we used a C-terminal deletion mutant of the SnRK2 OST1, which was unable to interact with both BRMN and BRMC. The interaction was nuclear and spread across the nucleoplasm, whereas the interaction with BRMC2C3 always showed nuclear speckles, which might represent specialized regions associated to chromatin.

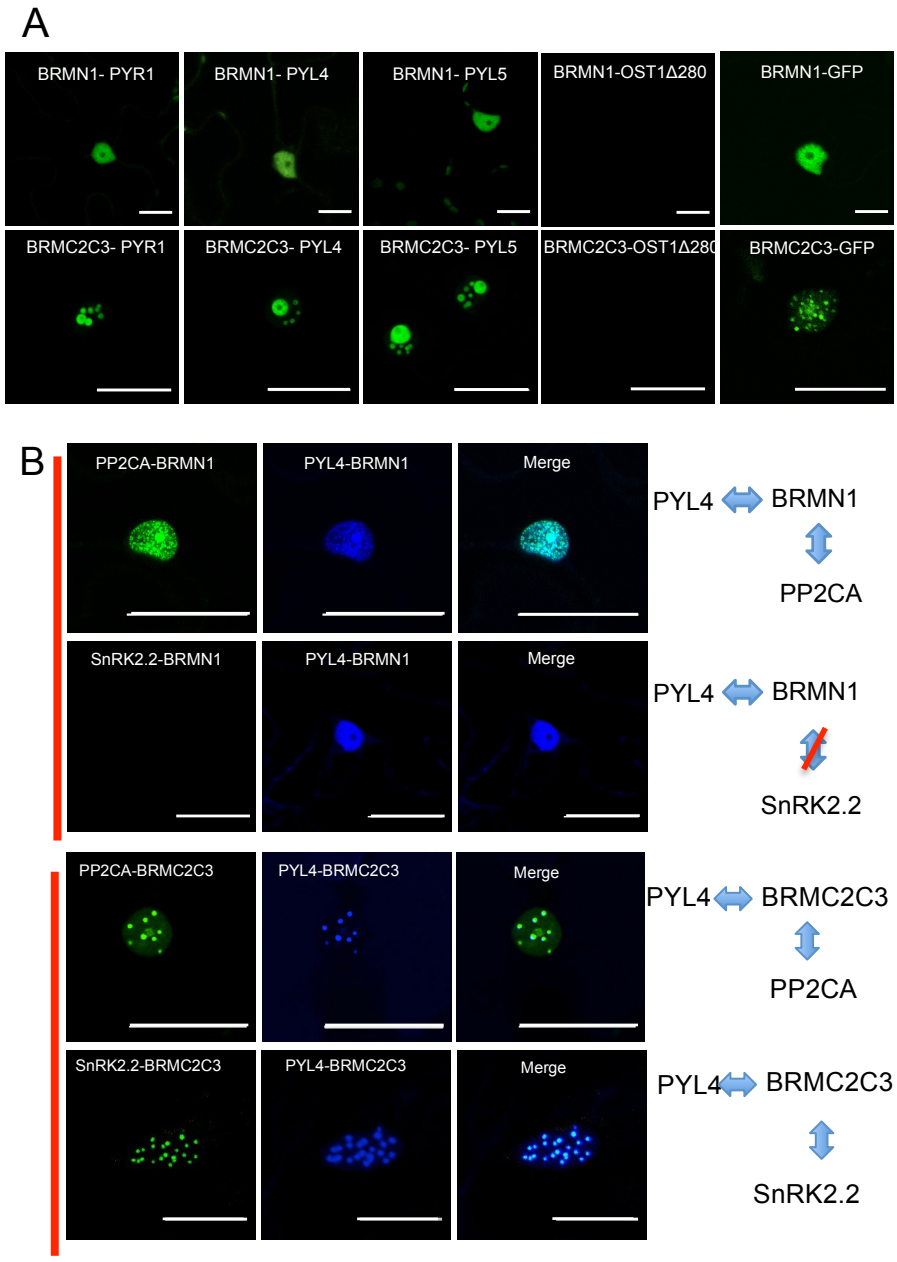

Figure 43. BiFC and mcBiFC assays show interaction of BRM with ABA signalosome in the nucleus of tobacco leaves. (A) BiFC confocal images of transiently transformed tobacco epidermal cells co-expressing BRMN1-YFP^{N} or YFP^{N}-BRMC2C3 and YFP^{C}-PYLs. The interaction of BRMN with all PYLs tested (top panels) was visualized in the

nucleoplasm, whereas the BRMC2C3-PYLs interaction (bottom panels) showed nuclear speckles. BRMN1/C2C3 and OST1Δ280 were used as negative controls and BRMN1/C2C3 fused to GFP as localization controls. (B) mcBiFC confocal images of transiently transformed tobacco epidermal cells co-expressing $SCFP^N$-PYL4, $VENUS^N$-PP2CA/$VENUS^N$-SnRK2.2 and $SCFP^C$-BRMN1 (top panels) and $SCFP^N$-PYL4, $VENUS^N$-PP2CA/ $VENUS^N$-SnRK2.2 and $SCFP^C$-BRMC2C3 (bottom panels). The interaction of BRMN1/BRMC2C3 with PP2CA and BRMN1/BRMC2C3 with SnRK2.2 gave rise to $VENUS^N$/$SCFP^C$ fluorescent protein that can be visualized in green, whereas the BRMN1/BRMC2C3-PYL4 interactions were visualized by the reconstitution of SCFP in blue. Scale bars correspond to 30 μm.

We have demonstrated previously that both PP2CA and SnRK2.2 were able to interact with BRM (Peirats-Llobet et al., 2016). The above results shows that ABA receptors also interact with BRM, which suggests the whole ABA signalosome formed by ABA receptors, PP2Cs and SnRK2s can interact with the BRM platform to regulate BRM activity. In order to test whether both PP2CA and the ABA receptor PYL4 can interact simultaneously with BRM, we performed multicolor BiFC (mcBiFC) (Gehl et al., 2009). This technique uses different BiFC vectors that are compatible among them and allows the visualization of two simultaneous interactions of a protein using two different colors (Waadt et al., 2008, Gehl et al., 2009). We cloned BRMN1/BRMC2C3 into *p(MAS)-SCYCE,* PYL4 into *pDEST-SCYNE(R)* and PP2CA into *pDEST-VYNE(R)* vectors (Gehl et al., 2009, Waadt & Kudla, 2008). The interaction of the N-terminal part of the supercyan fluorescence protein ($SCFP^N$) and the C-terminal part, $SCFP^C$, results in reconstitution of SCFP

(477 nm fluorescence) whereas interaction of $Venus^N$ and $SCFP^C$ generates green (515 nm) fluorescence.

As a result, we found interaction of BRMN1 or BRMC2C3 with PYL4, which was visualized by the reconstitution of SCFP (cyan), whereas the BRMN1- or BRMC2C3-PP2CA interactions gave rise to $VENUS^N$/$SCFP^C$ fluorescent protein (visualized in green). The complex PYL4-BRMN1-PP2CA could be visualized along the nucleoplasm, whereas the complex PYL4-BRMC2C3-PP2CA was concentrated in nuclear speckles (Figure 43B, first and third panels). On the other hand we could detect simultaneous interaction of BRMC2C3 with SnRK2.2 and PYL4 but no interaction between SnRK2.2 and BRMN1 could be detected in presence of PYL4, which suggests that SnRK2.2 is targeted to the C-terminal region of BRM in presence of PYL4 (Figure 43B, second and forth panels). We have demonstrated previously that PYL4, in presence of ABA, prevents the interaction of PP2CA with full length BRM (Peirats-Llobet et al., 2016). Since PYL4 targets SnRK2.2 to the C-terminal region of BRM, which is a hotspot for ABA-dependent phosphorylation, and prevents the interaction between PP2CA and BRM in presence of ABA, these results support a model where BRM is phosphorylated by SnRK2.2 in an ABA- and receptor-dependent manner (Figure 44).

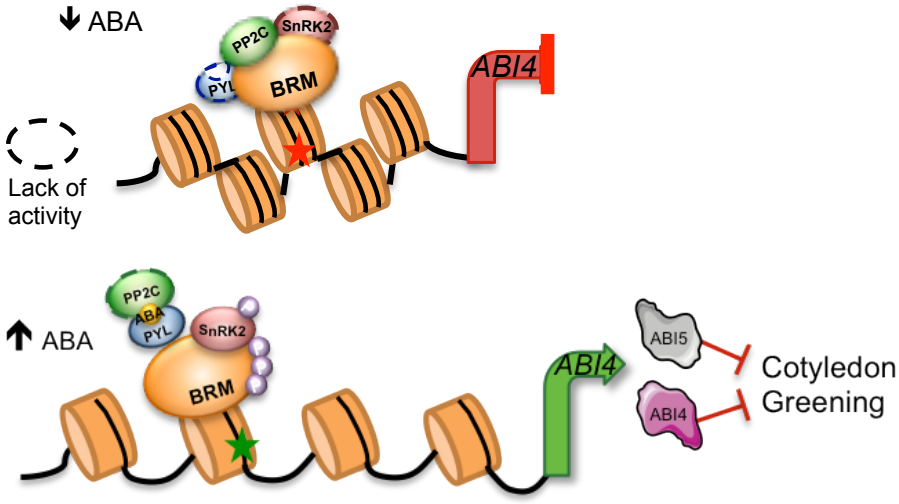

Figure 44. Suggested model for BRM function in ABI4 promoter. Top: With low levels of ABA, PP2CAs are active and blocking SnRK2s, BRM is also active to block *ABI4* expression. Bottom: With high ABA levels, PYR/PYLs bind ABA and are able to inhibit PP2Cs that will release SnRK2s that now will phosphorylate BRM. Phosphorylated BRM is inactive and *ABI4* can be expressed.

Figure 44 illustrates a model summarizing these novel data. Under low levels of ABA (Figure 44, top), data suggests BRM is interacting with PP2CA, SnRKs and PYR/PYLs at the same time, and this interaction blockade the transcription of ABA responsive genes, as *ABI4* gene in this model. When ABA levels are higher (Figure 44, bottom) PYR/PYLs interact with ABA and recruit PP2Cs in a ternary complex. But at the same time, PYR/PYL ABA receptors could be interacting with BRM protein. Moreover, SnRKs that are already interacting with BRM, now are active and can phosphorylate BRM leading to a reduction of BRM activity allowing the transcription of ABA related genes to occur.

Chapter Three: Characterization and biotechnological use of PP2CA promoter in *A. thaliana*

PP2CA PROMOTER CHARACTERIZATION

Expression pattern of *PP2CA* promoter

In contrast to ABA receptors (Gonzalez-Guzman et al., 2012) the spatio-temporal expression patterns of clade A PP2Cs are not well known for most of them. We focused our work to get a deeper knowledge of *PP2CA* expression pattern. PP2CA plays a key role in ABA signaling (Sheen, 1998, Kuhn et al., 2006, Yoshida et al., 2006) and additionally we discovered in chapter one a new role of PP2CA as regulator of BRM phosphorylation. To investigate *PP2CA* expression pattern we fusioned the promoter sequence of *PP2CA* to the GUS reporter (*ProPP2CA:GUS* construct). The *ProPP2CA* fragment, comprising 2000 base pairs 5‘ upstream of the ATG start codon of the *PP2CA* gene (AT3G11410), was amplified by PCR and cloned into *pCR8®/GW/TOPO®* vector. The PCR-generated DNA fragment was cloned into *pMDC163* vector by LR reaction (Curtis & Grossniklaus, 2003) to drive expression of the GUS gene (Figure 45). The final construct was transferred to *A. tumefaciens* by electroporation and used to transform Col-0 plants by the floral dip method (Clough & Bent, 1998). T1 seeds were selected by using 25 mg/mL hygromycin antibiotic. T1 resistant seedlings were transferred to the green house and grown in LD conditions to generate T2 seeds. These T2 seeds were again selected in hygromycin medium in order to obtain T3 homozygous progeny and that will be used for following studies.

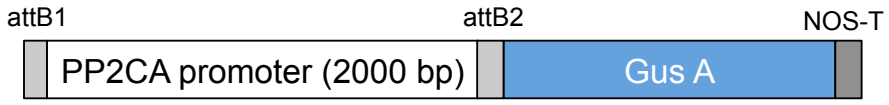

Figure 45. Construction for *ProPP2CA* fused to Gus A reporter gene with NOS terminator in *pMDC163* vector. *PP2CA* promoter comprises 2000 bp upstream ATG of *PP2CA*. The fragment was cloned into *pMDC163 GW* vector.

The analysis of the promoter of *PP2CA* gene showed expression in embryos, roots, guard cells and vascular tissue along the *A. thaliana* seedlings (Figure 46). The GUS expression was induced within 2 h of treatment with 10 µM ABA in most of the tissues as previously reported for the protein phosphatase HAB1 (Saez et al., 2004). GUS expression was induced by ABA treatment in 48 h-germinated embryos mainly along the radicle (Figure 46B) and also in leaves and stomata of 8 days-old seedlings (Figure 46D and 46F). In contrast, the expression in the hypocotyl junction showed no significant difference after ABA treatments (Figure 46G-H). *PP2CA* expression was found in root tip of 48 h-germinated embryos either with or without ABA treatment, but the expression was clearly up regulated after ABA treatment (Figure 46I-J). Staining of seed coats from 48-h imbibed seeds also detected up regulation of GUS expression in the endosperm (Figure 46K-L). The *PP2CA* was differentially expressed along the root. In fact, mature zones of the roots showed higher levels of GUS protein (Figure 46O-P) than immature ones (Figure 46Q-R). Interestingly, GUS signal appears in the elongation zone of the root and seems to be excluded from the meristematic zone. Curiously, the expression is up regulated in the root cap where the columella cells

are found, after ABA treatment (Figure 46S-T). The vasculature of the root, the stele, shows induction of GUS expression after ABA treatment. Altogether, these results indicate that expression of *PP2CA* is up-regulated by ABA in most of the plant tissues. Expression in seed and seedlings is in agreement with the relevant role of PP2CA in the regulation of seed germination and establishment (Yoshida et al., 2006, Kuhn et al., 2006). Additionally, the observed expression in other tissues indicates that PP2CA can be a global regulator of ABA signaling.

Propidium iodide pseudo shift (PS-PI) staining technique was also used to visualize the root tip with more detail (Truernit et al., 2008). Expression of *PP2CA* was up-regulated by ABA and localized in the stele (Figure 47A). This technique does not allow a correct visualization of the columella due to the background generated by the amyloplasts. Interestingly, Antoni et al. (2013) described that GUS expression driven by several promoters of the PYR/PYL/RCAR receptors is also localized in the stele (Figure 47B) whereas ProPYL8 is found in epidermis in addition to the stele. These results indicate an overlap in the expression patters of phosphatases and receptors that could be important for an efficient ABA signaling.

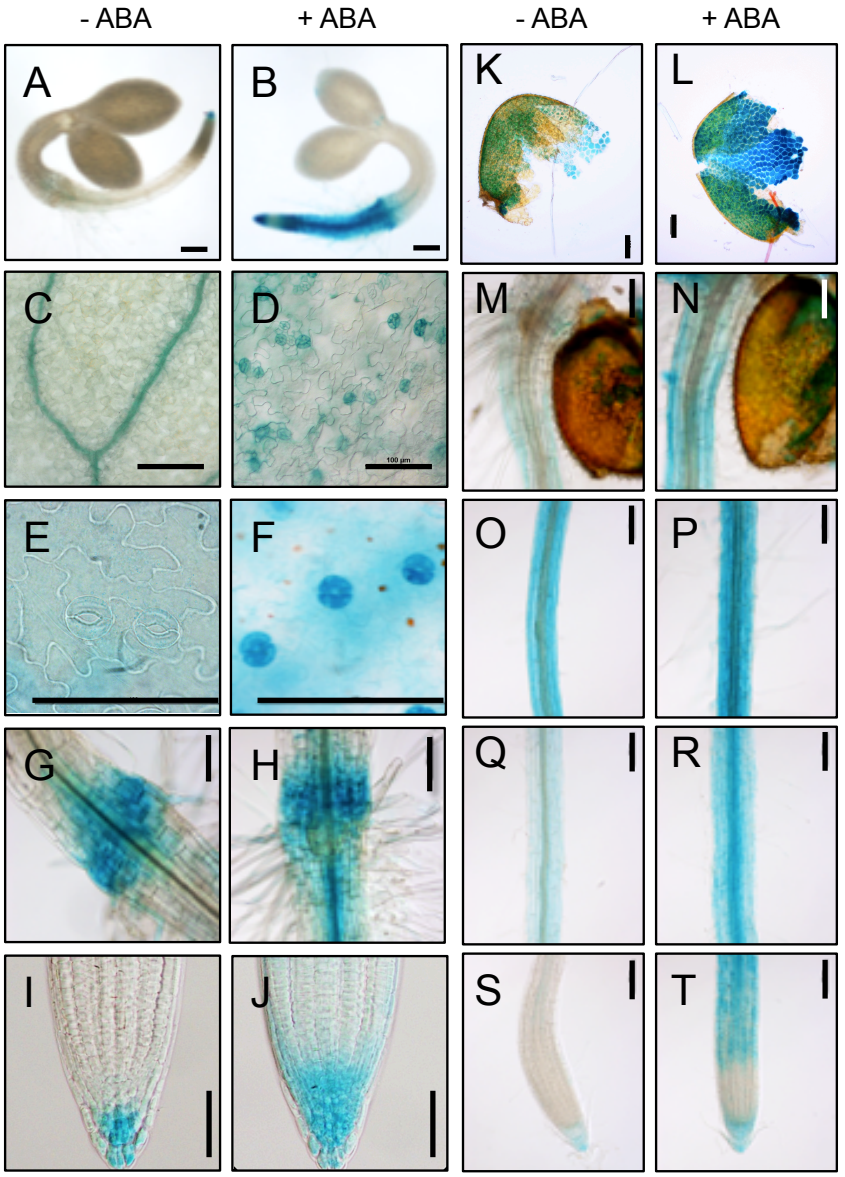

Figure 46. Images showing GUS expression driven by *ProPP2CA:GUS* gene in different tissues and developmental stages. Scale bar = 100 µm. The generation of *ProPP2CA:GUS* lines and imaging of histochemical GUS staining was performed as described in Gonzalez-Guzman et al. (2012). Material was mock or 10 µM ABA-treated for 2 h. (A) Mock and (B) ABA-treated 48 h embryos; (C) mock and (D) ABA-

treated leaves; (E) mock and (F) ABA-treated guard cells in leaves of 8-d-old seedlings; (G) mock and (H) ABA-treated root-hypocotyl junction; (I) mock and (J) ABA-treated root tips; (K) mock and (L) ABA-treated endosperms of embryos imbibed for 48 h; (M) mock and (N) ABA-treated hypocotyl; (O) mock and (P) ABA-treated mature root; (Q) mock and (R) ABA-treated root at the elongation zone; (S) mock and (T) ABA-treated root tips.

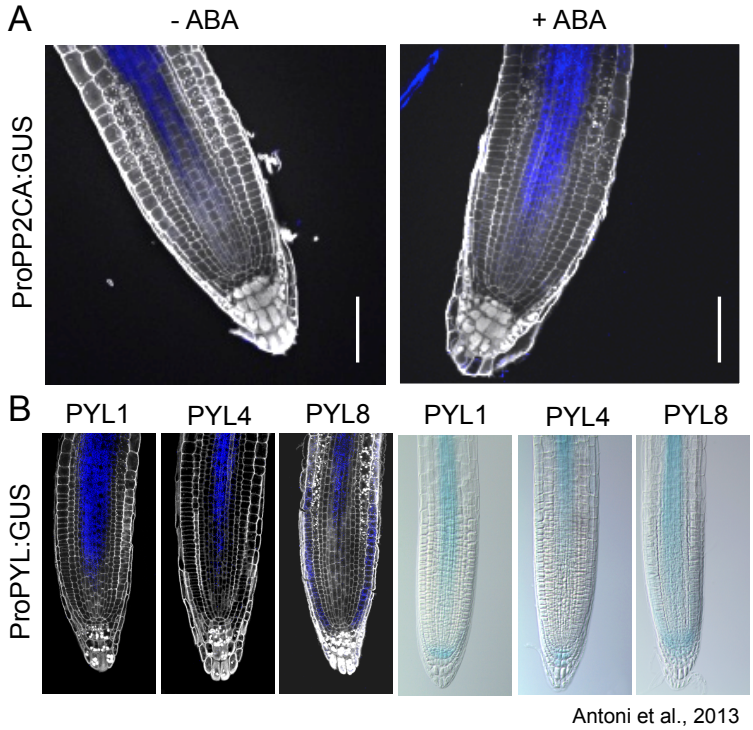

Figure 47. Core ABA-signaling element promoters driving the expression of GUS reporter gene in root tips of *A. thaliana* seedlings. GUS expression is visualized using modified PS-PI staining and confocal laser scanning microscopy. (A) ABA-inducible GUS expression driven by ProPP2CA. Seedlings of 8-d-old were treated with 10 μM ABA for 2 h. (B) GUS expression driven by PYR/PYLs promoters in the root tip (Antoni et al., 2013). The expression of GUS protein is localized in the stele in all the

PYR/PYL receptors, but also in the epidermis of ProPYL8. Scale bar = 100 µm.

After the analysis of *PP2CA* expression, we generated transgenic plants expressing HA-tagged PP2CA fusion protein driven by its own promoter in a *pp2ca-1* background. We generated this material because PP2CA protein dynamics were not known at the beginning of this work.

PP2CA PROTEIN DYNAMICS

ProPP2CA drives the expression of *PP2CA* in *pp2ca-1 A. thaliana* mutant

pALLIGATOR2 vector (Bensmihen et al., 2004) was digested using HindIII-SacI enzymes to remove 35S promoter and 1 out of 3 of the HA tags. The *PP2CA* promoter sequence was excised from *pCR8-ProPP2CA* using a double HindIII-SacI digestion and ligated to double digested *pAlligator2* to generate the construct *pALLIGATOR2-ProPP2CA:2HA*. Next, the open reading frame of *PP2CA* from *pCR8-PP2CA* (Antoni et al., 2012) was recombined by LR reaction into *pALLIGATOR2-ProPP2CA:2HA* to obtain *pALLIGATOR2-ProPP2CA:2HA-PP2CA* (Figure 48). The final construct in *pALLIGATOR2* vector was transferred to *A. tumefaciens* by electroporation and used to transform *pp2ca-1* plants by the floral dip method (Clough & Bent, 1998). T1 seeds generated were selected via the GFP expression driven by the At2S3 seed-specific promoter (Bensmihen et al., 2004) under GFP filter in the microscope. 100% GFP positive T3 lines were used for the following studies.

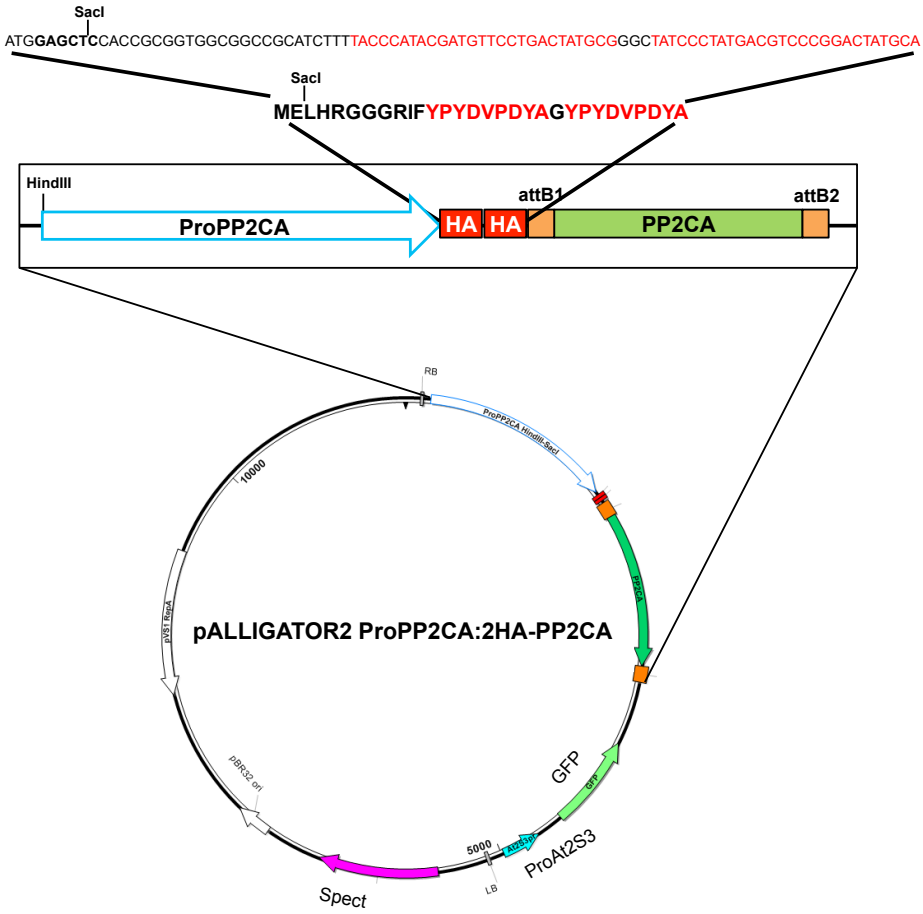

Figure 48. *pALLIGATOR2-ProPP2CA:2HA-PP2CA* expression vector generated by SeqBuilder software (DNASTAR® Lasergene). *ProAt2S3* corresponds to a seed specific promoter; GFP is the marker gene for seed selection; Spectinomycin resistance is used for bacterial selection.

Three independent transgenic *A. thaliana* lines expressing *PP2CA* driven by the *PP2CA* promoter in *pp2ca-1* background were selected. We studied the accumulation of PP2CA in those lines and we found that PP2CA protein was hardly detectable unless ABA treatment was performed. Additionally, the expected molecular

weight of the protein was close to that of the Rubisco large subunit, which might generate some problems for detection by immunoblot analysis. Therefore, we isolated roots from ABA-treated plants in all our experiments in order to obtain Rubisco-free protein samples. Additionally, *ProPP2CA:2HA-PP2CA* seedlings were treated with 50 µM ABA + 50 µM MG-132 for 3 h (Figure 49).

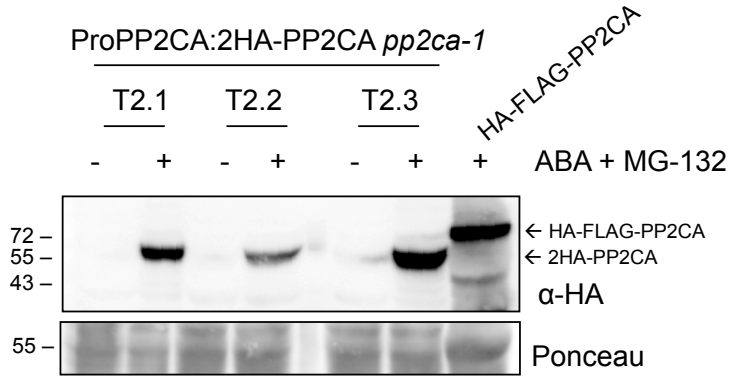

Figure 49. Expression of PP2CA is induced by ABA in root tissue of *ProPP2CA:2HA-PP2CA* transgenic lines. Root material from 12-d-old plants was mock (+) or treated with 50 µM ABA + 50 µM MG-132 (+) for 3 h. *35S:HA-FLAG PP2CA* (Wu et al., 2016) leaf material treated with 50 µM ABA + 50 µM MG-132 for 3 h was used as positive control. WB analysis was performed using anti-HA.

Western blot analysis revealed low to undetectable expression of PP2CA in roots in the absence of ABA treatment. However, the expression was markedly induced upon ABA treatment in the three independent lines in agreement with the expression of the GUS reporter driven by the *PP2CA* promoter (Figure 46).

PP2CA degradation is induced by ABA

The up-regulation of PP2CA (this thesis) and other clade A PP2Cs in response to ABA (Santiago et al., 2009b, Szostkiewicz et al., 2010), suggests the existence of a negative feedback mechanism to modulate ABA signaling. To analyze PP2CA protein dynamics *in vivo* we also used *Pro35S:HA-PP2CA* lines (Antoni et al., 2012) to avoid ABA up-regulation of the *PP2CA* promoter. We treated 10-d-old seedlings with different drugs, 100 µM CHX, 50 µM MG-132 or 50 µM ABA and took samples at several time points (4, 7 and 9 h).

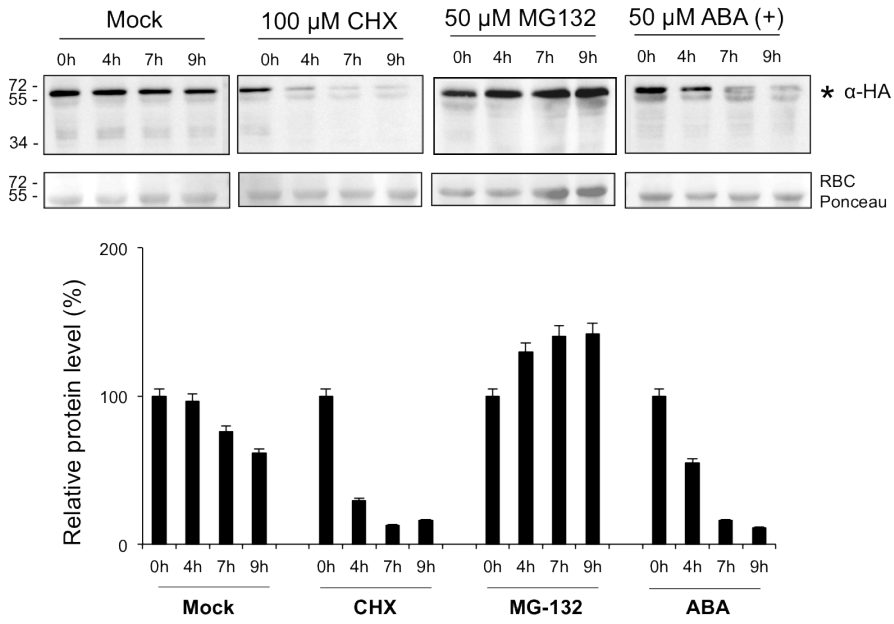

Figure 50. Effect of CHX, MG-132 and ABA treatment on PP2CA protein level. Top panel, 10-d-old seedlings expressing HA-tagged PP2CA protein were either mock- or chemically treated with 100 µM CHX, 50 µM MG-132 or 50 µM ABA for the indicated time period. Bottom panel, Histogram shows quantification of the anti-HA immunoblot. Error bars correspond to averages of relative intensity of the bands. The data analysis was performed by ImageJ analysis software.

Interestingly, PP2CA protein level was found to diminish with CHX and ABA treatments whereas the protein accumulates with MG-132 treatment (Figure 50). These results suggest that PP2CA is degraded via the 26S proteasome. Moreover, ABA treatment induces PP2CA degradation when the protein expression was driven by a *35S* promoter. These results opened new questions to be explored.

Next, we analyzed PP2CA ABA-dependent degradation, by carrying out a degradation kinetic assay performed as described in the figure 51, using the transgenic lines expressing PP2CA driven by its own promoter, *ProPP2CA:2HA-PP2CA*. The material was pre-treated with 50 μM ABA for 3 h in order to induce and accumulate PP2CA protein before drug treatments.

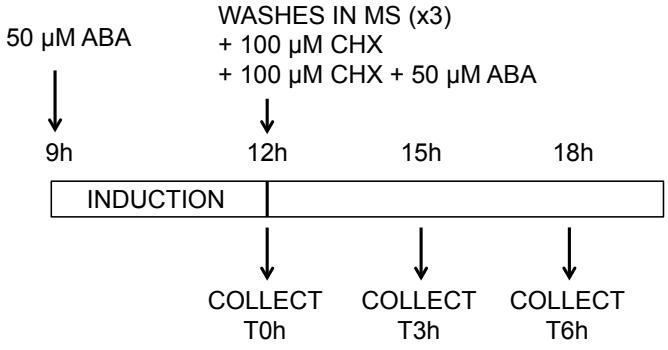

Figure 51. Experimental design for PP2CA degradation assay. The samples were pre-treatment with 50 μM ABA for 3 h and then, washed 3 times with MS media to remove all the residual ABA. The experimental treatments with 100 μM CHX or 100 μM CHX + 50 μM ABA were applied for 3 and 6 h. The treated material was frozen in liquid nitrogen until future processing.

After treating the plants with the translation inhibitor, CHX, for 3 h, all PP2CA protein was degraded (Figure 52A). This result suggested a fast turnover of PP2CA. Therefore, we repeated the experiment using a shorter time-course. We applied 20 min lapses between each material collection (Figure 52B). The results confirmed a quick degradation of PP2CA protein indicating that the protein has a short half-life. After 1 h of treatment with CHX most of the PP2CA protein is degraded. To further analyze ABA effect on PP2CA stability we also compared PP2CA protein levels in CHX-treated seedlings in the absence (CHX) or in the presence of exogenous ABA (CHX+ABA). CHX treatment showed a rapid degradation of PP2CA, whereas the combined treatment with CHX and ABA did not show a significant difference at 40-60 min. At 20 min, enhanced degradation was observed after CHX+ABA treatment. These data suggest that ABA promotes PP2CA protein degradation. However, since these experiments were performed using transgenic plants we could not conclude that PP2CA protein accumulation patterns were the same as in wild type plants. To this end, we developed a specific PP2CA antibody in collaboration with Professor An's lab.

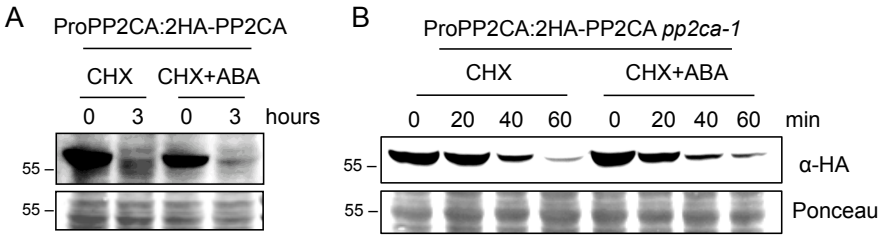

Figure 52. PP2CA protein is degraded *in vivo*. 10-d-old seedlings expressing HA-tagged PP2CA protein were pre-treated with 50 µM ABA for 3 h and either mock- or chemically treated with 100 µM CHX or 100 µM CHX + 50 µM ABA for the indicated time periods. WB analysis of root tissue was performed using anti-HA. A) Root material treated for 3 h with CHX or CHX + ABA. B) Short time course experiment (20, 40 and 60 min) treated with CHX or CHX + ABA.

The ProPP2CA:2HA-PP2CA *pp2ca-1* line was a crucial material for the high-throughput screening of crude PP2CA antibodies generated by our colleges at Peking University. Figure 53A shows a PP2CA antibody that was successfully used in our laboratory for detection of PP2CA. Next, Professor An group assayed antigen-affinity purified antibodies in protein samples of Col and *pp2ca-1*, obtaining the α-E2663 antibody for detection of endogenous PP2CA (Figure 53B).

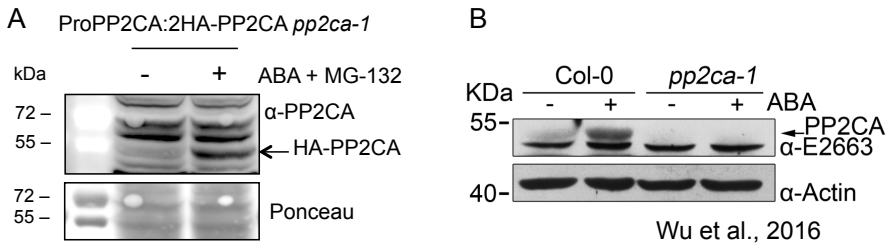

Figure 53. α-E2663 is a specific antibody for PP2CA. (A) Crude extract of α-PP2CA identified HA tagged PP2CA. Root material from 12-d-old ProPP2CA:2HA-PP2CA *pp2ca-1* seedlings were treated without (-) or with (+) 50 μM ABA for 3 h. Total proteins were extracted and equal protein amounts of each treatment were subjected to western blot analysis. α-PP2CA was used to detect HA-PP2CA with a dilution of 1:8000. HA-PP2CA (arrow) was markedly induced by ABA treatment. (B) Purified α-E2663 antibody. 2-week-old Col-0 and *pp2ca-1* etiolated seedlings were treated without (-) or with (+) 50 μM ABA for 6 h in darkness. Then total proteins were extracted and equal amounts of each treatment were subjected to western blot analysis. α-E2663 was used to detect endogenous PP2CA with a dilution of 1:3500. anti-Actin was analyzed as a loading control. Endogenous PP2CA (arrow) was detected in Col-0 and it was markedly induced by ABA treatment, whereas it was absent in *pp2ca-1* mutant (-/+ABA).

ProPP2CA AS AN INDUCIBLE PROMOTER FOR PROTEIN EXPRESSION

ProPP2CA drives stress-inducible expression of *Arabidopsis thaliana* and *Solanum lycopersicum* ABA receptors

Overexpression of monomeric ABA receptors confers drought tolerance (Santiago et al., 2009b, Gonzalez-Guzman et al., 2014, Yan & Chen, 2016, Yang et al., 2016b), but a penalty on growth under normal conditions has been described in some cases (Kim et al., 2014). Expression driven by an ABA-inducible promoter might solve this problem. To this aim, we decided to use the PP2CA promoter to drive inducible expression of ABA receptors. A previous study from Pizzio et al. (2013) had showed that PYL4 (AT2G38310) is an important ABA receptor for enhancing drought tolerance in *A. thaliana* plants. The mutant version of PYL4, named as PYL4^{A194T}, was more sensitive to ABA than the wild type version of the receptor. Transgenic plants overexpressing the mutant receptor PYL4^{A194T} were hypersensitive to ABA in different stages of development but also displayed reduced water-loss and enhanced drought tolerance (Pizzio et al., 2013).

In crops, constitutive overexpression of ABA receptors might impair growth in the absence of stress. Therefore, we decided to generate PYL4^{A194T} overexpressing plants using the ABA-inducible PP2CA promoter. At the same time, the work of Gonzalez-Guzman et al. (2014) identified and characterized tomato PYR/PYL receptors. Monomeric tomato receptors were highly expressed in roots and

able to enhance plant drought resistance (Gonzalez-Guzman et al., 2014). We selected Sl3g007310 a good candidate for inducible expression.

Our previous construct, *pALLIGATOR2-ProPP2CA:2HA*, was used to generate constructs where the above ABA receptors were driven by the ABA-inducible PP2CA promoter. To this end, *pCR8-PYL4* and *pCR8-PYL4^{A194T}* generated by Pizzio et al. (2013) and *pCR8-Sl3g007310* were recombined by LR reaction to generate the constructs showed in the figure 10. The constructs *pALLIGATOR2-ProPP2CA:2HA-PYLs* were transferred to *A. tumefaciens* by electroporation and used to transform Col-0 wild type plants by the floral dip method (Clough & Bent, 1998). T1 seeds generated were selected via the GFP expression driven by the At2S3 seed-specific promoter (Bensmihen et al., 2004) under GFP filter in the microscope. 100% GFP T3 lines were used for the following studies.

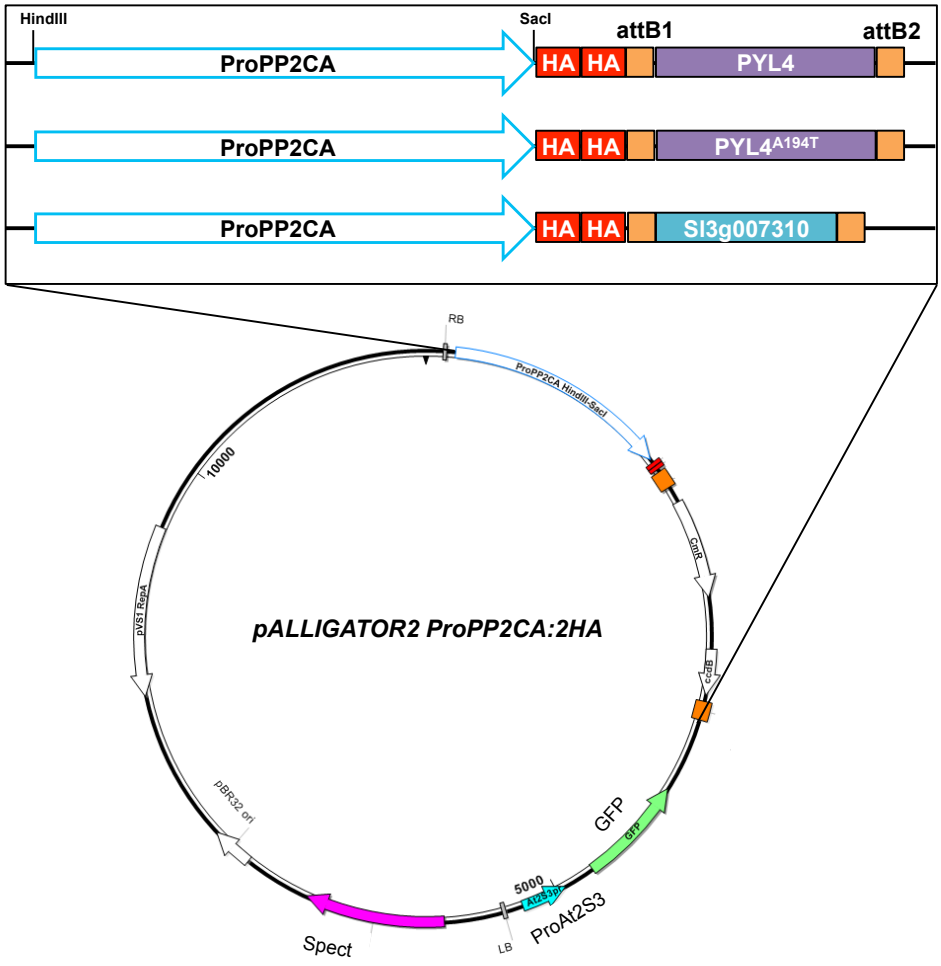

Figure 54. *ProPP2CA* fusions to different ABA receptors in *pALLIGATOR2*. PYL4 and PYL4^{A194T} are *A. thaliana* ABA receptors and Sl3g007310 is a *S. lycopersicum* ABA receptor. All the constructs expressed proteins tagged with HA tags for WB analysis.

First, we checked the inducible expression of of receptors driven by the PP2CA promoter under greenhouse conditions. Transgenic lines containing the *ProPP2CA* fused to *PYL4* and the mutant version, *PYL4*^{A194T}, were analyzed by WB. The results of the analysis of leaf material showed a strong ABA-inducible expression in both receptor lines (Figure 55).

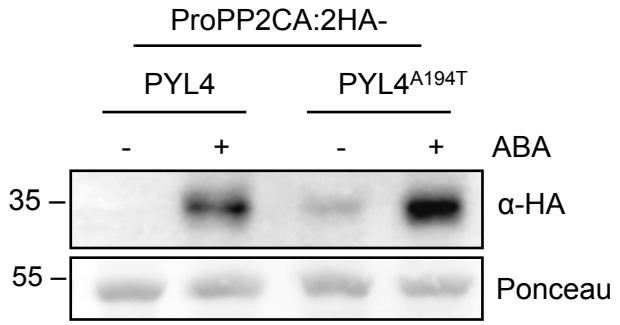

Figure 55. Inducible expression of the receptors PYL4 and PYL4^{A194T} driven by *ProPP2CA*. 3 weeks-old plants grown in the greenhouse were mock (-) or sprayed with 100 μM ABA (+) solution every hour during 3 h. WB analysis was performed using anti-HA antibody.

Additionally, we carried out a time-course experiment to analyze the ABA induction in transgenic lines expressing PYL4, PYL4^{A194T} and Sl3g007310 receptors. Seedlings of the transgenic lines were grown in liquid culture for 12 days and treated with 50 μM ABA for the indicated time periods. Figure 56 shows ABA-inducible expression of PYL4, PYL4^{A194T} and Sl3g007310 receptors. These lines showed undetectable or very low expression in mock conditions whereas high induction was observed after the ABA treatment.

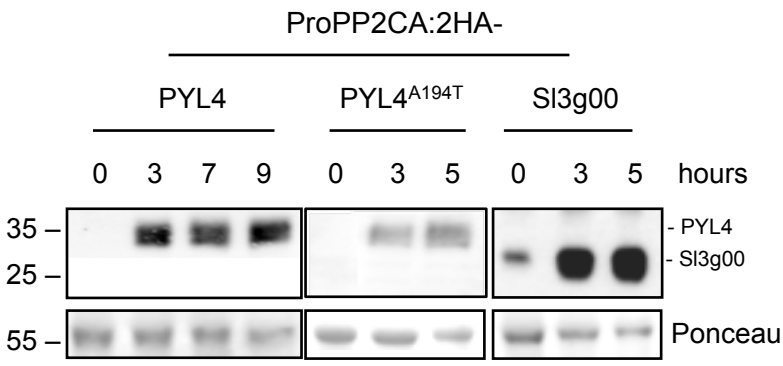

Figure 56. Inducible expression of ABA receptors from *A. thaliana* and *S. lycopersicum* directed by ProPP2CA in *A. thaliana* transgenic stable lines. Protein extracts from plants were grown in MS liquid media for 12 days and time-course were treated with 50 μM ABA solution. WB was analyzed anti-HA.

After confirming the ABA-inducibility of the transgenic lines, we conducted drought stress experiments to validate the approach. To this aim, ProPP2CA:2HA-PYL4 and ProPP2CA:2HA-PYL4^{A194T} plants were grown under normal watering conditions for 2 weeks, and then irrigation was stopped (0D). Severe wilting of the leaves was observed at 17 days in the PYL4 wild type plants, in contrast to PYL4^{A194T}. Then watering was restored and survival of the plants was scored on 22nd day. ProPP2CA:2HA-PYL4 plants did not survive after drought stress, whereas around 60% to 70% of ProPP2CA:2HA-PYL4^{A194T} plants survived (Figure 57).

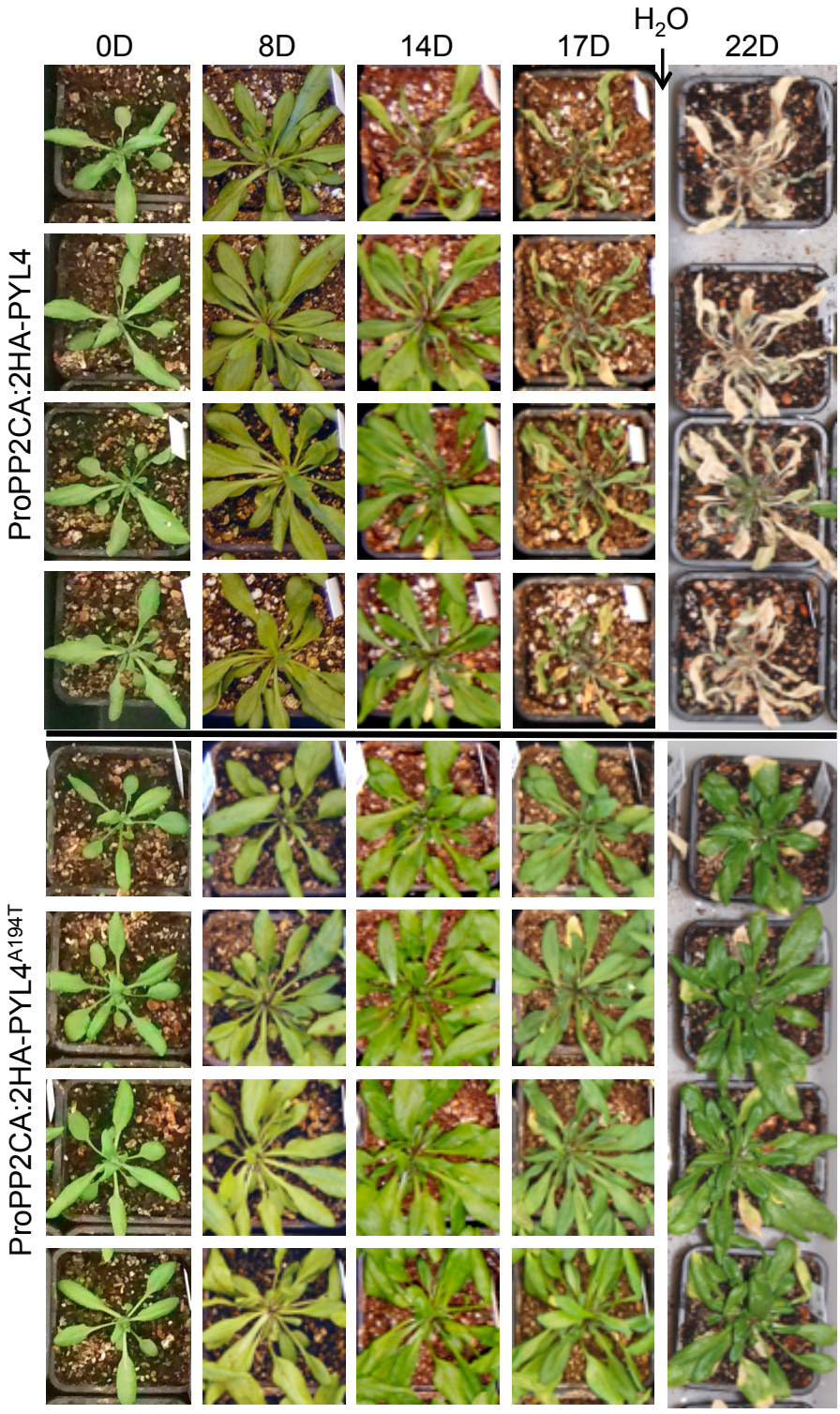
0D
8D
14D
17D
H2O
22D
ProPP2CA:2HA-PYL4
ProPP2CA:2HA-PYL4A194T

Figure 57. *ProPP2CA:2HA-PYL4^{A194T}* transgenic plants are drought tolerant. *ProPP2CA:2HA-PYL4* and *ProPP2CA:2HA-PYL4^{A194T}* plants were grown in the greenhouse for 2 weeks before removing the watering for other 17 days. All plants were watered again and 5 days after (22D) recovery pictures were taken.

This result suggested that the expression of PYL4^{A194T} driven by ProPP2CA was more efficient to activate ABA signaling pathway than PYL4 wt plants. This is in agreement with the increased sensitivity of PYL4^{A194T} for ABA in PP2C-activity assays (Pizzio et al., 2013). To verify that the plants express the ABA receptors during the drought stress treatment, we analyzed them by WB (Figure 58). The induction of the ABA receptors was detected in all the samples but certain variability in protein expression was found among the different lines.

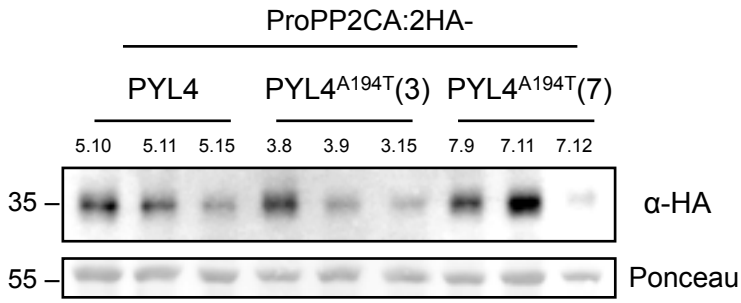

Figure 58. ABA inducibility of ABA receptors in leaves from adult plants of ProPP2CA:2HA-Receptor. 3-week-old plants grown in the greenhouse were sprayed with 100 μM ABA solution repeatedly for 3 h. One line of *ProPP2CA:2HA-PYL4* and two lines of the mutant version, PYL4^{A194T}, were used. WB was analyzed anti-HA.

Expression of abi1-1 driven by ProPP2CA leads to ABA-insensitivity in root

Another interesting question not yet resolved in the ABA signaling field was to know how interchangeable were the phosphatases in terms of spatio-temporal localization. To address that idea, the hypermorphic version of the ABI1 protein, *abi1-1* mutant, was cloned into the customized *pALLIGATOR2-ProPP2CA:2HA* vector. *pCR8-abi1-1* generated in our laboratory, was recombined by LR reaction to generate the *pALLIGATOR2-ProPP2CA:2HA-abi1-1* vector. The final construct in *pALLIGATOR2* was transferred to *A. tumefaciens* by electroporation and used to transform Col-0 wild type plants by the floral dip method (Clough & Bent, 1998).

Transgenic lines of *ProPP2CA:2HA-abi1-1* were mock (-) or 50 µM ABA treated (+) for 5 h. Root material was separated from the leaves and used for WB analysis. *ProPYL8:2HA-abi1-1* plants that was previously generated in our lab (Antoni et al., 2013) were used as a control of non-inducible promoter.

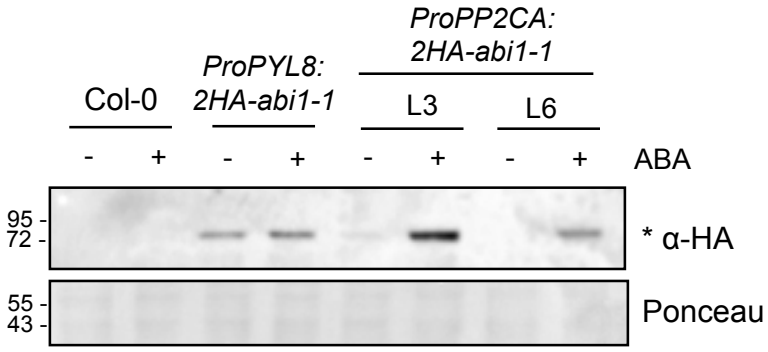

Figure 59. ABA-inducible phenotype of two different stable lines of *ProPP2CA:2HA-abi1-1*. Material was extracted from roots mock (-) or 50 µM ABA treated (+) for 5 h. Col-0 roots were used as a negative control

and *ProPYL8:2HA-abi1-1* as non-inducible promoter control. WB was analyzed anti-HA.

As shown in the Figure 59, the ABA treatment (50 µM ABA for 5 h) induces *abi1-1* protein expression in the two independent lines tested. On the other hand, *abi1-1* expression directed by PYL8 promoter was constitutive whereas inducible expression of the protein was generated with ProPP2CA plants.

abi1-1 is a hypermorphic mutant that shows strong ABA insensitivity (Leung et al., 1994, Meyer et al., 1994). To investigate whether *abi1-1* expressed under the PP2CA or PYL8 promoter affects ABA sensitivity, we analyzed germination and seedling establishment of *ProPP2CA2HA-abi1-1* and *ProPYL8:2HA-abi1-1* lines. After 3 days growing in 1 µM ABA (Figure 60A) approximately 90% of the seeds of both lines were germinated. The seedling establishment was also higher in both transgenic lines compared to wt. Therefore both transgenic plants showed reduced sensitivity to ABA compared to wt. We also analyzed ABA-mediated inhibition of the root growth (Figure 60B and C). Both transgenic lines, *ProPYL8* and *ProPP2CA:2HA-abi1-1* showed ABA-insensitivity in root growth compared to wt. These results suggest that *abi1-1* protein acts likely in the same tissues as PP2CA and PYL8. Additionally, selective expression of abi1-1 driven by either PP2CA or PYL8 promoters confers reduced sensitivity to ABA.

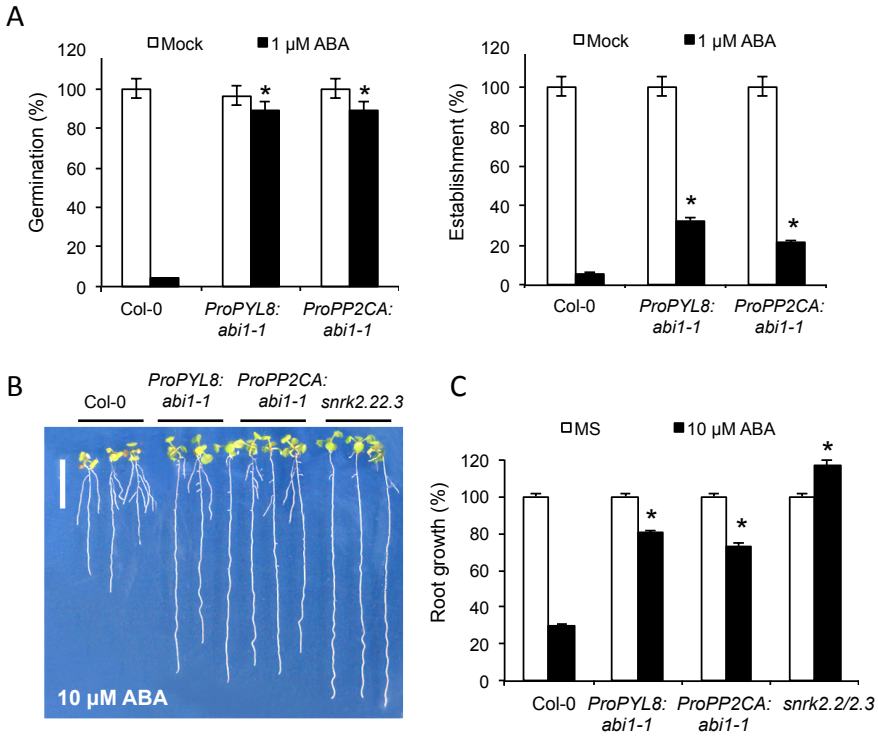

Figure 60. *abi1-1* displays an ABA-insensitive phenotype in germination, seedling establishment and root growth inhibition. (A) Quantification of the germination and seedling establishment of Col-0 wild-type, *ProPP2CA:2HA-abi1-1* and *ProPYL8:2HA-abi1-1* genetic backgrounds sown in plates lacking or supplemented with 1 µM ABA. Germination was scored at 3 days and establishment, as the presence of green cotyledons and the first pair of true leaves, at 7 days. Approximately 50 seeds per genotype were used in each experiment. Values are averages ± SE of three independent experiments. *$P < 0.01$ (Student's *t-test*) compared to Col-0 in the same experiment conditions. (B) The root growth ABA-insensitivity of *abi1-1* is driven by both promoters, PYL8 and PP2CA. Photographs of Col-0, *ProPYL8:2HA-abi1-1*, *ProPP2CA:2HA-abi1-1* and *snrk2.22.3* mutants grown for 10 days in MS medium supplemented with 10 µM ABA. Scale bar correspond to 1 cm. (C) Quantification of pictures in B. Values are averages ± SE of three

independent experiments (*n*=30). **P* < 0.05 (Student's *t-test*) compared to Col-0 in the same assay conditions.

Figure 61 summarizes the use of the PP2CA promoter to drive inducible expression of ABA receptors or PP2Cs. In the case of ABA receptors, ABA treatment will activate ABA signaling further creating a positive feedback. In the case of PP2Cs, ABA signaling will be blocked and the loop will be negative. As a result, receptor levels obtained after ABA-treatment are high, however, when we use *abi1-1* we can see induction but lower expression level is achieved.

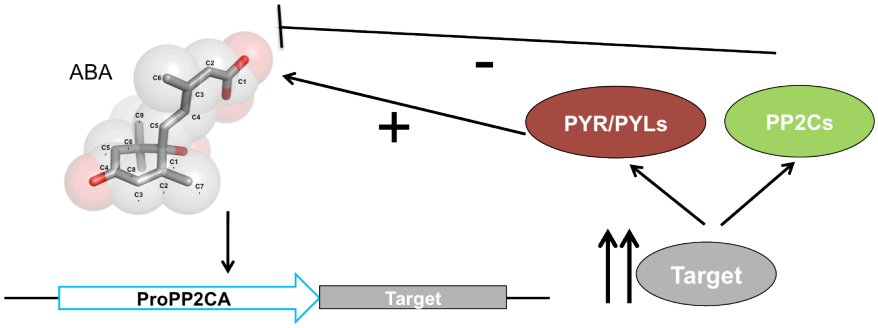

Figure 61. ABA activates PP2CA promoter producing high levels of target protein. In case the target is the receptor, the loop is positive and the level of the target will be increased, whereas if the target protein is a PP2C, the loop will be negative and the induction will be blocked.

DISCUSSION

The SWI/SNF ATPase BRM represses ABA responses in the absence of stress to balance plant growth and stress response (Han et al., 2012). Both the *brm-1* and *brm-3* loss-of-function alleles show enhanced ABA-mediated inhibition of seedling establishment. We show in this work that this phenotype can be rescued by removing ABI5 or ABI4 function since *brm-3 abi5-7* and *abi4 brm-3* double mutants are less sensitive to ABA than *brm-3* in root growth assays. This suggests that *ABI4* and *ABI5* are targets of BRM to regulate the ABA response. In fact, BRM represses *ABI5* expression in the absence of the stress signal by stabilizing a nucleosome close to the *ABI5* transcription start site (Han et al., 2012). Similarly, *ABI4* posses a well-positioned nucleosome close to the TSS and our results indicate that BRM could bind to this same region of the *ABI4* promoter. This data suggests a mechanism by which BRM prevents *ABI4* expression and could explain the increased expression of *ABI4* in the *brm3* mutant found in this work. In the case of *ABI5*, BRM does not prevent ABA-mediated destabilization of the nucleosome since it still resides at the ABI5 locus in conditions of elevated ABA (Han et al., 2012). This raises the possibility that BRM might be inactivated in the presence of ABA, for example by a post-translational modification. In this work, we provide evidence to propose a model where ABA/SnRK2-mediated phosphorylation impairs BRM activity (BRM OFF), which releases BRM repression and leads to *ABI5* induction (Figure 37). Conversely, PP2C-mediated BRM dephosphorylation could restore BRM activity (BRM ON) to maintain repression of ABA responses (and *ABI5* expression) under non-stressed plant growth conditions.

ABA signaling relies on a phosphorylation cascade, and analysis of the phosphoproteome in response to ABA had suggested that BRM might be phosphorylated by SnRK2s (Umezawa et al., 2013, Wang et al., 2013a). In this work, we provide direct evidence that OST1 is able to phosphorylate at least four Ser/Thr residues in the C-terminal region of BRM and that introduction of two phosphomimetic S1760D S1762D mutations impairs BRM function. Moreover, we have established that both SnRK2s and PP2Cs interact with the N- and C-terminal domains of BRM and co-immunoprecipitate with full-length BRM in the absence of exogenous ABA. Interestingly, whereas ABA treatment did not significantly affect the interaction of SnRK2 and BRM, this treatment dramatically reduced the interaction be- tween PP2CA and BRM. These results were corroborated by yeast two-hybrid and three-hybrid analyses. Thus, ABA perception through PYR/PYL ABA receptors may abrogate the PP2CA interaction with BRM (Figure 32 and Figure 37). Additionally, multicolor BiFC experiments, that help to study multicomponent interactions, showed the whole ABA signalosome (PYR/PYLs, PP2Cs and SnRK2s) interacting with BRM. Both N- and C-terminal BRM domains interacted with PP2CA and PYL4 simultaneously. However, in the case of SnRK2.2, interaction with BRM N-terminal region was prevented when PYL4 was present. Altogether these data indicate that ABA perception though PYR/PYL ABA receptors may promote the SnRK-mediated phosphorylation of BRM to de-repress the expression of important transcription factors in ABA signaling such as ABI4 and ABI5 (Figure 44).

ABA leads to phosphorylation of the activation loop of SnRK2s, which is a requisite for kinase activation (Umezawa et al., 2009;

Vlad et al., 2010). We have demonstrated that recombinant OST1/SnRK2.6 is able to phosphorylate the C-terminal region of BRM. According to the high number of SnRK2-dependent phosphopeptides identified in PhosPhAt database (Umezawa et al., 2013, Wang et al., 2013a), C-terminal region seems to be a hotspot for ABA-dependent phosphorylation. What effect on BRM activity could be expected from this phosphorylation? In the absence of a biochemical assay for BRM activity, we relied on the generation of a phosphomimetic mutant, BRMS1760D S1762D, which was introduced in the hypomorphic *brm-3* allele. The *ProBRM:BRM*$^{S1760D\ S1762D}$*::brm-3* mutant showed enhanced ABA sensitivity compared with the wt. Moreover, the *ProBRM:BRM*$^{S1760D\ S1762D}$*::brm-3* mutant displayed increased *ABI5* expression, which suggests that irreversible introduction of negative charge in certain Ser residues of BRM impairs its function in ABA signaling. ABA treatment led to a similar fold increase of *ABI5* expression in the wt, in both *brm-3* and *ProBRM:BRM*$^{S1760D\ S1762D}$*::brm-3*, consistent with the prior conclusion that BRM is inactivated upon ABA sensing (Han et al., 2012).

The combined data point to a model (Figure 37) whereby reversible phosphorylation of BRM by SnRK2s might lead to transient inactivation of the ATPase, which could be reverted by PP2CA. Our results also suggest that ABA-mediated induction of ABI5 requires phosphorylation of BRM by ABA-activated SnRK2s. Once the ABA levels diminish when plants return to non-stress conditions, PP2CA might dephosphorylate BRM to restore its activity and allow BRM to repress *ABI5* expression. *Arabidopsis* mutants lacking PP2CA or HAB1 show enhanced ABA-mediated inhibition of germination and seedling establishment, and higher expression of ABI5 than wt

(Nishimura et al., 2007; Rubio et al., 2009), which is in agreement with a role of PP2CA/HAB1 in maintaining BRM activity for repression of *ABI5* expression.

The *in vivo* identified SnRK2-dependent phosphorylation sites were concentrated around the AT hook and bromodomain of BRM, which are important domains for BRM function (Farrona et al., 2007). These domains constitute a module that allows BRM to interact with linker and nucleosomal DNA as well as the histone octamer (Farrona et al., 2007). These domains are required for BRM function since the *brm-3* mutant, which lacks most of this module (yet retains the AT hook), behaves as a hypomorphic allele (Farrona et al., 2007). In contrast, no phosphorylation sites were found in other important regions of BRM, such as the ATPase region required for ATP hydrolysis or the SnAC domain, which couples ATP hydrolysis to nucleosome movement (Sen et al., 2011, 2013). Therefore, we suggest that the C-terminal region located after the AT-hook domain and the bromodomain represents a hotspot for regulation through phosphorylation/dephosphorylation events. Interestingly, human BRM and BRG1 are phosphorylated and excluded from the condensed chromosomes during mitosis (Muchardt et al., 1996). Numerous phosphorylated Ser/Thr residues were identified before and after the bromodomain of the human BRM and BRG1 proteins (PhosphositePlus; http://www.phosphosite.org/proteinAction.do?id=5848&showAllSites=true). Therefore, phosphorylation of the C-terminal domain of BRM may be evolutionarily conserved. In the case of *Arabidopsis* BRM, the phosphomimetic BRM$^{S1760D\ S1762D}$ mutant phenocopies ABA hypersensitivity of *brm* loss-of-function alleles, which strongly suggests that SnRK2-dependent phosphorylation releases BRM

repression of ABA signaling. Conversely, PP2CA and HAB1, which are key negative regulators of ABA signaling, cooperate to maintain dephosphorylated and active BRM in the absence of the cue. In summary, our work provides a direct link between the core ABA signaling pathway and the chromatin-remodeling ATPase BRM. This link enables ABA-dependent modulation of BRM activity and a possible entry point for increasing response to water stress in plants.

In addition to the new role of PP2CA as a regulator of BRM phosphorylation status, we characterized the PP2CA promoter and identify that it is ABA-inducible. We also studied the stability of PP2CA showing that the protein was degraded by the proteasome and its degradation was induced by ABA (Wu 2016). This could represent a mechanism to enhance the stress response when ABA signaling is active. The acquired knowledge about the ABA inducibility of the PP2CA promoter prompted us to exploit this as a biotechnological tool. The use of ABA inducible promoters could potentially avoid the growth penalty observed in transgenic lines with a constitutive overexpression of ABA signaling core components observed before (Santiago et al., 2009b, Kim et al., 2014). Our results suggested this is a good strategy to direct the expression of ABA receptors only under stress conditions in order to enhance drought resistance in commercial crops. Reduced water availability, will induce ABA accumulation, which will activate PP2CA promoter leading to increased *PYR/PYL* expression. This could help the plant to tolerate the stress since plants overexpressing PYR/PYL receptors are drought tolerant (Santiago et al., 2009b, Kim et al., 2014, Yang et al., 2016a). In turn, by generating *ProPP2CA:abi1-1* transgenic plants we could efficiently

repress ABA signaling under stress conditions. Here we show how the ABA-inducible expression either of PYR/PYL ABA receptor or PP2CA could be used for biotechnological purposes.

CONCLUSIONS

1. We have identified the interactions among SWI/SNF ATPase BRM and the core elements of the ABA signaling pathway, i.e. PYR/PYL/RCAR receptors, clade A PP2Cs and SnRK2s.

2. OST1 phosphorylates four BRM Ser/Thr residues at the C-terminal region, which is a hotspot of phosphorylation.

3. PP2CA dephosphorylates BRM. This can be prevented by the formation of the PYL8-ABA-PP2CA ternary complex.

4. BRM phosphomimetic mutants are impaired to repress ABA-induced *ABI5* expression.

5. BRM represses *ABI4* expression and binds to ABI4 promoter region.

6. PP2CA promoter is ABA-inducible and can be used to generate drought tolerant plants.

MATERIALS AND METHODS

Biological Materials

Bacterial Strains

Escherichia coli (E. coli) chemocompetent cells (DH5*α* and TOP10® (Invitrogen)).

E. coli electrocompetent cells (DH10*β*).

E. coli DB3.1 strain from Life Technologies for *GATEWAY*™ plasmids containing *ccdB* toxic gene.

E. coli BL21 (DE3) pLysS chemocompetent strain for protein expression.

Agrobacterium tumefaciens (*A. tumefaciens*) C58C1 containing disarmed Ti plasmid *pGV2260* (Deblaere et al., 1985).

Yeast strains

S. cerevisiae AH109 (Clontech Laboratories).

S. cerevisiae PJ69-4A strain.

Plant Material

A. thaliana Col-0 ecotype.

N. benthamiana.

Mutants and transgenic stable lines in *A. thaliana* (Table 1).

Mutants and Transgenic Lines	Reference
*brm-3 (*SALK_088462)	(Farrona et al., 2007)
snrk2.2/2.3	(Fujii et al., 2007)
snrk2.2/2.3/brm-3	In this work
Pro35S:HAB1	(Saez et al., 2004)
Pro35S:HAB1/brm-1	(Han et al., 2012)
pp2ca-1 (SALK_028132)	(Kuhn et al., 2006)

abi4 (SALK_080095)	(Finkelstein, 1994)
abi4 brm-3	In this work
ProBRM:BRM-HA brm-1	(Han et al., 2012)
ProBRM:BRM-GFP brm-1	(Wu et al., 2012)
Pro35S:PP2CA-HA/ProBRM:BRM-GFP	In this work
Pro35S:SnRK2.2-HA/ProBRM:BRM-GFP	In this work
ProBRM:BRM$^{S1760D\ S1762D}$ brm-1	In this work
ProBRM:BRM$^{S1760A\ S1762A}$ brm-1	In this work
Pro35S:3HA-PP2CA	(Antoni et al., 2012)
Pro35S:3HA-SnRK2.2	(Planes et al., 2015)
Pro35S:3HA-SnRK2.3	(Planes et al., 2015)
ProPP2CA:2HA-PP2CA Col-0	In this work
ProPP2CA:2HA-PP2CA pp2ca-1	In this work
ProPP2CA:2HA-PYL4 Col-0	In this work
ProPP2CA:2HA-PYL4^{A194T} Col-0	In this work
ProPP2CA:2HA-Sl3g007310 Col-0	In this work

Table 1. *A. thaliana* mutant and transgenic lines generated and used in this work.

Growing Conditions and Transformation

Bacterial Culture

Luria-Bertani media (LB; 10 g/L triptone, 5 g/L yeast extract and 10 g/L NaCl, pH7.0 (2% agar in case of solid media preparation)) was used for bacterial culture. Different antibiotic-containing media was used depending on bacterial resistances (50 µg/mL Kanamycin

(Kan^R), 50 µg/mL Spectinomycin (Spec^R), 100 µg/mL Ampicillin (Amp^R)). The optimal temperature used for *E. coli* growth was 37ºC and for *A. tumefaciens*, 28ºC. In both cases, the liquid growth was performed in an orbital shaker at 250 rpm.

Transformation

For bacterial transformations, two techniques were used:

Heat shock method

100 ng of pDNA were incubated in 50 µL of *E. coli* competent cells suspension for 30 min on ice; the heat-shock was performed in a water bath at 42ºC for 45 sec followed by 2 min on ice. 500 µL of S.O.C. Medium (Invitrogen) was added to the mixture and was incubated for 1 h at 37ºC. After, the mixture was spinned down to collect the pellet and plated in LB medium containing the proper antibiotic.

Electroporation method

100 ng of pDNA were mixed with 50 µL of *A. tumefaciens pGV2260* competent cells suspension. The mixture was introduced in 0.2 cm pre-cooled electroporation cuvettes (Bio-Rad). Electroporation procedure was performed in Eppendorf Eporator®, 2000V/pulse (5-6 ms) conditions. Immediately 1 mL of LB medium was added and the mixture was incubated for 1-2 h in an orbital agitator at 28ºC. 200 µL of the mixture was plated in LB medium supplemented with the proper antibiotic.

Same amount of pDNA was mixed with 50 µL of *E. coli* DH10*β* competent cells suspension. The mixture was introduced in 0.1 cm pre-cooled electroporation cuvettes (Bio-Rad). Electroporation

procedure was performed in Eppendorf Eporator®, 1800V/pulse (5-6 ms) conditions. Immediately 500 µL of S.O.C. Medium (Invitrogen) was added to the mixture and incubated for 1 h at 37ºC. After, the mixture was spinned down to collect the pellet and plated in LB medium containing the proper antibiotic.

Yeast Culture

For *S. cerevisiae* culture, synthetic complete defined (SCD) culture medium (20% glucose, 7% yeast nitrogen base, 0.5 M succinic acid pH5.5, 20x Drop Out solution (DO) 2% agar in case of solid media) and synthetic defined (SD) culture medium (20% glucose, 7% yeast nitrogen base (YNB), 0.5 M succinic acid pH 5.5) were used.

For yeast transformants selection, SD basic culture medium was supplemented with extra aminoacids depending on the autotrophy generated by the vector:
-Trp -Leu/SD: Nitrogen base supplemented with DO, His and Ade
-Trp -Leu -His -Ade/SD: Nitrogen base supplemented with DO
-Trp -Leu -Ade/SD: Nitrogen base supplemented with DO and His

-Trp -Leu -Ade/SD culture medium (+His) was also supplemented with different concentrations of 3-amino 1, 2, 4-triazol (3AT) in the indicated experiments. 3AT is an inhibitor of *HIS3* gene product, which is part of the histidine biosynthesis in *S. cerevisiae.* Yeast was grown at 28ºC in an orbital shaker at 250 rpm.

Protocol for generation of *S. cerevisiae* competent cells was done according to MATCHMAKER GAL4 Two-Hybrid System 3 Manual (Clontech Laboratories).

Yeast Co-Transformation

1 µg of plasmidic DNA (pDNA) from the two partners we are interested to test the interaction were mixed in an aliquot of *AH109* yeast competent cells. 0.7 mL of PEG-Li-TE Solution (4 mL 45% PEG, 0.5 mL 10x LiAc-TE, 0.5 mL milli-Q water) was added. After vortex agitation, samples were incubated for 30 min at 28ºC. Vortex again was needed prior to next incubation for 20 min at 42ºC. Final centrifugation for 5 min at 1000×*g* was used to collect the cells and resuspended in 100 µL of milli-Q water. Glass beads were used to spread the culture on –Trp –Leu/SCD selective media. Plates were incubated for at least 2 days at 28ºC.

Arabidopsis thaliana

In Vitro Tissue Culture

For *in vitro* growing assays, seed sterilization was performed using Sterilization Solution I (70% ethanol, 0.01% Triton X-100) for 10 min followed by Sterilization solution II (50% Sodium hypochlorite) for 5 min. Removal of the sterilization solution II was done rinsing the seeds for 4 times with mili-Q water to fill the tube and changing the liquid with the pipette. Seeds were sown right after sterilization on Murashige–Skoog (MS) plates supplemented or not with different ABA concentrations per experiment. Stratification was conducted in the dark at 4ºC for 3 days and after it, the plates were incubated in controlled-environment growth chamber at 22ºC under

long day (LD) photoperiod conditions (16-h-light/8-h-dark photoperiod) at 80 to 100 µE m^{-2} s^{-2}.

Plant Treatments

Treatments were performed differently depending on the nature of the media used:

ABA stock solution was prepared from solid (+)-ABA (Sigma-Aldrich). 26.4 mg of powdered ABA were dissolved in 1 mL of 50 mM Tris-HCl pH8.0 buffer in order to get 10 mM ABA stock solution.

- Solid media treatment

MS plates were prepared with different concentrations of ABA. Germination and establishment experiments required ABA concentrations from 0.5 to 1 µM. Root growth working concentration was 10 µM ABA.

- Liquid culture treatments

Analyses of protein expression under several drug treatments were done using liquid cultures. Plants were grown in liquid MS medium cultures and treated with different drugs.

For ABA treatment concentrations vary from 50-100 µM (+)-ABA prepared from stock solution of 10 mM ABA. In case of MG-132 (Sigma-Aldrich) the working concentration was 50 µM prepared by dilution from 5 mM stock solution. CHX (Sigma-Aldrich) was used at 100 µM from a stock solution of 100 mM..

- Spray treatment

Exogenous application of ABA was done by spraying 100 µM solution onto 3 week-old leaves of adult plants grown in the greenhouse. Spray treatment was done for 3 h and the spray application was repeated each hour.

Greenhouse Culture

To propagate plants and for crosses, 1 week-old seedlings were transferred to soil (50% peat, 25% vermiculite, 25% perlite) and grown under LD conditions in the greenhouse 23°C/20°C temperature, 60% air relative humidity and 150 µmol m^{-2} s^{-1} light.

Generation of Mutants

To obtain mutants in *A. thaliana* such as *snrk2.2/2.3/brm-3* and *abi4 brm-3*, mutant parental plants were sowed on soil for 3 weeks. Closed flowers from mother plants were peeled to isolate the ovaries. Pollen from father mutant plants was incorporated to the ovaries and the cross was kept in a plastic wrap for two days, allowing the cross to develop. Seeds generated from the cross, F1 seeds, were grown in MS plates under LD conditions. To get homozygous lines, F2 seeds were grown and selected on MS media containing ABA (concentration was different depending on the strength of the parentals). ABA selection facilitates isolation of the homozygous mutants relying on their expected sensitivity to ABA.

For example, to obtain *snrk2.2/2.3/brm-3* triple mutant, F2 seeds were grown in normal MS media (¼ of the population in the cross is

expected to be the triple mutant). Rosette leaves were used to extract genomic DNA (gDNA) and genotyping. In this specific case, F2 1.1 line was homozygous for *snrk2.2* and *snrk2.3* mutations (this double mutant was used as the mother) and heterozygous for *brm-3* mutant (this mutant was used as pollen donor). Seeds derived from this F2 1.1 line, the F3 seeds, were sown in 1 μM ABA selective media. This amount of ABA will assure us to introduce bias in the germination rate. We expected to have good germination in seeds containing double *snrk2.2/2.3* and delay in germination in putative triple mutants because *brm-3* hypersensitivity. With this assumption, we transfer to soil different phenotypes of seedlings; insensitive seedlings and the other seedlings that show delayed germination. After genotyping the F3 plants, triple mutants were obtained in the delayed seeds indicating that the assumption was correct.

Arabidopsis thaliana Transgenic Lines Generation

pALLIGATOR2 and *pMDC163* vectors carrying the described constructions were transferred to *A. tumefaciens* by electroporation and used to transform *Col-0* wild-type or specific mutant plants by the floral dip method (Clough & Bent, 1998).

In the case of *pALLIGATOR2* constructions, T1 seeds were selected via the GFP expression driven by the *At2S3* seed-specific promoter (Bensmihen et al., 2004) under GFP filter in the microscope. T1 seeds were grown in the greenhouse to obtain T2. Same GFP selection strategy used before was followed with T2 and T3 transgenic lines. 100% GFP T3 lines were used for the following studies.

In the case of *pMDC163* vectors, the T1 seeds were selected by using 25 mg/mL hygromycin antibiotic. T1 resistant seedlings were transferred to the green house and grown in LD conditions to generate T2 seeds. These T2 seeds were again selected in hygromycin medium in order to obtain T3 homozygous progeny and that will be used for following studies.

Physiological Assays

Seed Germination and Seedling Establishment Assays

Approximately 100 seeds of each genotype were sown after sterilization on MS plates supplemented or not with different ABA concentrations. Stratification was conducted in the dark at 4ºC for 4 days. The plates were transferred to *in vitro* growing chamber under LD conditions. Radical emergence was analyzed at 72 h after sowing to score seed germination. Seedling establishment was scored as the percentage of seeds that developed green expanded cotyledons and the first pair of true leaves at 5 or 7 days.

Root Growth Assays

For root growth assays, seeds were sterilized and stratified as explained in a previous paragraph. Seedlings were grown on vertically oriented MS plates for 3-4 days. Afterwards, 20 plants were transferred to new MS plates lacking or supplemented with the indicated concentrations of ABA. The plates were scanned on a flatbed scanner after 10 days to produce image files suitable for quantitative analysis of root growth using the ImageJ v1.37 software.

Drought Stress Assays

For drought studies, transpiration rate was measured with water loss experiments. Seeds of all the genotypes were grown in MS plates for 7 days and transfer into soil in the greenhouse and grown under LD conditions for 2-3 weeks.

Long-term drought assays for *ProPP2CA:PYLs* plants, were performed after withholding water in plants maintained under greenhouse conditions basically as described by Saez et al. (2006). Eight plants of each genotype (two independent experiments) were grown in the greenhouse with LD conditions under normal watering conditions for 17 days and then subjected to drought stress by completely terminating irrigation for 17 days. Representative pictures were taken at several time points during the experiment (8D, 14D and 17D). Plants subjected to the water deprivation were afterwards watered with Hoagland solution and data were collected after 4 days. Pictures were taken after each time point for qualitative data analysis.

Nucleic Acids Extraction and Analysis Methods

DNA Extraction

Escherichia coli

pDNA was extracted from the bacteria using alkaline lysis of the cells. 1.5 mL of saturated cultures of *E. coli* were centrifuged at 12000×*g* for 1 min. Supernatant was discarded and the pellet was resuspended in 100 µL of ultrapure water of Type 1 (milli-Q water) and 100 µL of Lysis Solution (0.1 M NaOH, 10 mM ethylene

diamine tetraacetic acid (EDTA), 2% sodium dodecyl sulfate (SDS)). Samples were heated at 95ºC for 2 min and next kept on ice. 50 µL of 1M $MgCl_2$ were added and after vortexing the solution, the tubes were centrifuged at 12000×*g* for 5 min. Neutralization was performed with 50 µL of 5 M AcK (balanced with acetic acid at pH 5.0). The pDNA was precipitated with 2 volumes of pre-cooled 96% ethanol. After 15 min of incubation on ice, the precipitate was collected by centrifugation at 12000×*g* for 15 min. After discarding the supernatant, the pellet was rinsed with 500 µL of 70% ethanol and centrifuged at 12000×*g* for 5 min. The pellet was air-dried and resuspended with 30 µL of milli-Q water.

Arabidopsis thaliana

For gDNA extraction, 100 mg of leaf material from 2 weeks-old plants was collected in tubes and freeze into liquid nitrogen. The material was grinded with a glass pistil until fine powder. 2 volumes of Extraction Buffer (EB, 2% cetyl trimethyl ammonium bromide (CTAB), 100 mM Tris-HCl pH8.0, 20 mM EDTA, 1.4 M NaCl) were added to the sample and incubated at 65ºC for 10 min. 1 volume of chloroform/isoamyl alcohol (24:1) was added next and after vortexing, the sample was centrifuged at 12000×*g* for 10 min. 1 volume of the aqueous phase was transferred to a new tube and 1/10 of 10% CTAB was added (10% CTAB is very viscous so pre-warming of the solution at 65ºC has to be done prior to use) followed by an incubation at 65ºC for 2 min. For induction of the CTAB/DNA-RNA complex precipitation, 2 volumes of milli-Q water were added and followed by 15 min of ice incubation. Centrifugation of 12000×*g* for 10 min was performed to collect the pellet. After discarding the supernatant, 400 µL of 1 M NaCl was

used to resuspend the pellet. To precipitate de DNA, 800 µL of 96% ethanol were added followed by incubation on ice for 15 min. Last step was collecting the gDNA by centrifugation at 12000×*g* for 15 min. Samples were rinsed with 70% ethanol, as described before and the gDNA was resuspended with 30 µL of milli-Q water.

DNA Analysis by PCR Reaction

For open reading frame (ORF) amplifications and their posterior *GATEWAY*™ cloning in *pCR®8/GW/TOPO®,* the proofreading *Pfx 50™ DNA polymerase* (Life Technologies) was used. Table 2 shows the primer list used for cloning along this work.

Amplification	Primer Name	Sequence (5'-3')
BRM-N1 (1-949 aa)	F-BRMn	ATGCAATCTGGAGGCAGTGGCGG
	R-BRMN nostop	TGGCGCATTCATTTCCGTAAATC
BRM-D2 (691-949 aa)	FBRM-D2 *BamHI*	GGATCCATGTGTGAAGAAGGTGCAGAGTTC
	R-BRMN nostop	TGGCGCATTCATTTCCGTAAATC
BRM-C2C3 (691-2193 aa)	FBRM-C2 *NcoI*	ACCATGGTTGAGTTATTTGATCAGATG
	RBRM-C1 nostop	TAAATGGCTAGGCCGTCTTTTACC
BRM-C2 (1541-1890 aa)	FBRM-C2 *NcoI*	ACCATGGTTGAGTTATTTGATCAGATG
	RBRM-C2 Stop	CTAATTTGAAGAGCTAATAGGACT
BRM-C3 (1891-2193 aa)	FBRM-C3 *NcoI*	ACCATGGCTGGTGCAAGAATGTCCCAC

	RBRM-C3 *BamHI*	AAAGGATCCCTATAAATGGCTAG GCCGTCT
BRM-D2 (684-949 aa)	FBRM-D2 *NcoI*	ACCATGGATATTAAAGATCTGATT TGTGAAG
	RBRM-D2 Stop	CTATGGCGCATTCATTTCCGTAAA TCT
PP2CA	F*Not*NdePP2C A	TTTGCGGCCGCCATATGGCTGGG ATTTGTTGCGGTGTT
	R*Not*PP2CA	TTTGCGGCCGCTTAAGACGACGC TTGATTATTCCT
ABI4	FABI4*NcoI*	ACCATGGACCCTTTAGCTTCCCA A
	RABI4Stop	TTAATAGAATTCCCCCAAGATGG G
ProPP2CA	FproPP2CA *HindIII*	AAGCTTGGTTTTACCCGAACTTAA CCCAAATGC
	RproPP2CA *SacI*	GAGCTCCATTTGATCTCTAACAAA ACTTCTCCA
Sl03g007310	F*Nco*03g00731 0	ACCATGGACGCTAATGGATTCTG CGGTG
	R03g007310	TTAGACCTGATCAATGGGTTCTG

Table 2. Primer sequences for amplification of ORFs. Restriction sites are highlighted in green and Stop codons, in red. In brackets are the amplification size measured in aa.

For genotyping of the mutants, CTAB protocol for genomic DNA extraction was performed and *Taq polymerase* (produced in our laboratory) was used for PCR analysis. Primers used for genotyping each mutant and insertions (SALK and SAIL T-DNA, GABI-KAT insertions), are listed in table 3.

Mutants	Primer Name	Sequence (5'-3')
brm-3 genomic	FBRM-C2 *NcoI*	ACCATGGTTGAGTTATTTGATCAGAT G
	RBRM-C2 Stop	CTAATTTGAAGAGCTAATAGGACT
brm-3 T-DNA	newpROK2	GCCGATTTCGGAACCACCATC
	FBRM-C2 *NcoI*	ACCATGGTTGAGTTATTTGATCAGAT G
snrk2.2 genomic	LP2.2	CAAGACCATACATCTGCAAGCTGG
	RP2.2	ACACCTTGATGTTTCTTCTGTGTG
snrk2.2 T-DNA	LP2.2	CAAGACCATACATCTGCAAGCTGG
	GK-o8474	ATAATAACGCTGCGGACATCTACATT TT
snrk2.3 genomic	LP2.2	TTGGTTTTGAGTGTTCTGCTTTTG
	RP2.2	CACCACATGACCATACATCTGCAA
snrk2.3 T-DNA	LP2.3	TTGGTTTTGAGTGTTCTGCTTTTG
	GK-o8474	ATAATAACG CTG CGGACATCTACATTTT
abi4 genomic	FABI4*NcoI*	ACCATGGACCCTTTAGCTTCCCAA
	RABI4Stop	TTAATAGAATTCCCCCAAGATGGG
abi4 T-DNA	FABI4*NcoI*	ACCATGGACCCTTTAGCTTCCCAA
	newpROK2	GCCGATTTCGGAACCACCATC

Table 3. Primer sequences for genotyping of double/triple mutants generated in this work.

Generation of Entry Vectors

GATEWAY™ Cloning

The *GATEWAY*™ system *pCR®8/GW/TOPO® TA Cloning®* Kit (Life Technologies) was used for generating entry clones following manufacturer's instructions.

Generation of Destiny Vectors

For the generation of most of the destiny vectors *GATEWAY*™ technology was used.

GATEWAY™ LR Clonase II Reaction

50-150 ng of entry vector DNA and 150 ng of destiny vector DNA were mixed with 1.5 µL LR *Clonase™ II enzyme mix* (Life technologies). Volume was brought to 7.5 µL with milli-Q water and incubated at 25ºC for 1 h. To inactivate the clonase enzyme, 1 µL of 1% Proteinase K solution was added to the sample and incubated at 37ºC for 10 min. 5 µL of reaction was transformed in a 50 µL aliquot of DH5α *E. coli* chemocompetent cells.

Constructions for Yeast-Two and -Three Hybrid

For yeast-two and -three hybrid (Y2H-Y3H) assays, *pGADT7* and *pGBKT7-GW* versions and *pGADT7* and *pGBKT7* in their restriction versions were used. Moreover, other compatible vectors, as *pACT2™* and *pGBT9™* (Clontech Laboratories) that were already generated in our laboratory, were also used. The genes cloned in these vectors were fused to GAL4 activation domain (GAD) in *pGADT7*, *pACT2™* vectors or to the GAL4 binding

domain (GBD) in *pGBKT7*, *pGBT9*^{TM} vectors. In case of Y3H, *pBridge*^{TM} vector (Clontech Laboratories) was used because this vector can express two proteins at the same time: one fused to the DNA-binding domain and another additional protein.

Constructions (Y2H)	**Plasmid**	**Bacterial Selection**	**References**
GAD-HA-BRMN1	*pGADT7 GW*	Amp^{R}	In this work
GBD-myc-BRMN1	*pGBKT7 GW*	Kan^{R}	In this work
GBD-BRM N	*pDEST32*	Gen^{R}	In this work
GAD-HA-BRMC1	*pGADT7 GW*	Amp^{R}	In this work
GBD-myc-BRMC1	*pGBKT7 GW*	Kan^{R}	In this work
GBD-BRMD1	*pGBKT7 GW*	Kan^{R}	In this work
GBD-BRMD2	*pGBKT7 GW*	Kan^{R}	In this work
GAD-SWI3B	*pACT2*	Amp^{R}	(Saez et al., 2008)
GAD-HAB1	*pGADT7*	Amp^{R}	(Santiago et al., 2009b)
GAD-HAB1	*pDEST22*	Amp^{R}	In this work
GAD-HAB2	*pGADT7*	Amp^{R}	(Fujii et al., 2009)
GAD-ABI1	*pGADT7*	Amp^{R}	(Vlad et al., 2010)
GAD-ABI2	*pGADT7*	Amp^{R}	(Fujii et al., 2009)
GAD-PP2CA	*pGADT7*	Amp^{R}	(Fujii et al., 2009)
GAD-HAI1	*pGADT7*	Amp^{R}	In this work
GAD-AHG1	*pGADT7*	Amp^{R}	In this work
Constructions (Y3H)	**Plasmid**	**Bacterial Selection**	**References**
GBD-SnRK2.2	*pBridge*	Amp^{R}	(Fujii et al., 2009)
GBD-SnRK2.3	*pBridge*	Amp^{R}	(Fujii et al., 2009)
GBD-SnRK2.6/OST1	*pGBT9*	Amp^{R}	(Fujii et al., 2009)

GBD-BRMN	*pBridge*	Amp^R	In this work
GBD-BRMN-HA-PYL4 (MCSII)	*pBridge*	Amp^R	In this work
GBD-BMN-HA-PYL5 (MCSII)	*pBridge*	Amp^R	In this work

Table 4. Constructs used in this work for Y2H and Y3H assays in yeast.

Constructions for In Planta Expression

For *in planta* expression vector generation, *GATEWAY*™ system was used. The proteins of interest were fused to the green fluorescent protein (GFP) in C-terminal position and expressed under the control of *35S promoter*. These constructs were used for protein localization in tobacco epidermal cells.

Constructions	Plasmid	Bacterial Selection	
35S:BRMN-GFP	*pMDC83*	Kan^R	In this work
35S:BRMC2C3-GFP	*pMDC83*	Kan^R	In this work
35S:BRMC2-GFP	*pMDC83*	Kan^R	In this work
35S:BRMC3-GFP	*pMDC83*	Kan^R	In this work

Table 5. Constructions for *in planta* localizations of BRM fragments.

Constructions for Bi-molecular Fluorescence Complementation (BiFC) and multicolor BiFC (mcBiFC) in *Nicotiana benthamiana*

For BiFC experiments, destiny vectors for protein expression were generated. The *pSPYNE-35S* and *pSPYCE-35S* vectors used in this work were obtained from Walter et al. (2004) and *pYFPN43* and *pYFPC43* vectors were kindly provided by Alejandro Ferrando (Belda-Palazon et al., 2012). The proteins of interest were fused to N-terminal or C-terminal part of the yellow fluorescent protein (YFP) under *35S* promoter control. For mcBiFC the vectors used were obtained from Gehl et al. (2009).

Constructions	Plasmid	Bacterial Selection	References
Pro35S:BRMN1-c-myc-YFP^N	*pSPYNE-35S*	Kan^R	In this work
Pro35S:YFP^N-BRMC2C3	*pYFN43*	Kan^R	In this work
Pro35S:BRMN1-HA-YFP^C	*pSPYCE-35S*	Kan^R	In this work
Pro35S:BRMC2C3-HA-YFP^C	*pSPYCE-35S*	Kan^R	In this work
Pro35S:YFP^C-SnRK2.2	*pYFC43*	Kan^R	In this work
Pro35S:YFP^C-SnRK2.3	*pYFC43*	Kan^R	In this work
Pro35S:YFP^C-SnRK2.6/OST1	*pYFC43*	Kan^R	(Vlad et al., 2009)
Pro35S: YFP^C-SnRK2.6/OST1 Δ280	*pYFC43*	Kan^R	(Vlad et al., 2009)
Pro35S:YFP^N-ΔNPP2CA	*pYFN43*	Kan^R	(Saez et al., 2008)
Pro35S:YFP^N-PP2CA	*pYFN43*	Kan^R	(Antoni et al., 2012)
Pro35S:PP2CA-YFP^N	*pSPYNE*	Kan^R	(Pizzio et al., 2013)
Pro35S:YFP^N-ABI1	*pYFN43*	Kan^R	In this work
Pro35S:YFP^N-HAI1	*pYFN43*	Kan^R	In this work

Pro35S:YFP^{N}-HAB1	*pYFN43*	Kan^{R}	(Pizzio et al., 2013)
Constructions for protoplasts	**Plasmid**	**Bacterial Selection**	
Pro35S:eYFP^{N}-c-myc-BRMN	*pSPYNE (R)173*	Kan^{R}	In this work
Pro35S:eYFP^{N}-c-myc-BRMC	*pSPYNE (R)173*	Kan^{R}	In this work
Pro35S:eYFP^{C}-HA-HAB1	*pSPYCE (MR)*	Kan^{R}	In this work
Pro35S:eYFP^{C}-HA-OST1	*pSPYCE (MR)*	Kan^{R}	In this work
Constructions for mcBiFC	**Plasmid**	**Bacterial Selection**	
Pro35S: SCFP^{C}-HA-BRMN1	*p(MAS)DEST-SCYCE (R)^{GW}*	Kan^{R}	In this work
Pro35S: SCFP^{C}-HA-BRMC2C3	*p(MAS)DEST-SCYCE (R)^{GW}*	Kan^{R}	In this work
Pro35S:VENUS^{N}-c-myc-PP2CA	*pDEST–VYNE (R)^{GW}*	Kan^{R}	In this work
Pro35S:VENUS^{N}-c-myc-SnRK2.2	*pDEST–VYNE (R)^{GW}*	Kan^{R}	In this work
Pro35S:SCFP^{N}-FLAG-PYL4	*pDEST–SCYNE (R)^{GW}*	Kan^{R}	In this work

Table 6. Constructions used for BiFC/mcBiFC experiments in *N. benthamiana*.

Constructions for Protein Purification in *Escherichia coli*

For expression of recombinant proteins, two systems were used. *pETM-11* vector was used for expressing proteins tagged with 6His tail fused in the N-terminal part of the protein and *pMAL-c2* vector (Biolabs) was also used for recombinant protein expression but in

this case, the tag was maltose binding protein (MBP) fused in N-terminal position.

Constructions	Plasmid	Bacterial Selection	References
6His-BRM C2	*pETM-11*	Kan^R	In this work
6His-BRM C3	*pETM-11*	Kan^R	In this work
MBP-BRM D2	*pMAL-c2*	Amp^R	In this work
6His-SnRK2.6/OST1	*pETM-11*	Kan^R	(Santiago et al., 2009b)
6His-PP2CA	*pETM-11*	Kan^R	(Antoni et al., 2012)
6His-ABF2 ΔC	*pETM-11*	Kan^R	(Antoni et al., 2012)
6His-PYL8	*pETM-11*	Kan^R	(Antoni et al., 2012)

Table 7. Constructions used for protein expression and purification in *E. coli.*

Constructions for Transgenic Lines Generation

For the generation of transgenic lines *pALLIGATOR2* vector (Bensmihen et al., 2004) was used. This vector combines a GFP selection marker expressed under seed specific promoter, *At2S3*, making the transgenic lines easy to select under GFP filter in the microscope.

Constructions	Plasmid	Bacterial Selection	
ProPP2CA:2HA-PYL4	*pALLIGATOR2*	$Spect^R$	In this work
ProPP2CA:2HA-PYL4^{A194T}	*pALLIGATOR2*	$Spect^R$	In this work
ProPP2CA:2HA-	*pALLIGATOR2*	$Spect^R$	In this work

3g007310			
ProPP2CA:2HA-PP2CA	*pALLIGATOR2*	Spect^R	In this work

Table 8. Constructions for expressing PYR/PYL receptors/PP2CA under the control of PP2CA promoter.

Phosphomimetics and Phosphomutants Generation

A part of genomic *BRM* fragment of 2850 bp (*BamHI–EagI gBRM*), was cloned into *pENTR3C* vector (Invitrogen). The S1760 and S1762 residues were mutated either to aspartic acid (phosphomimetic) or alanine (phosphomutant) by site-directed mutagenesis. To achieve this aim, we used primers described in the table 9 following http://openwetware.org/wiki/Knight:Site-directed_mutagenesis/

Single_site procedure and the Stratagene QuickChange Site-Directed Mutagenesis manual. After verification of the mutagenesis by nucleotide sequencing, the *BamHI–EagI gBRM* fragment containing the S1760D/A and S1762D/A changes replaced the wt fragment in *ProBRM:gBRM-GFP* (Wu et al., 2012). Subsequently, *ProBRM:gBRM-GFP* was recombined into *pGWB1* by *GATEWAY*™ LR clonation. The resulting binary expression vector was transformed into *A. tumefaciens* and introduced into *brm-3* mutants (Farrona et al., 2004) by floral dip method (Clough & Bent, 1998).

Primer Name	Primer sequence (5'-3')
BRM S1760D S1762D	GATTCTCACATAGATCTCCAACGA**GA** **T**GGA**GAT**TGGGCCCATGACCGTGATG AAGG
BRM S1760A S1762A	GATTCTCACATAGATCTCCAACGA**GC** **T**GGA**GCT**TGGGCCCATGACCGTGATG

	AAGG

Table 9. Primers for phosphomimetic and phosphomuntant generation in *brm-3* mutant plants.

RNA extraction and PCR analysis of gene expression

Analysis of *ABI5* Expression

Two-day-old seedlings that were mock treated or treated with 50 μM ABA for 1 h, were used for *ABI5* expression analysis. RNA was extracted as Peirats-Llobet et al. (2016). In briefly, Trizol reagent (Invitrogen) was used for RNA extraction and further purified through DNaseI treatment and the RNA purification RNeasy mini kit (Qiagen). cDNA was synthesized using the Superscript IV kit (Invitrogen). Real-time PCR (StepOnePlus Real-Time PCR system; Applied Biosystems) was performed using Power SYBR Green PCR Master Mix (Life Technologies) and platinum *Taq* DNA polymerase (Invitrogen). *ABI5* transcript levels were normalized over that of the reference *UBQ10* gene (Czechowski et al., 2005).

Primer name	Primer sequence (5'-3')
qABI5_F	AACATGCATTGGCGGAGT
qABI5_R	TTGTGCCCTTGACTTCAAACT
qUBQ10_F	CCCTCCACTTGGTCCTCAG
qUBQ10_R	GTCAGAACTCTCCACCTCCAA

Table 10. Primers for analysis of ABI5 expression by RT-qPCR in *A. thaliana*.

Analysis of *ABI4* Expression

For RNA extraction material from 40 h germinated embryos (or 100 mg from 12 dag (days after germination) seedlings) was mock or 50 µM ABA treated for 1 h and samples were collected with liquid nitrogen. RNA extraction was performed with NucleoSpin® RNA Plant kit from Machery-Nagel, following the manufacturer's instructions. cDNA was synthesized from 2 µg of total purified RNA using 30U of RevertAid Reverse Transcriptase (Thermo Scientific) following the manufacturer's instructions.

RT-qPCR was performed using PyroTaq EvaGreen qPCR Master Mix 5X from Cultek (or EvaGreen® Dye 20X in water, carboxy-X-rhodamine (ROX) as a passive reference dye, both from Biotium and *Taq* DNA polymerase). The reaction was performed in a final volume of 10 µL using 0.4 µL of cDNA. The primer pairs used for this analysis are listed in table 11. The equipment used for the RT-qPCR was the 7500 Fast Real-Time PCR System from Applied Biosystems. The PCR conditions used were 1 cycle of denaturation for 15 sec at 95ºC, 40 cycles of denaturation (15 sec at 95ºC), primer hybridation (30 sec at 55ºC) and extension (30 sec at 60ºC); 1 cycle of DNA dissociation (15 sec at 95ºC, 1 min at 60ºC, 15 sec at 95ºC). *ABI4* transcript levels were normalized over that of the reference Act8 gene (or *PDF2* gene (Czechowski et al., 2005)). RT-qPCR results were analyzed by 7500 Software v2.0.4 (Applied Biosystems) using $2^{\Delta\Delta Ct}$ method for relative genic expression as described in (Livak & Schmittgen, 2001).

Primer name	Primer sequence
FwABI4-721	TTAGGGCAGGAACAAGGAGG

RvABI4-831	CGGCGGTGGATGAGTTATTG
FAct8	AGTGGTCGTACAACCGGTATTGT
RAct8	GAGGATAGCATGTGGAAGTGAGAA
FPDF2	TCAACATCTGGGTCTTCACTTAGC
RPDF2	GATGCAATCTCTCATTCCGATAGTC

Table 11. Primers for semiquantitative/quantitative analysis of ABI4 expression in *A. thaliana* mutants.

Analysis of ABI4 Promoter

For ChIP analysis of the ProBRM:BRM-HA material, we used the following list of primers.

Primer name	Final Concentration	Primer sequence (5'-3')
F1 pABI4	500 nM	CCGTTAGCCGTTATGTAATGATTTA
R1 pABI4	500 nM	GGAACAGAGATATCATTTTTGTTTGT
FnewP2.1	500 nM	CAATTTAAATTGACAAGTACTTAG
RnewP2.1	500 nM	GAACTGAATCAAATTCACCAAGG
FnewP2.2	500 nM	CAGTTCTCTCTGGTTGAATCCTC
RnewP2.2	500 nM	GGGTAACTATAGCAAATCATGAGC
F3 pABI4	500 nM	CGCTCATGATTTGCTATAGTTACC
R3 pABI4	500 nM	GAGAAAAATAGTGGAGAGGACGAA
F4 pABI4	500 nM	CGTCCTCTCCACTATTTTTCTCA
R4 pABI4	500 nM	GTGGAATCGGATTGAGGATTATT
FPDF2	300 nM	TCAACATCTGGGTCTTCACTTAGC
RPDF2	900 nM	GATGCAATCTCTCATTCCGATAGTC
FpABI5e1	500 nM	AATTCTCCGGCGGCTTTT
RpABI5e1	500 nM	CCGGTGGCTTTGTGTTCC

Table 12. Primers for ABI4 promoter analysis by RT-qPCR in *A. thaliana*.

Protein Technology

Recombinant Protein Induction In *Escherichia coli*

Purification of recombinant proteins was performed as described previously in Santiago et al. (2009b); Antoni et al. (2012), except in the case of BRMD2, which was fused to MBP protein. BRM protein fragments corresponding to the C-terminal region, BRMC2 (1541–1890 aa) and BRMC3 (1891–2193 aa) were amplified using PCR and cloned into *pETM11*, and BRMD2 (684–950 aa) corresponding to the last fragment of N-terminal region, was cloned into *pMAL-c2*. For the expression of each recombinant protein in *E. coli* BL21 (DE3) cells or DH5α, transformed with *pETM11/pMAL-c2* construct, respectively, bacteria were grown in LB medium to an optical density (OD_{600}) of 0.6-0.8. At this point, 1 mM of Isopropyl *β*-D-1-thiogalactopyranoside (IPTG) was added for the induction of this protein system and bacteria were harvested after 3 h incubation at 28ºC. To collect the bacterial pellet, culture was centrifuged at 3000×*g* for 15 min. After discarding the supernatant, pellet was washed with 2 mL of MBP buffer (20 mM Tris-HCl pH7.4, 200 mM NaCl, 1 mM EDTA and 10 mM *β*-mercaptoethanol (added prior to use)) centrifuged at 13000×*g* for 1.5 min at 4ºC and kept in -80ºC.

Recombinant Protein Purification in *Escherichia coli*

His-tag proteins culture and purification

6His-tagged recombinant proteins were purified to homogeneity using nickel-nitrilotriacetic (Ni-NTA) affinity chromatography (Antoni et al., 2012). Shortly, the protein pellet was resuspended in 2 mL of

histidine buffer (HIS buffer, 50 mM Tris-HCl, pH 7.6, 250 mM KCl, 10% glycerol, 0.1% Tween 20, and 10 mM *β*-mercaptoethanol), and the cells were sonicated with 2 pulses of 30 sec (hold position, 50% of the power) in a Branson Sonifier. A cleared lysate was obtained after centrifugation at 14000×*g* for 15 min at 4ºC, and it was diluted with 2 volumes of HIS buffer. The protein extract was applied to a 0.5 mL Ni-NTA acid agarose column, and the column was washed with 10 mL of HIS buffer supplemented with 20% glycerol and 30 mM imidazole. Bounded protein was eluted with HIS buffer supplemented with 20% glycerol and 250 mM imidazole. Recovery of the columns was done by adding 5 mL of 0.2 M acetic solution supplemented with 30% glycerol, washed with 8 mL of milli-Q water and the resin was kept at 4ºC with 5 mL of 30% ethanol.

MBP-tag proteins culture and purification

Maltose binding protein (MBP) is a big and soluble protein used when solubility problems happens in purifications.

Purification of MBP-BRMD2 protein was performed using amylose affinity chromatography. The matrix for the protein separation was amylose resin (New England, Biolabs), which is a polymer with high affinity for MBP protein. 1 mL of the resin was added to the column for the matrix generation, flow-through was discarded and the resin was washed once with 10 mL of MBP buffer (20 mM Tris-HCl pH 7.4, 200 mM NaCl, 1 mM EDTA and 10 mM *β*-mercaptoethanol). The samples have to be kept on ice during all the process but especially in the sonication step, to preserve the integrity of the proteins. 2 mL protein pellet was resuspended in MBP lysis buffer (1x MBP buffer, 10 mM *β*-mercaptoethanol and

0.25% Tween 20) for sonication 2 pulses of 30 sec (hold position, 50% of the power) in a Branson Sonifier. The samples were centrifuged at 13000×*g* for 10 min and 4ºC. Around 2 mL of the sample was collected and diluted 5 times with MBP dilution/wash buffer (1x MBP buffer, 10 mM *β*-mercaptoethanol). 10 mL of the sample were loaded into the column, washed with 10 mL of MBP dilution/wash buffer and eluted in protein fractions with 0.3 mL of MBP elution buffer (1x MBP buffer, 10 mM *β*-mercaptoethanol, 200 µL 0.5 M maltose).

Quantification of the protein in both purification protocols was done by Bradford assay (Bio-Rad). Samples are loaded in a one dimension SDS-polyacrylamide gel electrophoresis (SDS-PAGE).

Coomassie staining

For protein visualization, acrylamide gels were incubated in Instant*Blue*™ (Expedeon) staining solution for 15 min. Unstaining of the gel was done rinsing the gel with milli-Q water until the background was removed.

Protein Extraction

Saccharomyces cerevisiae

Yeast cultures for protein extraction were grown O/N in selective medium at 28ºC. The OD_{600} of the cultures were adjusted to 5, centrifuged at 1000×*g* for 2 min, washed with 1 mL of milli-Q water and resuspended again in 100 µL milli-Q water. 100 µL of 0.2 M NaOH, 1% *β*-mercaptoethanol were added and incubated 10 min at room temperature (RT). Samples were centrifuged and

resuspended in 100 µL of milli-Q water. Quantification of the samples was done by Bradford assay (Bio-Rad). Samples were mixed with 5x Laemmli buffer (30 mM Tris-HCl pH6.8, 7.5% SDS, 0.1 M dithiothreitol (DTT), 10 mM EDTA, 30% Sucrose, 0.25 mg/mL Bromophenol Blue), boiled for 3 min at 95ºC, cooled on ice for 1 min and spinned down prior to separate the proteins in SDS-PAGE.

Nicotiana benthamiana

2x Laemmli buffer was used for total protein extraction from *N. benthamiana* leaves (2 volumes of 2x Laemmli buffer per each gram of pulverized vegetal tissue). The mixture between sample and buffer was vortexed and heated at 95ºC for 15 min. Afterward, the sample was cooled on ice, spinned down and it was ready for SDS-PAGE analyses.

Arabidopsis thaliana

For protein extraction from *A. thaliana* material, 2 volumes of Lysis Buffer (50 mM Tris-HCl pH8.0, 150 mM NaCl, 1% Triton X-100, 3 mM DTT, 50 µM proteasome inhibitor MG-132 (UBPBio) and 1 tablet of antiprotease cocktail Roche (1 tablet/10mL buffer)) were added to sample. The mixture was kept on ice for 30 min and vortexed every 10 min. Samples were centrifuged at 12000×*g* at 4ºC for 30 min. The supernatant was transferred into a new tube and the protein quantification was performed by Bradford assay (Bio-Rad).

Biochemical Fractionation

Protein extracts for immunodetection experiments were prepared from tobacco leaves 48–72 h after agro-infiltration or from *A. thaliana* transgenic lines expressing GFP- and HA-tagged versions of BRM and PP2Cs/SnRK2s, respectively. Grinded plant material (100 mg) for direct WB analysis was extracted in 2xLaemmli buffer, proteins were run in a gradient 4%-15% SDS-PAGE *Mini-Protean® Precast gel* (Bio-Rad), and analyzed by WB. Nuclear fractionation of GFP- or HA-tagged proteins was performed as described previously (Saez et al., 2008, Antoni et al., 2012). Briefly, material from 40 h germinated embryos of *ProBRM:BRM-HA* were grown in MS –sucrose (suc) plates, ground in liquid nitrogen and homogenized in Lysis Buffer (20 mM Tris-HCl pH 7.6, 25% Glycerol, 20 mM KCl, 2.5 mM $MgCl_2$, 250 mM sucrose, 0.8 mM phenylmethylsulfonyl fluoride (PMSF), 5 mM *β*-mercaptoethanol, 1 tablet Protease Inhibitor Cocktail (Roche)/10mL of buffer). The lysate was filtered thought two layers of miracloth paper and was centrifuged at 12000×*g* at 4ºC for 20 min. Cytoplasmic fraction was stored at -20ºC and nuclear pellet was rinsed 3 times with Nuclei Resuspension Buffer (NRB, 20 mM Tris-HCl pH7.6, 25% glycerol, 2.5 mM $MgCl_2$, 0.5% Triton X-100, 0.8 mM PMSF, 5 mM *β*-mercaptoethanol). Nuclei were lysed with Medium Salt Buffer (MSB, 20 mM Tris-HCl pH7.6, 0.4 M NaCl, 1 mM EDTA, 5% glycerol, 0.5 mM PMSF, 0.1% Triton X-100, 1xProtease Inhibitor Cocktail and nuclear soluble fraction was collected for analysis. Soluble proteins from the nuclear fraction were immunoprecipitated using super-paramagnetic micro MACS beads (Miltenyi Biotec) coupled to monoclonal anti-GFP or anti-HA antibody according to the manufacturer's instructions. Purified immunocomplexes were

eluted with pre-heated elution buffer, run in a 10% SDS–PAGE gel and analyzed by WB.

SDS-PAGE Electrophoresis

Mixed samples with Laemmli buffer were boiled for 10 min at 95ºC and spinned down. The system used for protein analysis was Mini-Protean® System from Bio-Rad. Running gel containing 8-12% Acrylamide (19:1 Acrylamide/Bis-acrylamide from National diagnostics), 375 mM Tris-HCl pH8.8, 0.1% SDS, 0.2% N,N,N',N'-tetramethyl ethylenediamine (TEMED) and 0.08% ammonium persulfate (APS). Stacking gel is composed by 4% acrylamide/bis-acrylamide, 125 mM Tris-HCl pH 6.8, 0.1% SDS, 0.8% TEMED and 0.1% APS.

Western Blot Analyses

After SDS-PAGE, wet transfer method was used for protein visualization. Proteins were transferred to a polyvinylidene difluoride (PVDF) membrane *Immobilon®-P* (Millipore™), previously activated in 100% methanol solution, using *Mini Trans-Blot® Cell system* (Bio-Rad). Transfer buffer used was 1x Towbin Buffer (25 mM Tris-HCl pH7.6, 192 mM glycine, 20% (v/v) methanol, 0.1% SDS).

To check the transference, the membrane was incubated in Ponceau S Solution (0.1% (w/v) Ponceau S (Sigma-Aldrich) in 5% acetic acid) for 15 min in an orbital shaker. 1% acetic acid was used for membrane unstaining and 1x Tris-buffered saline (TBS, 50

mM Tris-HCl pH 7.6, 150 mM NaCl) was used to remove completely the staining.

For protein detection, the membrane was incubated for at least 2 h in blocking solution (1x TBS, 0.1% Tween-20 with 5% (w/v) nonfat dry milk). The antibodies (Table 13) were incubated at least for 1 h at room temperature in 5% blocking solution. After the antibody incubation, 3 washes with 1x TBST for 10 min were performed to remove the excess of primary antibody, and next, secondary antibody which was also diluted in 5% blocking solution was incubated for 1 hour and 3 washes were done as previously described. Detection was performed using the ECL advance western blotting chemiluminescent detection kit (GE Healthcare). Image capture was done using the image analyzer LAS3000, and quantification of the protein signal was done using Image Gauche V4.0 software.

Primary Antibodies	**Type**	**Manufacturer**	**Dilution**
Anti-GFP	Monoclonal	Clontech (JL8)	1:10000
Anti-HA/HRP	Monoclonal	Roche (3F10)	1:1000
Anti-c-myc	Monoclonal	Roche (9E10)	1:700
Anti-Histone3	Polyclonal	Abcam	1:10000
Anti-GAL4 AD	Monoclonal	Clontech	1:1000
Anti-GAL4 DNA-BD	Monoclonal	Clontech	1:1000
Secondary Antibodies	**Type**	**Manufacturer**	**Dilution**
Anti-IgG(mouse)-HRP	Polyclonal	GE Healthcare	1:5000
Anti-IgG(rabbit)-HRP	Polyclonal	GE Healthcare	1:5000

ChIP antibodies	Type	Manufacturer	Dilution
Anti-HA High Affinity	Monoclonal	Roche (3F10)	1:500

Table 13. Primary and secondary antibodies used in this work for chemiluminescent detection of the proteins of interest. ChIP, Chromatin Immunoprecipitation; HRP, horseradish peroxidase.

In vitro phosphorylation and phosphopeptide proteomic analysis

Phosphorylation assays were done basically as described previously in Dupeux et al. (2011a). In brief, a reaction mixture containing 1 µg of 6His-OST1 and 1 mg of 6His-BRMC2, 6His-BRMC3 or MBP-BRMD2 was incubated for 60 min at room temperature in 30 µL of Kinase Buffer (20 mM Tris–HCl pH 7.8, 10 mM $MgCl_2$, 2 mM $MnCl_2$, 0.5 mM DTT, and 3.5 µCi of γ^{-32P} ATP (3000 Ci/mmol)). When indicated, ABF2ΔC recombinant protein (100 ng) was added as a substrate of OST1. Reactions were stopped by adding Laemmli buffer, proteins were separated by SDS–PAGE using an 8% (w/v) acrylamide gel, transferred to an PVDF membrane, and detected using a phosphorimaging system (FLA5100; Fujifilm).

Cold phosphorylation of 6His-BRMC2 and 6His-BRMC3 substrates was performed in the presence of 1 mM ATP. Next, samples were run on a SDS-PAGE and Coomassie stained, and the gel bands corresponding to the different proteins were cut and in-gel digested. In brief, following reduction and alkylation (10 mM DTT and 50 mM Iodoacetamide, respectively, both in 25 mM ammonium

bicarbonate), BRMC2 and BRMC3 samples were digested with trypsin (1:50 enzyme/protein ratio) and incubated O/N at 37ºC. Peptides were recovered in 50% acetonitrile (ACN)/1% trifluoroacetic acid (TFA), dried in speed-Vac, and kept at -20ºC until phosphopeptide enrichment. The enrichment procedure concatenated two in-house packed microcolumns, the IMAC microcolumn and the Oligo R3 reversed-phase column, which provides selective purification and sample cleanup prior to liquid chromatography coupled to mass/mass (LC–MS/MS) analysis. Reversed-phase LC was performed on an Ultimate 3000 nano High-performance liquid chromatography (nanoHPLC) (Dionex). A 5-mL volume of the reconstituted peptide samples was injected on a C18 Acclaim™ PepMap™ 100 LC Column (Dionex) (5 µm, 100 Å, 300 µm I.D. x5 mm) at a flow rate of 30 mL/min, using H_2O/ACN/TFA (98:2:0.1) as loading mobile phase for 5 min. Then the trap column was switched online in back-flush mode to a C18 PepMap™ 100 analytical column (3 µm, 100 Å, 75 mm I.D. x15 cm). A 60-min linear gradient of 4%–50% B was delivered from the micro pump at a flow rate of 300 nL/min, where mobile phase A was 0.1% formic acid in milli-Q water and B was 20% milli-Q water and 0.1% formic acid in ACN. For rinsing the column, the percentage of B was increased to 95% in 6 min and then returned to initial conditions in 2 min. Afterward the column was re-equilibrated for 15 min. The UV detector wavelengths were monitored at 214 and 280 nm.

NanoHPLC was coupled to a 3D ion-trap mass spectrometer amaZon speed (Bruker Daltoniks) via CaptiveSpray ion source operating in positive ion mode, with capillary voltage set at 1.3 kV. The ion-trap mass spectrometer was operated in a data-dependent

mode, performing full scan (m/z 350–1500) MS spectra followed by MS/MS, alternating Collision-induced Dissociation (CID)/Electron Transfer Dissociation (ETD) fragmentation of the eight most abundant ions. Dynamic exclusion was applied to prevent the same *m/z* from being isolated for 1 min after its fragmentation. For protein identification, CID and ETD spectra obtained by LC-MS/MS system were searched against the SwissProt database using a licensed version v.2.3.02 of Mascot (Matrix Science) as search engine. ETD preserves the phosphoryl moiety during peptide fragmentation, which facilitates phospho-site characterization. Peptides with scores above a threshold that indicates a reliable identification were selected, and based on these individual scores protein identifications were assigned. In addition, manual validation of phosphopeptide MS/MS spectra was performed.

Yeast Two-Hybrid and Triple-Hybrid Assays

Interaction assays were usually performed as described by Saez et al. (2008), using the AH109 yeast strain and testing yeast growth in medium lacking Histidine (-His) and Adenine (-Ade). The resulting transformants, in both cases, were grown O/N in liquid –Triptophan (-Trp) –Leucine (-Leu)/SD culture medium and adjusted to equal cell density. Serial dilutions of cells were spotted on -Trp -Leu -His/SD culture medium with 0.1 mM 3-amino-1, 2, 4-triazole (3-AT).

To perform triple-hybrid experiments whereby ABA receptors interfere with the binding of PP2CA to BRMN, the sequence of BRMN was fused to GBD in *pBridge* vector. Next, the coding sequences of PYL4 or PYL5 were cloned into the NotI site (multicloning site II, abbreviated as MCSII) of *pBridge-BRMN*. For

triple-hybrid experiments with PP2CA and SnRK2.3, the sequence of SnRK2.3 was firstly fused to GBD in *pBridge*. Next, the coding sequence of PP2CA was cloned into the NotI site of *pBridge-SnRK2.3*. Yeast growth in triple-hybrid experiments was tested either in medium lacking His supplemented with 3-AT or medium lacking His and Ade. For triple-hybrid experiments, we cloned BRMN *BamHI-SalI* fragment into *pBridge* vectors containing PYL4 and PYL5 coding sequences. BRMN coding sequence is fused to GBD. Yeast host AH109 was co-transformed with one of the following plasmids, *pGADT7-PP2CA*, encoding GAD-PP2CA fusing and *pBridge-BRMN*, encoding GBD-BRMN fusion; whereas to test the interference of ABA-receptors on this interaction, *pBridge-BRMN+PYL4* and *pBridge-BRMN+PYL5* were employed.

β-Glucuronidase Staining

GUS Histochemical assay

Seeds were sterilized and stratified as in the germination experiments. Whole seedlings or organs of *A. thaliana* plants were submerged for incubation in GUS-staining solution at 37ºC. This solution contains 1:1 of X-Gluc: K^+ ferricyanide (0.5 mM)/ ferrocyanide (0.5 mM), where 5-bromo-4-chloro-3-indolyl glucuronide (X-Gluc) is the substrate for the *β*-glucoronidase activity, *GUS* gene. The product of glucuronidase action on X-Gluc is not colored. Instead, the indoxyl derivate produced must undergo an oxidative dimerization to form an insoluble and highly colored indigo dye (ClBr indigo). This dimerization is induced by atmospheric oxygen, and can be enhanced by using an oxidation catalyst such as a K^+ ferricyanide/ferrocyanide.

For **leaf staining**, GUS solution was infiltrated into the tissue subjecting the samples to vacuum for 10 min prior to O/N incubation in at 37ºC.

For **root staining**, samples were incubated 15-30 min at 37ºC. Previous to visualization and after the GUS incubation, roots need a clarification process, which consists in an incubation of the samples in acidified methanol solution for 20 min at 55ºC, followed by 15 min in sodium hydroxide (NaOH) solution. Rehydration of the roots was performed in decreasing ethanol series: 40%, 20% and 10%, keeping the samples more than 15 min each ethanol.

In case of **whole seedlings**, after GUS incubation for 15-30 min, samples were incubated, at least O/N with chloral hydrate solution (8 g chloral hydrate: 1 mL 100% glycerol: 2 mL H_2O). After, the samples were kept 50% glycerol for at least 2 h and were mounted in 50% glycerol for further visualization.

In case of **embryos**, GUS incubation was performed for 15-30 min at 37ºC and O/N incubation was performed for seed coats (testas). Embryos were kept in Fixative solution (50% Methanol and 10% acetic acid) O/N at 4ºC. Tissue was rinsed with milli-Q water twice prior to incubate it in 50% glycerol for at least 2 h.

The samples in all cases were ABA treated with 10 µM ABA for 2 h and after GUS staining protocol, they were stored in 50% glycerol from at least 2 h to O/N and mounted on microscope slides for further analysis with Leica EZ4D microscope (Leica Microsystems).

GUS Fluorogenic assay

Jefferson et al. (1987) described the method used for GUS quantification. Shortly, 150 mg of plant material was grinded with a mortar in liquid nitrogen until fine powder. Samples were homogenized with 2 volumes of extraction buffer (50 mM $NaPO_4$ pH 7.0, 10 mM *β*-mercaptoethanol, 10 mM EDTA, 0.1% sodium lauril sarcosine (inhibitor of the initiation of DNA transcription), 0.1% Triton X-100, 25 µg/mL PMSF), mixed 3 times for 30 sec with a vortex and centrifuged at 12000×*g* for 15 min at 4ºC. Supernatant was collected in a new tube. The assay buffer (1 mM of 4-methylumbelliferyl *β*-D-glucuronide (MUG) in extraction buffer) had to be pre-heated at 37ºC for 30 min in order to perform the assay at 37ºC. 5 µL of extract were used per each 500 µL of assay buffer. After mixing with the pipette, the assay can start. 100 µL of this mixture had to be collected in each time point and had to be added to 900 µL of Stop Buffer (0.2 M Na_2CO_3). Time points will depend on the expression of the line, here were measured every 20 min and the substrate was quantified with TECAN® spectrophotometer using the following parameters, Excitation 365 nm/Emission 455 nm.

Pseudo-Schiff-Propidium Iodide Root Staining

Pseudo-Schiff-Propidium Iodide protocol (mPS-PI) for root staining used was adapted from Truernit et al. (2008) by Mary Paz Gonzalez-Garcia. 5-7 days-old seedlings were fixed in 50% methanol, 10% acetic acid solution and stored at 4°C O/N. Samples were rinsed 3 times for 5 min with milli-Q water, transferred to 1% periodic acid solution (Sigma-Aldrich 3951) and incubated at RT in fume hood for 30 min. Samples were rinsed

again 3 times for 5 min with milli-Q water. The staining solution was composed of 540 µL Schiff reagent (100 mM sodium metabisulphite ($Na_2S_2O_5$) and 0.15N HCl; propidium iodide to a final concentration of 100 µg/mL was freshly added) and incubate at RT for 1 h. Seedlings were placed on microscope slides and some drops of chloral hydrate solution (2 mg/mL choral hydrate, 40% glycerol) were added to cover the roots. Microscope slides were stored O/N in a box with wet paper in the bottom to protect it from dehydration and light. chloral hydrate excess was removed with paper towels. Some drops of Hoyer's solution (32.5 g chloral hydrate, 3.2 mL glycerol, 5 g arabic gum (Sigma-Aldrich G9752)) were added to the samples and sealed with covers. The preparations were stored for drying at RT in the dark for at least 1 week before imaging at confocal. Microscope slides can be completely sealed with nail polish to obtain permanent samples.

Agro-transformation, Transient Expression and Bi-molecular Fluorescence Complementation Assays

Pre-culture of single isolated colony of *A. tumefaciens* was grown in liquid media at 28ºC for 2 days to saturate the culture. 1/100 dilution of the pre-culture was added to the fresh culture and grown O/N. *A. tumefaciens* cells were harvested by centrifugation at 3000×*g* for 30 min and resuspended in infiltration solution (10 mM MES buffer pH5.6, 100 µM acetosyringone, 10 mM $MgCl_2$) to an OD_{600nm} of 1. These cells were mixed with an equal volume of *A. tumefaciens* C58C1 (*pCH32 35S:p19*) expressing the silencing suppressor p19 of tomato bushy stunt virus (Voinnet et al., 2003)

so that the final density of *A. tumefaciens* solution was approximately 1. Bacteria were incubated for 3 h at room temperature and then injected into young fully expanded leaves of 4-week-old *N. benthamiana* plants. Leaves were examined 48–72 h after infiltration using Confocal Laser Scanning Microscopy (CLSM).

Arabidopsis thaliana Protoplast Generation and Transient Expression Assays

A. thaliana protoplast isolation and transformation was performed as described by Yoo et al. (2007). Briefly, around 25 leaves from 2-3 weeks-old rosettes grown in the greenhouse were cut in fine stripes. Enzyme solution for cell wall digestion (20 mM MES, 1.5% (w/v) cellulase R10, 0.4% (w/v) macerozyme, 0.4 M mannitol, 20 mM KCl) was warmed at 55ºC for 10 min and cooled down before adding 10 mM $CaCl_2$ and 0.1% Bovine serum albumin (BSA). Enzyme solution was filtered (0.45 µm) added to the tissue samples and kept in a rocker for 3 hours. Sample was filtered with a mesh and protoplasts were washed with salt solution W5 (2 mM MES, 154 mM NaCl, 125 mM $CaCl_2$, 5 mM KCl). After critical centrifugation of 100×*g* in each step for 3 times, incubation of 30 min of the protoplasts on ice was required. Centrifugation of the protoplasts at 100×*g* for 30 sec was used to change the previous buffer into mannitol-magnesium buffer (MMG, 4 mM MES, 0.4 mM mannitol, 15 mM $MgCl_2$).

For BiFC assay with protoplasts, pDNA, protoplasts and a polyethylene glycol (PEG) solution for transformation (40% PEG 4000, 0.2 M mannitol, 100 mM $CaCl_2$) were gently mixed and

incubate at RT for 10-15 min. 1 mL of salt solution W5 was added to wash the PEG solution followed by a centrifugation at 150×*g* for 2 min, and second round at 200×*g* for 2 min. New salt solution W5 was added and samples were kept O/N in dark for expression of the proteins.

Confocal Laser Scanning Microscopy

Confocal imaging was performed using a Zeiss LSM 780 AxioObserver.Z1 laser scanning microscope with C-Apochromat 403/1.20-W corrective water immersion objective. The following fluorophores, which were excited and fluorescence emission detected by frame switching in the single or multi-tracking mode at the indicated wavelengths, were used in tobacco leaf infiltration experiments: GFP (488 nm/500–530 nm) and YFP (488 nm/529–550 nm). Pinholes were adjusted to one Air Unit for each wavelength. Post-acquisition image processing was performed using ZEN (ZEISS Efficient Navigation) Lite 2012 imaging software and ImageJ v1.37 (http://rsb.info.gov/ij/) for image analyses.

Chromatin Immunoprecipitation (ChIP)

50 mg of seeds for each of the treatments were grown in MS – sucrose and 2% agar. Seeds were stratified at 4ºC in the dark for 4 days and grown in continuous light in the growing chamber for 36 h. Liquid treatment with 50 µM of ABA was applied to the plates for 1 h. Next, the material was collected and treated with 5 mL of **fixation buffer** (0.4 M sucrose, 10 mM Tris-HCl pH 8, 0.05 % Triton X-100, 1% Formaldehyde, 1 mM PMSF). To improve the crosslinking efficiency vacuum was applied for 15 min while the

tubes were kept on ice. To stop the fixation process, 2 M of **glycine** was added to the sample containing the fixation buffer and 5 more min of vacuum were applied. Samples were washed three times with cold milliQ water, mixed gently and filtered with a strainer to remove the remaining formaldehyde. Dry samples were freeze in liquid nitrogen and stored at -80ºC for the next level of processing.

The material was grinded with a mortar and pistil with liquid nitrogen until a fine powder was obtained. 5 mL of **extraction buffer 1** (0.4 M sucrose, 10 mM Tris-HCl pH8.0, 1 mM EDTA, protease inhibitors, 1 mM PMSF, 5 mM β-mercaptoethanol) was used for homogenizing the material prior to filter it twice with miracloth. The material was centrifuged at 1000×*g* and 4ºC for 20 min to collect the nuclei. The pellet was resuspended in 2 mL of **extraction buffer 2** (0.25 M sucrose, 10 mM Tris-HCl pH8.0, 1 mM EDTA, 10 mM $MgCl_2$, 1% Triton X-100, protease inhibitors, 1 mM PMSF, 5 mM β-mercaptoethanol) and centrifuged at 1000×*g* and 4ºC for 10 min. This processes has to be repeated at least two times or until obtain a white pellet. The intact nuclei pellet should be resuspended in 1 mL **lysis buffer** (50 mM Tris-HCl pH8.0, 10 mM EDTA, 1% SDS, 1 mM PMSF). The sonication was performed with Bioruptor® from Diagenode and the conditions were 5 cycles of 10 sec ON and 30 sec OFF. The sonicated chromatin was centrifuged at 13000×*g* and 4ºC for 10 min. The IP with 200 µL of the sonicated chromatin and 1:500 dilution of the α-HA from Roche was performed in the rocker at 4ºC for 2 h. The immunoprecipitated material was eluted with 300 µL of **elution buffer** (1% SDS, 0.1 M $NaHCO_3$) in the shaker (1100 rpm) for 1 h at 65ºC. The IP material and the input sample DNA was treated with 13 µL of NaCl 5 M and kept O/N in the shaker (900 rpm) at 65ºC. DNA was purified with

columns using Qiagen DNA gel extraction kit according to the manufacturer instructions.

REFERENCES

Abe H, Urao T, Ito T, Seki M, Shinozaki K, Yamaguchi-Shinozaki K, 2003. Arabidopsis AtMYC2 (bHLH) and AtMYB2 (MYB) function as transcriptional activators in abscisic acid signaling. *Plant Cell* **15**, 63-78.

Abrams E, Neigeborn L, Carlson M, 1986. Molecular analysis of SNF2 and SNF5, genes required for expression of glucose-repressible genes in Saccharomyces cerevisiae. *Mol Cell Biol* **6**, 3643-51.

Ahmad A, Zhang Y, Cao XF, 2010. Decoding the epigenetic language of plant development. *Mol Plant* **3**, 719-28.

Antoni R, Gonzalez-Guzman M, Rodriguez L*, et al.*, 2013. PYRABACTIN RESISTANCE1-LIKE8 plays an important role for the regulation of abscisic acid signaling in root. *Plant Physiol* **161**, 931-41.

Antoni R, Gonzalez-Guzman M, Rodriguez L, Rodrigues A, Pizzio GA, Rodriguez PL, 2012. Selective inhibition of clade A phosphatases type 2C by PYR/PYL/RCAR abscisic acid receptors. *Plant Physiol* **158**, 970-80.

Antoni R, Rodriguez L, Gonzalez-Guzman M, Pizzio GA, Rodriguez PL, 2011. News on ABA transport, protein degradation, and ABFs/WRKYs in ABA signaling. *Curr Opin Plant Biol* **14**, 547-53.

Archacki R, Buszewicz D, Sarnowski TJ*, et al.*, 2013. BRAHMA ATPase of the SWI/SNF chromatin remodeling complex acts as a positive regulator of gibberellin-mediated responses in arabidopsis. *PLoS One* **8**, e58588.

Archacki R, Sarnowski TJ, Halibart-Puzio J*, et al.*, 2009. Genetic analysis of functional redundancy of BRM ATPase and ATSWI3C subunits of Arabidopsis SWI/SNF chromatin remodelling complexes. *Planta* **229**, 1281-92.

Arenas-Huertero F, Arroyo A, Zhou L, Sheen J, Leon P, 2000. Analysis of Arabidopsis glucose insensitive mutants, gin5 and gin6, reveals a central role of the plant hormone ABA in the regulation of plant vegetative development by sugar. *Genes Dev* **14**, 2085-96.

Bai G, Yang DH, Zhao Y*, et al.*, 2013. Interactions between soybean ABA receptors and type 2C protein phosphatases. *Plant Mol Biol* **83**, 651-64.

Bao Y, Aggarwal P, Robbins NE, 2nd*, et al.*, 2014. Plant roots use a patterning mechanism to position lateral root branches toward available water. *Proc Natl Acad Sci U S A* **111**, 9319-24.

Bari R, Jones JD, 2009. Role of plant hormones in plant defence responses. *Plant Mol Biol* **69**, 473-88.

Bauer H, Ache P, Lautner S*, et al.*, 2013. The stomatal response to reduced relative humidity requires guard cell-autonomous ABA synthesis. *Curr Biol* **23**, 53-7.

Bechtold U, Penfold CA, Jenkins DJ*, et al.*, 2016. Time-Series Transcriptomics Reveals That AGAMOUS-LIKE22 Affects Primary Metabolism and Developmental Processes in Drought-Stressed Arabidopsis. *Plant Cell* **28**, 345-66.

Belda-Palazon B, Ruiz L, Marti E*, et al.*, 2012. Aminopropyltransferases involved in polyamine biosynthesis localize preferentially in the nucleus of plant cells. *PLoS One* **7**, e46907.

Bensmihen S, To A, Lambert G, Kroj T, Giraudat J, Parcy F, 2004. Analysis of an activated ABI5 allele using a new selection method for transgenic Arabidopsis seeds. *FEBS Lett* **561**, 127-31.

Bezhani S, Winter C, Hershman S*, et al.*, 2007. Unique, shared, and redundant roles for the Arabidopsis SWI/SNF chromatin remodeling ATPases BRAHMA and SPLAYED. *Plant Cell* **19**, 403-16.

Bossi F, Cordoba E, Dupre P, Mendoza MS, Roman CS, Leon P, 2009. The Arabidopsis ABA-INSENSITIVE (ABI) 4 factor acts as a central transcription activator of the expression of its own gene, and for the induction of ABI5 and SBE2.2 genes during sugar signaling. *Plant J* **59**, 359-74.

Boudsocq M, Barbier-Brygoo H, Lauriere C, 2004. Identification of nine sucrose nonfermenting 1-related protein kinases 2 activated by hyperosmotic and saline stresses in Arabidopsis thaliana. *J Biol Chem* **279**, 41758-66.

Bourachot B, Yaniv M, Muchardt C, 1999. The activity of mammalian brm/SNF2alpha is dependent on a high-mobility-group protein I/Y-like DNA binding domain. *Mol Cell Biol* **19**, 3931-9.

Brachmann RK, Boeke JD, 1997. Tag games in yeast: the two-hybrid system and beyond. *Curr Opin Biotechnol* **8**, 561-8.

Brandt B, Brodsky DE, Xue S*, et al.*, 2012. Reconstitution of abscisic acid activation of SLAC1 anion channel by CPK6 and OST1 kinases and branched ABI1 PP2C phosphatase action. *Proc Natl Acad Sci U S A* **109**, 10593-8.

Burla B, Pfrunder S, Nagy R, Francisco RM, Lee Y, Martinoia E, 2013. Vacuolar transport of abscisic acid glucosyl ester is mediated by ATP-binding cassette and proton-antiport mechanisms in Arabidopsis. *Plant Physiol* **163**, 1446-58.

Cairns BR, 2009. The logic of chromatin architecture and remodelling at promoters. *Nature* **461**, 193-8.

Cao FY, Yoshioka K, Desveaux D, 2011. The roles of ABA in plant-pathogen interactions. *J Plant Res* **124**, 489-99.

Carrera E, Holman T, Medhurst A*, et al.*, 2008. Seed after-ripening is a discrete developmental pathway associated with specific gene networks in Arabidopsis. *Plant J* **53**, 214-24.

Chai YM, Jia HF, Li CL, Dong QH, Shen YY, 2011. FaPYR1 is involved in strawberry fruit ripening. *J Exp Bot* **62**, 5079-89.

Cheng A, Kaldis P, Solomon MJ, 2000. Dephosphorylation of human cyclin-dependent kinases by protein phosphatase type 2C alpha and beta 2 isoforms. *J Biol Chem* **275**, 34744-9.

Cheng WH, Endo A, Zhou L*, et al.*, 2002. A unique short-chain dehydrogenase/reductase in Arabidopsis glucose signaling and abscisic acid biosynthesis and functions. *Plant Cell* **14**, 2723-43.

Cherel I, Michard E, Platet N*, et al.*, 2002. Physical and functional interaction of the Arabidopsis K(+) channel AKT2 and phosphatase AtPP2CA. *Plant Cell* **14**, 1133-46.

Chodavarapu RK, Feng S, Bernatavichute YV*, et al.*, 2010. Relationship between nucleosome positioning and DNA methylation. *Nature* **466**, 388-92.

Choi H, Hong J, Ha J, Kang J, Kim SY, 2000. ABFs, a family of ABA-responsive element binding factors. *J Biol Chem* **275**, 1723-30.

Clapier CR, Cairns BR, 2012. Regulation of ISWI involves inhibitory modules antagonized by nucleosomal epitopes. *Nature* **492**, 280-4.

Clough SJ, Bent AF, 1998. Floral dip: a simplified method for Agrobacterium-mediated transformation of Arabidopsis thaliana. *Plant J* **16**, 735-43.

Corona DF, Tamkun JW, 2004. Multiple roles for ISWI in transcription, chromosome organization and DNA replication. *Biochim Biophys Acta* **1677**, 113-9.

Curtis MD, Grossniklaus U, 2003. A gateway cloning vector set for high-throughput functional analysis of genes in planta. *Plant Physiol* **133**, 462-9.

Cutler SR, Rodriguez PL, Finkelstein RR, Abrams SR, 2010. Abscisic acid: emergence of a core signaling network. *Annu Rev Plant Biol* **61**, 651-79.

Czechowski T, Stitt M, Altmann T, Udvardi MK, Scheible WR, 2005. Genome-wide identification and testing of superior reference genes for transcript normalization in Arabidopsis. *Plant Physiol* **139**, 5-17.

Daszkowska-Golec A, Szarejko I, 2013. Open or close the gate - stomata action under the control of phytohormones in drought stress conditions. *Front Plant Sci* **4**, 138.

Deak KI, Malamy J, 2005. Osmotic regulation of root system architecture. *Plant J* **43**, 17-28.

Deblaere R, Bytebier B, De Greve H*, et al.*, 1985. Efficient octopine Ti plasmid-derived vectors for Agrobacterium-mediated gene transfer to plants. *Nucleic Acids Res* **13**, 4777-88.

Dhalluin C, Carlson JE, Zeng L, He C, Aggarwal AK, Zhou MM, 1999. Structure and ligand of a histone acetyltransferase bromodomain. *Nature* **399**, 491-6.

Dietz KJ, Sauter A, Wichert K, Messdaghi D, Hartung W, 2000. Extracellular beta-glucosidase activity in barley involved in the hydrolysis of ABA glucose conjugate in leaves. *J Exp Bot* **51**, 937-44.

Dupeux F, Antoni R, Betz K*, et al.*, 2011a. Modulation of abscisic acid signaling in vivo by an engineered receptor-insensitive protein phosphatase type 2C allele. *Plant Physiol* **156**, 106-16.

Dupeux F, Santiago J, Betz K*, et al.*, 2011b. A thermodynamic switch modulates abscisic acid receptor sensitivity. *EMBO J* **30**, 4171-84.

Durek P, Schmidt R, Heazlewood JL*, et al.*, 2010. PhosPhAt: the Arabidopsis thaliana phosphorylation site database. An update. *Nucleic Acids Res* **38**, D828-34.

Efroni I, Han SK, Kim HJ*, et al.*, 2013. Regulation of leaf maturation by chromatin-mediated modulation of cytokinin responses. *Dev Cell* **24**, 438-45.

Ezcurra I, Wycliffe P, Nehlin L, Ellerstrom M, Rask L, 2000. Transactivation of the Brassica napus napin promoter by ABI3 requires interaction of the conserved B2 and B3 domains of ABI3 with different cis-elements: B2 mediates activation through an ABRE, whereas B3 interacts with an RY/G-box. *Plant J* **24**, 57-66.

Farrona S, Hurtado L, Bowman JL, Reyes JC, 2004. The Arabidopsis thaliana SNF2 homolog AtBRM controls shoot development and flowering. *Development* **131**, 4965-75.

Farrona S, Hurtado L, March-Diaz R*, et al.*, 2011. Brahma is required for proper expression of the floral repressor FLC in Arabidopsis. *PLoS One* **6**, e17997.

Farrona S, Hurtado L, Reyes JC, 2007. A nucleosome interaction module is required for normal function of Arabidopsis thaliana BRAHMA. *J Mol Biol* **373**, 240-50.

Finkelstein R, 2013. Abscisic Acid synthesis and response. *Arabidopsis Book* **11**, e0166.

Finkelstein R, Gampala SS, Lynch TJ, Thomas TL, Rock CD, 2005. Redundant and distinct functions of the ABA response loci ABA-INSENSITIVE(ABI)5 and ABRE-BINDING FACTOR (ABF)3. *Plant Mol Biol* **59**, 253-67.

Finkelstein R, Lynch T, Reeves W, Petitfils M, Mostachetti M, 2011. Accumulation of the transcription factor ABA-insensitive (ABI)4 is tightly regulated post-transcriptionally. *J Exp Bot* **62**, 3971-9.

Finkelstein RR, 1994. Maternal Effects Govern Variable Dominance of Two Abscisic Acid Response Mutations in Arabidopsis thaliana. *Plant Physiol* **105**, 1203-8.

Finkelstein RR, Gampala SS, Rock CD, 2002. Abscisic acid signaling in seeds and seedlings. *Plant Cell* **14 Suppl**, S15-45.

Finkelstein RR, Lynch TJ, 2000. The Arabidopsis abscisic acid response gene ABI5 encodes a basic leucine zipper transcription factor. *Plant Cell* **12**, 599-609.

Finkelstein RR, Rock CD, 2002. Abscisic Acid biosynthesis and response. *Arabidopsis Book* **1**, e0058.

Finkelstein RR, Wang ML, Lynch TJ, Rao S, Goodman HM, 1998. The Arabidopsis abscisic acid response locus ABI4 encodes an APETALA 2 domain protein. *Plant Cell* **10**, 1043-54.

Fujii H, Chinnusamy V, Rodrigues A*, et al.*, 2009. In vitro reconstitution of an abscisic acid signalling pathway. *Nature* **462**, 660-4.

Fujii H, Verslues PE, Zhu JK, 2007. Identification of two protein kinases required for abscisic acid regulation of seed germination, root growth, and gene expression in Arabidopsis. *Plant Cell* **19**, 485-94.

Fujii H, Verslues PE, Zhu JK, 2011. Arabidopsis decuple mutant reveals the importance of SnRK2 kinases in osmotic stress responses in vivo. *Proc Natl Acad Sci U S A* **108**, 1717-22.

Fujii H, Zhu JK, 2009. Arabidopsis mutant deficient in 3 abscisic acid-activated protein kinases reveals critical roles in growth, reproduction, and stress. *Proc Natl Acad Sci U S A* **106**, 8380-5.

Fujita Y, Fujita M, Satoh R*, et al.*, 2005. AREB1 is a transcription activator of novel ABRE-dependent ABA signaling that enhances drought stress tolerance in Arabidopsis. *Plant Cell* **17**, 3470-88.

Fujita Y, Fujita M, Shinozaki K, Yamaguchi-Shinozaki K, 2011. ABA-mediated transcriptional regulation in response to osmotic stress in plants. *J Plant Res* **124**, 509-25.

Fujita Y, Nakashima K, Yoshida T*, et al.*, 2009. Three SnRK2 protein kinases are the main positive regulators of abscisic acid

signaling in response to water stress in Arabidopsis. *Plant Cell Physiol* **50**, 2123-32.

Fujita Y, Yoshida T, Yamaguchi-Shinozaki K, 2013. Pivotal role of the AREB/ABF-SnRK2 pathway in ABRE-mediated transcription in response to osmotic stress in plants. *Physiol Plant* **147**, 15-27.

Gehl C, Waadt R, Kudla J, Mendel RR, Hansch R, 2009. New GATEWAY vectors for high throughput analyses of protein-protein interactions by bimolecular fluorescence complementation. *Mol Plant* **2**, 1051-8.

Geiger D, Scherzer S, Mumm P*, et al.*, 2009. Activity of guard cell anion channel SLAC1 is controlled by drought-stress signaling kinase-phosphatase pair. *Proc Natl Acad Sci U S A* **106**, 21425-30.

Gentry M, Hennig L, 2014. Remodelling chromatin to shape development of plants. *Exp Cell Res* **321**, 40-6.

Gimenez-Ibanez S, Solano R, 2013. Nuclear jasmonate and salicylate signaling and crosstalk in defense against pathogens. *Front Plant Sci* **4**, 72.

Giraud E, Van Aken O, Ho LH, Whelan J, 2009. The transcription factor ABI4 is a regulator of mitochondrial retrograde expression of ALTERNATIVE OXIDASE1a. *Plant Physiol* **150**, 1286-96.

Golldack D, Li C, Mohan H, Probst N, 2013. Gibberellins and abscisic acid signal crosstalk: living and developing under unfavorable conditions. *Plant Cell Rep* **32**, 1007-16.

Gonzalez-Guzman M, Abia D, Salinas J, Serrano R, Rodriguez PL, 2004. Two new alleles of the abscisic aldehyde oxidase 3 gene reveal its role in abscisic acid biosynthesis in seeds. *Plant Physiol* **135**, 325-33.

Gonzalez-Guzman M, Apostolova N, Belles JM*, et al.*, 2002. The short-chain alcohol dehydrogenase ABA2 catalyzes the conversion of xanthoxin to abscisic aldehyde. *Plant Cell* **14**, 1833-46.

Gonzalez-Guzman M, Pizzio GA, Antoni R*, et al.*, 2012. Arabidopsis PYR/PYL/RCAR receptors play a major role in quantitative regulation of stomatal aperture and transcriptional response to abscisic acid. *Plant Cell* **24**, 2483-96.

Gonzalez-Guzman M, Rodriguez L, Lorenzo-Orts L*, et al.*, 2014. Tomato PYR/PYL/RCAR abscisic acid receptors show high expression in root, differential sensitivity to the abscisic acid agonist quinabactin, and the capability to enhance plant drought resistance. *J Exp Bot* **65**, 4451-64.

Gosti F, Beaudoin N, Serizet C, Webb AA, Vartanian N, Giraudat J, 1999. ABI1 protein phosphatase 2C is a negative regulator of abscisic acid signaling. *Plant Cell* **11**, 1897-910.

Grondin A, Rodrigues O, Verdoucq L, Merlot S, Leonhardt N, Maurel C, 2015. Aquaporins Contribute to ABA-Triggered Stomatal Closure through OST1-Mediated Phosphorylation. *Plant Cell* **27**, 1945-54.

Gudesblat GE, Russinova E, 2011. Plants grow on brassinosteroids. *Curr Opin Plant Biol* **14**, 530-7.

Guo Y, Xiong L, Song CP, Gong D, Halfter U, Zhu JK, 2002. A calcium sensor and its interacting protein kinase are global regulators of abscisic acid signaling in Arabidopsis. *Dev Cell* **3**, 233-44.

Hacham Y, Holland N, Butterfield C*, et al.*, 2011. Brassinosteroid perception in the epidermis controls root meristem size. *Development* **138**, 839-48.

Han SK, Sang Y, Rodrigues A*, et al.*, 2012. The SWI2/SNF2 chromatin remodeling ATPase BRAHMA represses abscisic acid responses in the absence of the stress stimulus in Arabidopsis. *Plant Cell* **24**, 4892-906.

Han SK, Wagner D, 2014. Role of chromatin in water stress responses in plants. *J Exp Bot* **65**, 2785-99.

Han SK, Wu MF, Cui S, Wagner D, 2015. Roles and activities of chromatin remodeling ATPases in plants. *Plant J* **83**, 62-77.

Hao Q, Yin P, Li W*, et al.*, 2011. The molecular basis of ABA-independent inhibition of PP2Cs by a subclass of PYL proteins. *Mol Cell* **42**, 662-72.

Hargreaves DC, Crabtree GR, 2011. ATP-dependent chromatin remodeling: genetics, genomics and mechanisms. *Cell Res* **21**, 396-420.

Harris JM, 2015. Abscisic Acid: Hidden Architect of Root System Structure. *Plants (Basel)* **4**, 548-72.

Holdsworth MJ, Bentsink L, Soppe WJ, 2008. Molecular networks regulating Arabidopsis seed maturation, after-ripening, dormancy and germination. *New Phytol* **179**, 33-54.

Hrabak EM, Chan CW, Gribskov M*, et al.*, 2003. The Arabidopsis CDPK-SnRK superfamily of protein kinases. *Plant Physiol* **132**, 666-80.

Huijser C, Kortstee A, Pego J, Weisbeek P, Wisman E, Smeekens S, 2000. The Arabidopsis SUCROSE UNCOUPLED-6 gene is identical to ABSCISIC ACID INSENSITIVE-4: involvement of abscisic acid in sugar responses. *Plant J* **23**, 577-85.

Hurtado L, Farrona S, Reyes JC, 2006. The putative SWI/SNF complex subunit BRAHMA activates flower homeotic genes in Arabidopsis thaliana. *Plant Mol Biol* **62**, 291-304.

Imes D, Mumm P, Bohm J*, et al.*, 2013. Open stomata 1 (OST1) kinase controls R-type anion channel QUAC1 in Arabidopsis guard cells. *Plant J* **74**, 372-82.

Jarillo JA, Pineiro M, Cubas P, Martinez-Zapater JM, 2009. Chromatin remodeling in plant development. *Int J Dev Biol* **53**, 1581-96.

Jefferson RA, Kavanagh TA, Bevan MW, 1987. GUS fusions: beta-glucuronidase as a sensitive and versatile gene fusion marker in higher plants. *EMBO J* **6**, 3901-7.

Jerzmanowski A, 2007. SWI/SNF chromatin remodeling and linker histones in plants. *Biochim Biophys Acta* **1769**, 330-45.

Kaliff M, Staal J, Myrenas M, Dixelius C, 2007. ABA is required for Leptosphaeria maculans resistance via ABI1- and ABI4-dependent signaling. *Mol Plant Microbe Interact* **20**, 335-45.

Kanno Y, Hanada A, Chiba Y*, et al.*, 2012. Identification of an abscisic acid transporter by functional screening using the receptor complex as a sensor. *Proc Natl Acad Sci U S A* **109**, 9653-8.

Kanno Y, Jikumaru Y, Hanada A*, et al.*, 2010. Comprehensive hormone profiling in developing Arabidopsis seeds: examination of

the site of ABA biosynthesis, ABA transport and hormone interactions. *Plant Cell Physiol* **51**, 1988-2001.

Kerchev PI, Pellny TK, Vivancos PD*, et al.*, 2011. The transcription factor ABI4 Is required for the ascorbic acid-dependent regulation of growth and regulation of jasmonate-dependent defense signaling pathways in Arabidopsis. *Plant Cell* **23**, 3319-34.

Kilian J, Whitehead D, Horak J*, et al.*, 2007. The AtGenExpress global stress expression data set: protocols, evaluation and model data analysis of UV-B light, drought and cold stress responses. *Plant J* **50**, 347-63.

Kim H, Hwang H, Hong JW*, et al.*, 2012. A rice orthologue of the ABA receptor, OsPYL/RCAR5, is a positive regulator of the ABA signal transduction pathway in seed germination and early seedling growth. *J Exp Bot* **63**, 1013-24.

Kim H, Lee K, Hwang H*, et al.*, 2014. Overexpression of PYL5 in rice enhances drought tolerance, inhibits growth, and modulates gene expression. *J Exp Bot* **65**, 453-64.

Klessig DF, Durner J, Noad R*, et al.*, 2000. Nitric oxide and salicylic acid signaling in plant defense. *Proc Natl Acad Sci U S A* **97**, 8849-55.

Knizewski L, Ginalski K, Jerzmanowski A, 2008. Snf2 proteins in plants: gene silencing and beyond. *Trends Plant Sci* **13**, 557-65.

Kong L, Cheng J, Zhu Y*, et al.*, 2015. Degradation of the ABA co-receptor ABI1 by PUB12/13 U-box E3 ligases. *Nat Commun* **6**, 8630.

Konson A, Pradeep S, D'acunto CW, Seger R, 2011. Pigment epithelium-derived factor and its phosphomimetic mutant induce JNK-dependent apoptosis and p38-mediated migration arrest. *J Biol Chem* **286**, 3540-51.

Koornneef M, Reuling G, Karssen CM, 1984. The isolation and characterization of abscisic acid-insensitive mutants of Arabidopsis thaliana. *Physiologia Plantarum* **61**, 377-83.

Koussevitzky S, Nott A, Mockler TC*, et al.*, 2007. Signals from chloroplasts converge to regulate nuclear gene expression. *Science* **316**, 715-9.

Kuhn JM, Boisson-Dernier A, Dizon MB, Maktabi MH, Schroeder JI, 2006. The protein phosphatase AtPP2CA negatively regulates abscisic acid signal transduction in Arabidopsis, and effects of abh1 on AtPP2CA mRNA. *Plant Physiol* **140**, 127-39.

Kuromori T, Miyaji T, Yabuuchi H*, et al.*, 2010. ABC transporter AtABCG25 is involved in abscisic acid transport and responses. *Proc Natl Acad Sci U S A* **107**, 2361-6.

Kuromori T, Shinozaki K, 2010. ABA transport factors found in Arabidopsis ABC transporters. *Plant Signal Behav* **5**, 1124-6.

Kuromori T, Yamamoto M, 1994. Cloning of cDNAs from Arabidopsis thaliana that encode putative protein phosphatase 2C and a human Dr1-like protein by transformation of a fission yeast mutant. *Nucleic Acids Res* **22**, 5296-301.

Kwak JM, Mori IC, Pei ZM*, et al.*, 2003. NADPH oxidase AtrbohD and AtrbohF genes function in ROS-dependent ABA signaling in Arabidopsis. *EMBO J* **22**, 2623-33.

Kwon CS, Hibara K, Pfluger J*, et al.*, 2006. A role for chromatin remodeling in regulation of CUC gene expression in the Arabidopsis cotyledon boundary. *Development* **133**, 3223-30.

Kwon CS, Wagner D, 2007. Unwinding chromatin for development and growth: a few genes at a time. *Trends Genet* **23**, 403-12.

Laby RJ, Kincaid MS, Kim D, Gibson SI, 2000. The Arabidopsis sugar-insensitive mutants sis4 and sis5 are defective in abscisic acid synthesis and response. *Plant J* **23**, 587-96.

Lee KH, Piao HL, Kim HY*, et al.*, 2006. Activation of glucosidase via stress-induced polymerization rapidly increases active pools of abscisic acid. *Cell* **126**, 1109-20.

Lee SC, Lan W, Buchanan BB, Luan S, 2009. A protein kinase-phosphatase pair interacts with an ion channel to regulate ABA signaling in plant guard cells. *Proc Natl Acad Sci U S A* **106**, 21419-24.

Lee SC, Lan WZ, Kim BG*, et al.*, 2007. A protein phosphorylation/dephosphorylation network regulates a plant potassium channel. *Proc Natl Acad Sci U S A* **104**, 15959-64.

Leran S, Varala K, Boyer JC*, et al.*, 2014. A unified nomenclature of NITRATE TRANSPORTER 1/PEPTIDE TRANSPORTER family members in plants. *Trends Plant Sci* **19**, 5-9.

Leung J, Bouvier-Durand M, Morris PC, Guerrier D, Chefdor F, Giraudat J, 1994. Arabidopsis ABA response gene ABI1: features of a calcium-modulated protein phosphatase. *Science* **264**, 1448-52.

Leung J, Merlot S, Giraudat J, 1997. The Arabidopsis ABSCISIC ACID-INSENSITIVE2 (ABI2) and ABI1 genes encode homologous protein phosphatases 2C involved in abscisic acid signal transduction. *Plant Cell* **9**, 759-71.

Lim EK, Jackson RG, Bowles DJ, 2005. Identification and characterisation of Arabidopsis glycosyltransferases capable of glucosylating coniferyl aldehyde and sinapyl aldehyde. *FEBS Lett* **579**, 2802-6.

Liscum E, Reed JW, 2002. Genetics of Aux/IAA and ARF action in plant growth and development. *Plant Mol Biol* **49**, 387-400.

Liu Q, Kasuga M, Sakuma Y*, et al.*, 1998. Two transcription factors, DREB1 and DREB2, with an EREBP/AP2 DNA binding domain separate two cellular signal transduction pathways in drought- and low-temperature-responsive gene expression, respectively, in Arabidopsis. *Plant Cell* **10**, 1391-406.

Liu X, Yue Y, Li B*, et al.*, 2007. A G protein-coupled receptor is a plasma membrane receptor for the plant hormone abscisic acid. *Science* **315**, 1712-6.

Livak KJ, Schmittgen TD, 2001. Analysis of relative gene expression data using real-time quantitative PCR and the 2(-Delta Delta C(T)) Method. *Methods* **25**, 402-8.

Lopez-Molina L, Chua NH, 2000. A null mutation in a bZIP factor confers ABA-insensitivity in Arabidopsis thaliana. *Plant Cell Physiol* **41**, 541-7.

Lopez-Molina L, Mongrand S, Chua NH, 2001. A postgermination developmental arrest checkpoint is mediated by abscisic acid and requires the ABI5 transcription factor in Arabidopsis. *Proc Natl Acad Sci U S A* **98**, 4782-7.

Lopez-Molina L, Mongrand S, Mclachlin DT, Chait BT, Chua NH, 2002. ABI5 acts downstream of ABI3 to execute an ABA-dependent growth arrest during germination. *Plant J* **32**, 317-28.

Lu C, Fedoroff N, 2000. A mutation in the Arabidopsis HYL1 gene encoding a dsRNA binding protein affects responses to abscisic acid, auxin, and cytokinin. *Plant Cell* **12**, 2351-66.

Luan S, 2003. Protein phosphatases in plants. *Annu Rev Plant Biol* **54**, 63-92.

Luo M, Wang YY, Liu X*, et al.*, 2012. HD2C interacts with HDA6 and is involved in ABA and salt stress response in Arabidopsis. *J Exp Bot* **63**, 3297-306.

Lynch T, Erickson BJ, Finkelstein RR, 2012. Direct interactions of ABA-insensitive(ABI)-clade protein phosphatase(PP)2Cs with calcium-dependent protein kinases and ABA response element-binding bZIPs may contribute to turning off ABA response. *Plant Mol Biol* **80**, 647-58.

Ma Y, Szostkiewicz I, Korte A*, et al.*, 2009. Regulators of PP2C phosphatase activity function as abscisic acid sensors. *Science* **324**, 1064-8.

Manning BJ, Peterson CL, 2013. Releasing the brakes on a chromatin-remodeling enzyme. *Nat Struct Mol Biol* **20**, 5-7.

Mclachlan DH, Kopischke M, Robatzek S, 2014. Gate control: guard cell regulation by microbial stress. *New Phytol* **203**, 1049-63.

Melcher K, Ng LM, Zhou XE*, et al.*, 2009. A gate-latch-lock mechanism for hormone signalling by abscisic acid receptors. *Nature* **462**, 602-8.

Melotto M, Underwood W, Koczan J, Nomura K, He SY, 2006. Plant stomata function in innate immunity against bacterial invasion. *Cell* **126**, 969-80.

Merilo E, Jalakas P, Laanemets K*, et al.*, 2015. Abscisic Acid Transport and Homeostasis in the Context of Stomatal Regulation. *Mol Plant* **8**, 1321-33.

Merlot S, Mustilli AC, Genty B*, et al.*, 2002. Use of infrared thermal imaging to isolate Arabidopsis mutants defective in stomatal regulation. *Plant J* **30**, 601-9.

Meyer K, Leube MP, Grill E, 1994. A protein phosphatase 2C involved in ABA signal transduction in Arabidopsis thaliana. *Science* **264**, 1452-5.

Meyer S, Mumm P, Imes D*, et al.*, 2010. AtALMT12 represents an R-type anion channel required for stomatal movement in Arabidopsis guard cells. *Plant J* **63**, 1054-62.

Miyazono K, Miyakawa T, Sawano Y*, et al.*, 2009. Structural basis of abscisic acid signalling. *Nature* **462**, 609-14.

Mizuguchi G, Shen X, Landry J, Wu WH, Sen S, Wu C, 2004. ATP-driven exchange of histone H2AZ variant catalyzed by SWR1 chromatin remodeling complex. *Science* **303**, 343-8.

Mori IC, Murata Y, Yang Y*, et al.*, 2006. CDPKs CPK6 and CPK3 function in ABA regulation of guard cell S-type anion- and Ca(2+)-permeable channels and stomatal closure. *PLoS Biol* **4**, e327.

Munemasa S, Hauser F, Park J, Waadt R, Brandt B, Schroeder JI, 2015. Mechanisms of abscisic acid-mediated control of stomatal aperture. *Curr Opin Plant Biol* **28**, 154-62.

Mustilli AC, Merlot S, Vavasseur A, Fenzi F, Giraudat J, 2002. Arabidopsis OST1 protein kinase mediates the regulation of stomatal aperture by abscisic acid and acts upstream of reactive oxygen species production. *Plant Cell* **14**, 3089-99.

Nakashima K, Fujita Y, Kanamori N*, et al.*, 2009. Three Arabidopsis SnRK2 protein kinases, SRK2D/SnRK2.2, SRK2E/SnRK2.6/OST1 and SRK2I/SnRK2.3, involved in ABA signaling are essential for the control of seed development and dormancy. *Plant Cell Physiol* **50**, 1345-63.

Narlikar GJ, Sundaramoorthy R, Owen-Hughes T, 2013. Mechanisms and functions of ATP-dependent chromatin-remodeling enzymes. *Cell* **154**, 490-503.

Navajas R, Paradela A, Albar JP, 2011. Immobilized metal affinity chromatography/reversed-phase enrichment of phosphopeptides

and analysis by CID/ETD tandem mass spectrometry. *Methods Mol Biol* **681**, 337-48.

Nemhauser JL, Hong F, Chory J, 2006. Different plant hormones regulate similar processes through largely nonoverlapping transcriptional responses. *Cell* **126**, 467-75.

Ng LM, Soon FF, Zhou XE*, et al.*, 2011. Structural basis for basal activity and autoactivation of abscisic acid (ABA) signaling SnRK2 kinases. *Proc Natl Acad Sci U S A* **108**, 21259-64.

Nishimura N, Hitomi K, Arvai AS*, et al.*, 2009. Structural mechanism of abscisic acid binding and signaling by dimeric PYR1. *Science* **326**, 1373-9.

Nishimura N, Sarkeshik A, Nito K*, et al.*, 2010. PYR/PYL/RCAR family members are major in-vivo ABI1 protein phosphatase 2C-interacting proteins in Arabidopsis. *Plant J* **61**, 290-9.

Nishimura N, Yoshida T, Kitahata N, Asami T, Shinozaki K, Hirayama T, 2007. ABA-Hypersensitive Germination1 encodes a protein phosphatase 2C, an essential component of abscisic acid signaling in Arabidopsis seed. *Plant J* **50**, 935-49.

Nishimura N, Yoshida T, Murayama M, Asami T, Shinozaki K, Hirayama T, 2004. Isolation and characterization of novel mutants affecting the abscisic acid sensitivity of Arabidopsis germination and seedling growth. *Plant Cell Physiol* **45**, 1485-99.

Okamoto M, Kuwahara A, Seo M*, et al.*, 2006. CYP707A1 and CYP707A2, which encode abscisic acid 8'-hydroxylases, are indispensable for proper control of seed dormancy and germination in Arabidopsis. *Plant Physiol* **141**, 97-107.

Okamoto M, Peterson FC, Defries A*, et al.*, 2013. Activation of dimeric ABA receptors elicits guard cell closure, ABA-regulated gene expression, and drought tolerance. *Proc Natl Acad Sci U S A* **110**, 12132-7.

Papamichos-Chronakis M, Watanabe S, Rando OJ, Peterson CL, 2011. Global regulation of H2A.Z localization by the INO80 chromatin-remodeling enzyme is essential for genome integrity. *Cell* **144**, 200-13.

Parcy F, Valon C, Raynal M, Gaubier-Comella P, Delseny M, Giraudat J, 1994. Regulation of gene expression programs during Arabidopsis seed development: roles of the ABI3 locus and of endogenous abscisic acid. *Plant Cell* **6**, 1567-82.

Park SY, Fung P, Nishimura N*, et al.*, 2009. Abscisic acid inhibits type 2C protein phosphatases via the PYR/PYL family of START proteins. *Science* **324**, 1068-71.

Peirats-Llobet M, Han SK, Gonzalez-Guzman M*, et al.*, 2016. A Direct Link between Abscisic Acid Sensing and the Chromatin-Remodeling ATPase BRAHMA via Core ABA Signaling Pathway Components. *Mol Plant* **9**, 136-47.

Peret B, De Rybel B, Casimiro I*, et al.*, 2009. Arabidopsis lateral root development: an emerging story. *Trends Plant Sci* **14**, 399-408.

Pizzio GA, Rodriguez L, Antoni R*, et al.*, 2013. The PYL4 A194T mutant uncovers a key role of PYR1-LIKE4/PROTEIN PHOSPHATASE 2CA interaction for abscisic acid signaling and plant drought resistance. *Plant Physiol* **163**, 441-55.

Planes MD, Ninoles R, Rubio L*, et al.*, 2015. A mechanism of growth inhibition by abscisic acid in germinating seeds of Arabidopsis thaliana based on inhibition of plasma membrane H+-ATPase and decreased cytosolic pH, K+, and anions. *J Exp Bot* **66**, 813-25.

Raz V, Bergervoet JH, Koornneef M, 2001. Sequential steps for developmental arrest in Arabidopsis seeds. *Development* **128**, 243-52.

Razem FA, El-Kereamy A, Abrams SR, Hill RD, 2006. The RNA-binding protein FCA is an abscisic acid receptor. *Nature* **439**, 290-4.

Razem FA, El-Kereamy A, Abrams SR, Hill RD, 2008. Retraction. The RNA-binding protein FCA is an abscisic acid receptor. *Nature* **456**, 824.

Reeves R, Beckerbauer L, 2001. HMGI/Y proteins: flexible regulators of transcription and chromatin structure. *Biochim Biophys Acta* **1519**, 13-29.

Reeves WM, Lynch TJ, Mobin R, Finkelstein RR, 2011. Direct targets of the transcription factors ABA-Insensitive(ABI)4 and ABI5 reveal synergistic action by ABI4 and several bZIP ABA response factors. *Plant Mol Biol* **75**, 347-63.

Ren X, Chen Z, Liu Y*, et al.*, 2010. ABO3, a WRKY transcription factor, mediates plant responses to abscisic acid and drought tolerance in Arabidopsis. *Plant J* **63**, 417-29.

Risk JM, Macknight RC, Day CL, 2008. FCA does not bind abscisic acid. *Nature* **456**, E5-6.

Rodrigues A, Adamo M, Crozet P*, et al.*, 2013. ABI1 and PP2CA phosphatases are negative regulators of Snf1-related protein kinase1 signaling in Arabidopsis. *Plant Cell* **25**, 3871-84.

Rodriguez PL, Benning G, Grill E, 1998. ABI2, a second protein phosphatase 2C involved in abscisic acid signal transduction in Arabidopsis. *FEBS Lett* **421**, 185-90.

Rubio S, Rodrigues A, Saez A*, et al.*, 2009. Triple loss of function of protein phosphatases type 2C leads to partial constitutive response to endogenous abscisic acid. *Plant Physiol* **150**, 1345-55.

Ryu H, Cho H, Bae W, Hwang I, 2014. Control of early seedling development by BES1/TPL/HDA19-mediated epigenetic regulation of ABI3. *Nat Commun* **5**, 4138.

Saez A, Apostolova N, Gonzalez-Guzman M*, et al.*, 2004. Gain-of-function and loss-of-function phenotypes of the protein phosphatase 2C HAB1 reveal its role as a negative regulator of abscisic acid signalling. *Plant J* **37**, 354-69.

Saez A, Robert N, Maktabi MH, Schroeder JI, Serrano R, Rodriguez PL, 2006. Enhancement of abscisic acid sensitivity and reduction of water consumption in Arabidopsis by combined inactivation of the protein phosphatases type 2C ABI1 and HAB1. *Plant Physiol* **141**, 1389-99.

Saez A, Rodrigues A, Santiago J, Rubio S, Rodriguez PL, 2008. HAB1-SWI3B interaction reveals a link between abscisic acid signaling and putative SWI/SNF chromatin-remodeling complexes in Arabidopsis. *Plant Cell* **20**, 2972-88.

Saito S, Hirai N, Matsumoto C*, et al.*, 2004. Arabidopsis CYP707As encode (+)-abscisic acid 8'-hydroxylase, a key enzyme in the oxidative catabolism of abscisic acid. *Plant Physiol* **134**, 1439-49.

Sang Y, Silva-Ortega CO, Wu S*, et al.*, 2012. Mutations in two non-canonical Arabidopsis SWI2/SNF2 chromatin remodeling ATPases cause embryogenesis and stem cell maintenance defects. *Plant J* **72**, 1000-14.

Santiago J, Dupeux F, Betz K*, et al.*, 2012. Structural insights into PYR/PYL/RCAR ABA receptors and PP2Cs. *Plant Sci* **182**, 3-11.

Santiago J, Dupeux F, Round A*, et al.*, 2009a. The abscisic acid receptor PYR1 in complex with abscisic acid. *Nature* **462**, 665-8.

Santiago J, Rodrigues A, Saez A*, et al.*, 2009b. Modulation of drought resistance by the abscisic acid receptor PYL5 through inhibition of clade A PP2Cs. *Plant J* **60**, 575-88.

Santner A, Estelle M, 2009. Recent advances and emerging trends in plant hormone signalling. *Nature* **459**, 1071-8.

Sarnowska EA, Rolicka AT, Bucior E*, et al.*, 2013. DELLA-interacting SWI3C core subunit of switch/sucrose nonfermenting chromatin remodeling complex modulates gibberellin responses and hormonal cross talk in Arabidopsis. *Plant Physiol* **163**, 305-17.

Sarnowski TJ, Rios G, Jasik J*, et al.*, 2005. SWI3 subunits of putative SWI/SNF chromatin-remodeling complexes play distinct roles during Arabidopsis development. *Plant Cell* **17**, 2454-72.

Sato A, Sato Y, Fukao Y*, et al.*, 2009. Threonine at position 306 of the KAT1 potassium channel is essential for channel activity and is a target site for ABA-activated SnRK2/OST1/SnRK2.6 protein kinase. *Biochem J* **424**, 439-48.

Schachtman DP, Goodger JQ, 2008. Chemical root to shoot signaling under drought. *Trends Plant Sci* **13**, 281-7.

Schaller GE, Bishopp A, Kieber JJ, 2015. The yin-yang of hormones: cytokinin and auxin interactions in plant development. *Plant Cell* **27**, 44-63.

Schroeder JI, Allen GJ, Hugouvieux V, Kwak JM, Waner D, 2001. GUARD CELL SIGNAL TRANSDUCTION. *Annu Rev Plant Physiol Plant Mol Biol* **52**, 627-58.

Schwartz SH, Qin X, Zeevaart JA, 2003. Elucidation of the indirect pathway of abscisic acid biosynthesis by mutants, genes, and enzymes. *Plant Physiol* **131**, 1591-601.

Schweighofer A, Hirt H, Meskiene I, 2004. Plant PP2C phosphatases: emerging functions in stress signaling. *Trends Plant Sci* **9**, 236-43.

Sen P, Ghosh S, Pugh BF, Bartholomew B, 2011. A new, highly conserved domain in Swi2/Snf2 is required for SWI/SNF remodeling. *Nucleic Acids Res* **39**, 9155-66.

Sen P, Vivas P, Dechassa ML, Mooney AM, Poirier MG, Bartholomew B, 2013. The SnAC domain of SWI/SNF is a histone anchor required for remodeling. *Mol Cell Biol* **33**, 360-70.

Seo M, Peeters AJ, Koiwai H*, et al.*, 2000. The Arabidopsis aldehyde oxidase 3 (AAO3) gene product catalyzes the final step in abscisic acid biosynthesis in leaves. *Proc Natl Acad Sci U S A* **97**, 12908-13.

Shang Y, Yan L, Liu ZQ*, et al.*, 2010. The Mg-chelatase H subunit of Arabidopsis antagonizes a group of WRKY transcription repressors to relieve ABA-responsive genes of inhibition. *Plant Cell* **22**, 1909-35.

Sharp RE, Poroyko V, Hejlek LG*, et al.*, 2004. Root growth maintenance during water deficits: physiology to functional genomics. *J Exp Bot* **55**, 2343-51.

Sheen J, 1998. Mutational analysis of protein phosphatase 2C involved in abscisic acid signal transduction in higher plants. *Proc Natl Acad Sci U S A* **95**, 975-80.

Shen YY, Wang XF, Wu FQ*, et al.*, 2006. The Mg-chelatase H subunit is an abscisic acid receptor. *Nature* **443**, 823-6.

Shinozaki K, Yamaguchi-Shinozaki K, 2007. Gene networks involved in drought stress response and tolerance. *J Exp Bot* **58**, 221-7.

Shu K, Chen Q, Wu Y*, et al.*, 2016a. ABI4 mediates antagonistic effects of abscisic acid and gibberellins at transcript and protein levels. *Plant J* **85**, 348-61.

Shu K, Chen Q, Wu Y*, et al.*, 2016b. ABSCISIC ACID-INSENSITIVE 4 negatively regulates flowering through directly promoting Arabidopsis FLOWERING LOCUS C transcription. *J Exp Bot* **67**, 195-205.

Shu K, Liu XD, Xie Q, He ZH, 2016c. Two Faces of One Seed: Hormonal Regulation of Dormancy and Germination. *Mol Plant* **9**, 34-45.

Shu K, Zhang H, Wang S*, et al.*, 2013. ABI4 regulates primary seed dormancy by regulating the biogenesis of abscisic acid and gibberellins in arabidopsis. *PLoS Genet* **9**, e1003577.

Signora L, De Smet I, Foyer CH, Zhang H, 2001. ABA plays a central role in mediating the regulatory effects of nitrate on root branching in Arabidopsis. *Plant J* **28**, 655-62.

Sirichandra C, Davanture M, Turk BE*, et al.*, 2010. The Arabidopsis ABA-activated kinase OST1 phosphorylates the bZIP transcription factor ABF3 and creates a 14-3-3 binding site involved in its turnover. *PLoS One* **5**, e13935.

Sirichandra C, Gu D, Hu HC*, et al.*, 2009. Phosphorylation of the Arabidopsis AtrbohF NADPH oxidase by OST1 protein kinase. *FEBS Lett* **583**, 2982-6.

Smith CL, Peterson CL, 2005. ATP-dependent chromatin remodeling. *Curr Top Dev Biol* **65**, 115-48.

Soderman EM, Brocard IM, Lynch TJ, Finkelstein RR, 2000. Regulation and function of the Arabidopsis ABA-insensitive4 gene in seed and abscisic acid response signaling networks. *Plant Physiol* **124**, 1752-65.

Sokol A, Kwiatkowska A, Jerzmanowski A, Prymakowska-Bosak M, 2007. Up-regulation of stress-inducible genes in tobacco and Arabidopsis cells in response to abiotic stresses and ABA treatment correlates with dynamic changes in histone H3 and H4 modifications. *Planta* **227**, 245-54.

Soon FF, Ng LM, Zhou XE*, et al.*, 2012. Molecular mimicry regulates ABA signaling by SnRK2 kinases and PP2C phosphatases. *Science* **335**, 85-8.

Spoel SH, Dong X, 2008. Making sense of hormone crosstalk during plant immune responses. *Cell Host Microbe* **3**, 348-51.

Stark MJ, 1996. Yeast protein serine/threonine phosphatases: multiple roles and diverse regulation. *Yeast* **12**, 1647-75.

Struhl K, Segal E, 2013. Determinants of nucleosome positioning. *Nat Struct Mol Biol* **20**, 267-73.

Su Y, Kwon CS, Bezhani S*, et al.*, 2006. The N-terminal ATPase AT-hook-containing region of the Arabidopsis chromatin-remodeling protein SPLAYED is sufficient for biological activity. *Plant J* **46**, 685-99.

Sun L, Wang YP, Chen P*, et al.*, 2011. Transcriptional regulation of SlPYL, SlPP2C, and SlSnRK2 gene families encoding ABA signal core components during tomato fruit development and drought stress. *J Exp Bot* **62**, 5659-69.

Swain SM, Singh DP, 2005. Tall tales from sly dwarves: novel functions of gibberellins in plant development. *Trends Plant Sci* **10**, 123-9.

Swarup R, Kramer EM, Perry P*, et al.*, 2005. Root gravitropism requires lateral root cap and epidermal cells for transport and response to a mobile auxin signal. *Nat Cell Biol* **7**, 1057-65.

Szerlong H, Hinata K, Viswanathan R, Erdjument-Bromage H, Tempst P, Cairns BR, 2008. The HSA domain binds nuclear actin-related proteins to regulate chromatin-remodeling ATPases. *Nat Struct Mol Biol* **15**, 469-76.

Szerlong HJ, Hansen JC, 2011. Nucleosome distribution and linker DNA: connecting nuclear function to dynamic chromatin structure. *Biochem Cell Biol* **89**, 24-34.

Szostkiewicz I, Richter K, Kepka M*, et al.*, 2010. Closely related receptor complexes differ in their ABA selectivity and sensitivity. *Plant J* **61**, 25-35.

Tahtiharju S, Palva T, 2001. Antisense inhibition of protein phosphatase 2C accelerates cold acclimation in Arabidopsis thaliana. *Plant J* **26**, 461-70.

Takahashi N, Goto N, Okada K, Takahashi H, 2002. Hydrotropism in abscisic acid, wavy, and gravitropic mutants of Arabidopsis thaliana. *Planta* **216**, 203-11.

Takahashi N, Yamazaki Y, Kobayashi A, Higashitani A, Takahashi H, 2003. Hydrotropism interacts with gravitropism by degrading amyloplasts in seedling roots of Arabidopsis and radish. *Plant Physiol* **132**, 805-10.

Tamkun JW, Deuring R, Scott MP*, et al.*, 1992. brahma: a regulator of Drosophila homeotic genes structurally related to the yeast transcriptional activator SNF2/SWI2. *Cell* **68**, 561-72.

Tang X, Hou A, Babu M*, et al.*, 2008. The Arabidopsis BRAHMA chromatin-remodeling ATPase is involved in repression of seed maturation genes in leaves. *Plant Physiol* **147**, 1143-57.

Tiburcio AF, Altabella T, Bitrian M, Alcazar R, 2014. The roles of polyamines during the lifespan of plants: from development to stress. *Planta* **240**, 1-18.

Truernit E, Bauby H, Dubreucq B*, et al.*, 2008. High-resolution whole-mount imaging of three-dimensional tissue organization and gene expression enables the study of Phloem development and structure in Arabidopsis. *Plant Cell* **20**, 1494-503.

Tsay YF, Chiu CC, Tsai CB, Ho CH, Hsu PK, 2007. Nitrate transporters and peptide transporters. *FEBS Lett* **581**, 2290-300.

Ubeda-Tomas S, Federici F, Casimiro I*, et al.*, 2009. Gibberellin signaling in the endodermis controls Arabidopsis root meristem size. *Curr Biol* **19**, 1194-9.

Umezawa T, Sugiyama N, Mizoguchi M*, et al.*, 2009. Type 2C protein phosphatases directly regulate abscisic acid-activated protein kinases in Arabidopsis. *Proc Natl Acad Sci U S A* **106**, 17588-93.

Umezawa T, Sugiyama N, Takahashi F*, et al.*, 2013. Genetics and phosphoproteomics reveal a protein phosphorylation network in the

abscisic acid signaling pathway in Arabidopsis thaliana. *Sci Signal* **6**, rs8.

Uno Y, Furihata T, Abe H, Yoshida R, Shinozaki K, Yamaguchi-Shinozaki K, 2000. Arabidopsis basic leucine zipper transcription factors involved in an abscisic acid-dependent signal transduction pathway under drought and high-salinity conditions. *Proc Natl Acad Sci U S A* **97**, 11632-7.

Van De Poel B, Smet D, Van Der Straeten D, 2015. Ethylene and Hormonal Cross Talk in Vegetative Growth and Development. *Plant Physiol* **169**, 61-72.

Vercruyssen L, Verkest A, Gonzalez N*, et al.*, 2014. ANGUSTIFOLIA3 binds to SWI/SNF chromatin remodeling complexes to regulate transcription during Arabidopsis leaf development. *Plant Cell* **26**, 210-29.

Verma V, Ravindran P, Kumar PP, 2016. Plant hormone-mediated regulation of stress responses. *BMC Plant Biol* **16**, 86.

Vlad F, Droillard MJ, Valot B*, et al.*, 2010. Phospho-site mapping, genetic and in planta activation studies reveal key aspects of the different phosphorylation mechanisms involved in activation of SnRK2s. *Plant J* **63**, 778-90.

Vlad F, Rubio S, Rodrigues A*, et al.*, 2009. Protein phosphatases 2C regulate the activation of the Snf1-related kinase OST1 by abscisic acid in Arabidopsis. *Plant Cell* **21**, 3170-84.

Voinnet O, Rivas S, Mestre P, Baulcombe D, 2003. An enhanced transient expression system in plants based on suppression of gene silencing by the p19 protein of tomato bushy stunt virus. *Plant J* **33**, 949-56.

Waadt R, Kudla J, 2008. In Planta Visualization of Protein Interactions Using Bimolecular Fluorescence Complementation (BiFC). *CSH Protoc* **2008**, pdb.prot4995.

Waadt R, Schmidt LK, Lohse M, Hashimoto K, Bock R, Kudla J, 2008. Multicolor bimolecular fluorescence complementation reveals simultaneous formation of alternative CBL/CIPK complexes in planta. *Plant J* **56**, 505-16.

Walter M, Chaban C, Schutze K*, et al.*, 2004. Visualization of protein interactions in living plant cells using bimolecular fluorescence complementation. *Plant J* **40**, 428-38.

Wang P, Xue L, Batelli G*, et al.*, 2013a. Quantitative phosphoproteomics identifies SnRK2 protein kinase substrates and reveals the effectors of abscisic acid action. *Proc Natl Acad Sci U S A* **110**, 11205-10.

Wang RS, Pandey S, Li S*, et al.*, 2011. Common and unique elements of the ABA-regulated transcriptome of Arabidopsis guard cells. *BMC Genomics* **12**, 216.

Wang Y, Li L, Ye T, Lu Y, Chen X, Wu Y, 2013b. The inhibitory effect of ABA on floral transition is mediated by ABI5 in Arabidopsis. *J Exp Bot* **64**, 675-84.

Weake VM, Workman JL, 2010. Inducible gene expression: diverse regulatory mechanisms. *Nat Rev Genet* **11**, 426-37.

Whitehouse I, Flaus A, Cairns BR, White MF, Workman JL, Owen-Hughes T, 1999. Nucleosome mobilization catalysed by the yeast SWI/SNF complex. *Nature* **400**, 784-7.

Wilkinson S, Davies WJ, 2002. ABA-based chemical signalling: the co-ordination of responses to stress in plants. *Plant Cell Environ* **25**, 195-210.

Wind JJ, Peviani A, Snel B, Hanson J, Smeekens SC, 2013. ABI4: versatile activator and repressor. *Trends Plant Sci* **18**, 125-32.

Winter D, Vinegar B, Nahal H, Ammar R, Wilson GV, Provart NJ, 2007. An "Electronic Fluorescent Pictograph" browser for exploring and analyzing large-scale biological data sets. *PLoS One* **2**, e718.

Wu MF, Sang Y, Bezhani S*, et al.*, 2012. SWI2/SNF2 chromatin remodeling ATPases overcome polycomb repression and control floral organ identity with the LEAFY and SEPALLATA3 transcription factors. *Proc Natl Acad Sci U S A* **109**, 3576-81.

Wu Q, Zhang X, Peirats-Llobet M*, et al.*, 2016. Ubiquitin Ligases RGLG1 and RGLG5 Regulate Abscisic Acid Signaling by Controlling the Turnover of Phosphatase PP2CA. *Plant Cell*.

Xu Y, Guo C, Zhou B*, et al.*, 2016. Regulation of vegetative phase change by SWI2/SNF2 chromatin remodeling ATPase BRAHMA. *Plant Physiol*.

Xu ZY, Lee KH, Dong T*, et al.*, 2012. A vacuolar beta-glucosidase homolog that possesses glucose-conjugated abscisic acid hydrolyzing activity plays an important role in osmotic stress responses in Arabidopsis. *Plant Cell* **24**, 2184-99.

Xue L, Wang P, Wang L*, et al.*, 2013. Quantitative measurement of phosphoproteome response to osmotic stress in arabidopsis based on Library-Assisted eXtracted Ion Chromatogram (LAXIC). *Mol Cell Proteomics* **12**, 2354-69.

Yan A, Chen Z, 2016. The pivotal role of abscisic acid signaling during transition from seed maturation to germination. *Plant Cell Rep*.

Yang S, Li C, Zhao L*, et al.*, 2015. The Arabidopsis SWI2/SNF2 Chromatin Remodeling ATPase BRAHMA Targets Directly to PINs and Is Required for Root Stem Cell Niche Maintenance. *Plant Cell* **27**, 1670-80.

Yang W, Zhang W, Wang X, 2016a. Post-translational control of ABA signalling: the roles of protein phosphorylation and ubiquitination. *Plant Biotechnol J*.

Yang Z, Liu J, Tischer SV*, et al.*, 2016b. Leveraging abscisic acid receptors for efficient water use in Arabidopsis. *Proc Natl Acad Sci U S A* **113**, 6791-6.

Yin P, Fan H, Hao Q*, et al.*, 2009. Structural insights into the mechanism of abscisic acid signaling by PYL proteins. *Nat Struct Mol Biol* **16**, 1230-6.

Yoo SD, Cho YH, Sheen J, 2007. Arabidopsis mesophyll protoplasts: a versatile cell system for transient gene expression analysis. *Nat Protoc* **2**, 1565-72.

Yoshida R, Hobo T, Ichimura K*, et al.*, 2002. ABA-activated SnRK2 protein kinase is required for dehydration stress signaling in Arabidopsis. *Plant Cell Physiol* **43**, 1473-83.

Yoshida T, Fujita Y, Maruyama K*, et al.*, 2015. Four Arabidopsis AREB/ABF transcription factors function predominantly in gene

expression downstream of SnRK2 kinases in abscisic acid signalling in response to osmotic stress. *Plant Cell Environ* **38**, 35-49.

Yoshida T, Fujita Y, Sayama H*, et al.*, 2010. AREB1, AREB2, and ABF3 are master transcription factors that cooperatively regulate ABRE-dependent ABA signaling involved in drought stress tolerance and require ABA for full activation. *Plant J* **61**, 672-85.

Yoshida T, Nishimura N, Kitahata N*, et al.*, 2006. ABA-hypersensitive germination3 encodes a protein phosphatase 2C (AtPP2CA) that strongly regulates abscisic acid signaling during germination among Arabidopsis protein phosphatase 2Cs. *Plant Physiol* **140**, 115-26.

Zeng L, Zhou MM, 2002. Bromodomain: an acetyl-lysine binding domain. *FEBS Lett* **513**, 124-8.

Zhao M, Yang S, Chen CY*, et al.*, 2015a. Arabidopsis BREVIPEDICELLUS interacts with the SWI2/SNF2 chromatin remodeling ATPase BRAHMA to regulate KNAT2 and KNAT6 expression in control of inflorescence architecture. *PLoS Genet* **11**, e1005125.

Zhao M, Yang S, Liu X, Wu K, 2015b. Arabidopsis histone demethylases LDL1 and LDL2 control primary seed dormancy by regulating DELAY OF GERMINATION 1 and ABA signaling-related genes. *Front Plant Sci* **6**, 159.

Zhu Y, Rowley MJ, Bohmdorfer G, Wierzbicki AT, 2013. A SWI/SNF chromatin-remodeling complex acts in noncoding RNA-mediated transcriptional silencing. *Mol Cell* **49**, 298-309.

Zwanenburg B, Pospisil T, Cavar Zeljkovic S, 2016. Strigolactones: new plant hormones in action. *Planta* **243**, 1311-26.

ABBREVIATIONS

3AT: 3-Amino-1, 2, 4-Triazole

AA: Amino Acid

AAO: Abscisic Aldehyde Oxidase

ABA: Abscisic Acid

ABA-GE: ABA-Glucose Ester

aba1: ABA deficient 1

ABA2: ABA deficient 2

ABF1: ABA Binding Factor2

ABF2/AREB1: ABA Binding Factor2

ABI1/abi1: ABA-Insensitive1

ABI2: ABA-Insensitive2

ABI3: ABA Insensitive3

ABI4: ABA Insensitive4

ABI5: ABA Insensitive5

AD: Activation Domain

Ade: Adenine

AHG1: ABA-Hypersensitive Germination1

AHG3/PP2CA: ABA-Hypersensitive Germination 3

AmpR: Ampicillin resistance

AP2: APETALA2

APS: Ammonium Persulfate

ARE: ABA Responsive Element

AREB1/ABF2: ABA Responsive Element Binding Factor1

AtABCG25: *Arabidopsis thaliana* ATP-Binding Cassette G25

AtABCG40: *Arabidopsis thaliana* ATP-Binding Cassette G40

BD: Binding Domain

BR: Brassinosteroids

BRM: Brahma, ATPase

BSA: Bovine Serum Albumin

bZIP: Basic Leucine-Zipper transcription factor family protein

CID: Collision-induced Dissociation

CIP: Calf Intestinal alkaline Phosphatase

CIPK: Calcium Independent Protein Kinase

CK: Cytokinins

CLSM: Confocal Laser Scanning Microscopy

CO: Constans

co-IP: Co-immunoprecipitation

CR: Chromatin remodeling

CRC: Chromatin remodeling complexes

CTAB: Cetyl Trimethyl Ammonium Bromide

CUC: CUP-SHAPED COTYLEDON

DO: Drop Out solution

DTT: Di Tio Treitol

EDTA: Ethylene Diamine Tetraacetic Acid

EMS: Ethyl methanesulfonate

ET: Ethylene

ETD: Electron Transfer Dissociation

FLC: Flowering locus C

FT: FLOWERING LOCUS T

GAs: Gibberellins

GAD: GAL4 activation domain

GBD: GAL4 binding domain

GenR: Gentamycin resistance

GFP: Green Fluorescence Protein

GUS: β-Glucuronidase

HAB1: Hypersensitive to ABA1

HAB2: Hypersensitive to ABA2

HAI1: Highly ABA Inducible1

HAI2: Highly ABA Inducible2

HAI3: Highly ABA Inducible3

HAT/HDAC: Histone Acetyltransferase/Histone Deacetilase

His: Histidine

HSA: Helicase SANT-associated domain

hyl1: Hyponastic leaves

IPTG: β-D-1-thiogalactopyranoside

JA: jasmonates

KanR: Kanamycin resistance

KAT1: Potassium channel 1

Kd: dissociation constant

LB: Luria broth, Luria Bertani media

LC–MS/MS: Liquid chromatography coupled to mass/mass

LD: Long Day

Leu: Leucine

lncRNA: Long non coding RNA

MES: 2-(N-morpholino) ethanesulfonic acid

MMG: Mannitol-Magnesium buffer

mPS-PI: Pseudo-Schiff-Propidium Iodide protocol

MS: Murashige-Skoog

MUG: 4-methylumbelliferyl β-D-glucuronide

NADPH oxidase: Nicotinamide Adenine Dinucleotide Phosphate oxidase

nanoHPLC: nano High-performance liquid chromatography

NCED: 9-Cis-Epoxycarotenoid Dioxygenase

N_I: Nuclear insoluble fraction

Ni-NTA: Nickel-Nitrilotriacetic

NO: nitric oxide

N_S: Nuclear soluble fraction

N_T: Nuclear total fraction

OD600: Optical density mesured at a wavelenght of 600nm

OE: Overexpression

ORF: Open Reading Frame

OST1: Open Stomata1

PA: Polyamines

PcG: Polycomb proteins

PCR2: PcG repressive complex 2

PEG: Polyethylene glycol

PM-ATPase: Plasma Membrane ATPase

PMSF: Phenylmethylsulfonyl Fluoride

PP1: Protein Phosphatase Type 1

PP2A: Protein Phosphatase Type 2A

PP2C: Protein Phosphatase Type 2C

PP2CA/AHG3: Protein Phosphatase 2CA

ProGC1: Promoter of Guard Cells

PYL1 to 13: PYR1-Like1 to 13

PYR/PYL/RCAR: Pyrabactin Resistance 1/PYR1-Like/Regulatory Components of ABA Receptors

PYR1: Pyrabactin Resistance 1

QUAC1: R-Type Anion Channel

RAM: Root Apical Meristem

RFP: Red fluorescent protein

ROS: Reactive Oxygen Species

ROX: Carboxy-X-rhodamine

RT: Room Temperature

SA: Salicylic acid

SCD: Synthetic Complete Defined culture medium

SD: Synthetic Defined culture medium

SDS: Sodium DodecylSulphate

SDS-PAGE: SDS-PolyAcrylamide Gel Electrophoresis

Ser: Serine

SL: Strigolactones

SLAC1: Slow Anion Channel 1

SnAC: Snf2 ATP-coupling

SnRK1: Sucrose-Non Fermenting1 (SNF1)-Related Protein Kinase 1

SnRK2: Sucrose-Non Fermenting1 (SNF1)-Related Protein Kinase 2

SnRK2.2/D: SNF1-Related Protein Kinase 2.2

SnRK2.3/I: SNF1-Related Protein Kinase 2.3

SnRK2.6/E/OST1: SNF1-Related Protein Kinase 2.2

SpecR: Spectinomycin resistance

SWI/SNF: Switch/Sucrose Non-Fermenting

SWN: Swinger

TEMED: N,N,N',N'-Tetramethylethylenediamine

TF: Transcription Factor

TFA: Trifluoroacetic Acid

Trp: Triptophan

X-Gluc: 5-bromo-4-chloro-3-indolyl Glucuronide

YFPN: N terminal part of the yellow fluorescence protein

YNB: Yeast Nitrogen Base